PROTON EXCHANGE IN AQUEOUS SOLUTIONS OF POLYFUNCTIONAL ELECTROLYTES

JOHN NORMAN ATHERTON


CENTRE FOR NFLD. STUDIES
MEMORIAL UNIVERSITY
OF NEWFOUNDLAND

PROTON EXCHANGE IN AQUEOUS SOLUTIONS OF POLYFUNCTIONAL ELECTROLYTES

A Thesis

Presented to

The Department of Chemistry

Memorial University of Newfoundland

In Partial Fulfillment

of the Requirements for the Degree

Doctor of Philosophy

by

John Norman Atherton, B.Sc., M.Sc., Dip.Ed.

April 1977

ABSTRACT

The adiabatic half passage experiment was used to measure the rates of proton exchange reactions in acidified aqueous solutions of piperazine, N,N'-dimethylpiperazine and histamine. All of the reactions which were detected involved participation by water molecules. Reactions detected for piperazine included (a) the transfer of a proton from a piperazine species to a water molecule and (b) the transfer of a proton from one piperazine species to another piperazine species via at least one water molecule. For N,N'-dimethylpiperazine, reactions of type (b) could not be detected.

In the case of histamine, proton exchange from two different types of N-H site was distinguished. Reactions of types (a) and (b) were detected for proton transfer from both imidazolium and ammonium sites. An intramolecular proton exchange was also found in which a proton was transferred from an ammonium site to an imidazole site of the same histamine molecule with one or two water molecules participating. The rate constant for this reaction is $j_i = (1.87 \pm 0.09) \times 10^5$ sec.$^{-1}$.

Since the distances between active centers in enzymes is sometimes comparable to that in histamine, it follows that intramolecular proton transfer in enzymes is possible and perhaps even probable. If such an intramolecular reaction does occur in enzymes at about the same rate as it occurs in histamine then it will compete favourably with bimolecular reactions at physiological pH. The ability of the hydrogen bonded water molecules to fit the contours of the enzyme could result in

an intramolecular proton transfer even between centers which are severely sterically crowded.

ACKNOWLEDGEMENTS

My very sincere gratitude is expressed to the supervisor of this work, Dr. E.K. Ralph, who showed a very human understanding of my difficulties as well as a thorough competence in providing advice which was essential for the completion of the project. Other members of the faculty and staff of the Chemistry Department were also helpful in various ways. I particularly wish to thank Dr. J.M.W. Scott for helpful discussions and Miss T. Barker for some very valuable assistance when I was about to submit the thesis.

I must also thank my wife for her patience and understanding during times of stress as well as substantial assistance in preparation of the manuscript and type-script. Miss I.B. Anderson and Mrs B. Hibbert also helped in the typing of the manuscript. Technical Typing were engaged to produce the final type-script and Miss H. Hiscock drew all of the diagrams. Financial assistance was provided by a Memorial University Graduate Student Fellowship.

TABLE OF CONTENTS

LIST OF TABLES

Table — Page

Table — Page

LIST OF FIGURES

SYMBOLS USED FOR HISTAMINE RATE CONSTANTS

k is used for the rate constants of reactions in which a proton is transferred from an imidazolium site.

j is used for the rate constants of reactions in which a proton is transferred from an ammonium site.

ℓ is used for the rate constants of composite reactions involving proton transfers from both imidazolium and ammonium sites.

1 is used as the subscript to the rate constant if only one histamine species is involved in the reaction.

2 is used as the subscript to the rate constant if two histamine species are involved in the reaction.

Double numerical subscripts are used to designate specific component reactions in which two histamine species are involved. The two numbers represent the respective charges on the two reacting histamine species.

Other symbols are defined in the text with the appropriate mechanisms.

CHAPTER 1

INTRODUCTION

The mechanism of enzyme action has been of great interest to biochemists. This interest has arisen largely from the importance of enzymes as catalysts of physiological reactions. An additional reason for interest has been the very fast rate at which these catalysed reactions proceed. A major difficulty in elucidating the mechanisms lies in the complexity of the enzyme - substrate complex in which the reactions occur. One popular approach to the problem has been the investigation of intramolecular processes occurring in smaller molecules which have been selected as models for the enzyme - substrate complex [1, 2]. The present work uses the histamine molecule as such a model, with nuclear magnetic resonance being chosen as the most profitable method for investigating the reaction kinetics and mechanisms.

The histamine molecule (which is shown in Figure 4.2) contains two different types of acid-base reactive sites, and in acidic solutions it exists primarily as a doubly protonated species. Since little data was available for this charge type, initial work was carried out on simpler model systems. These simpler models were chosen with two equivalent acid-base reactive sites so that similar charge types to histamine could be investigated with fewer microscopic rate and equilibrium constants being involved. This was expected to lead to a simpler kinetic analysis which could delineate salt effects, acidity functions, etc., which might be useful in the case of histamine. Chapter 3 contains

results for piperazine and for N,N'-dimethylpiperazine which were both used as simple models.

The Intramolecular Model for Enzymic Catalysis

It is generally accepted that enzymic catalysis depends on the same basic chemical mechanisms which are utilized for simple reactions in solution [3]. Greater enzymic efficiency is then explained by a more favourable free energy change due to the binding of the reactants at the active site of the enzyme as described by Koshland's induced fit model [4]. Part of this effect is the entropic contribution to enzymic catalysis which arises from the enzyme holding the reactants together at the active site in the optimum position for reaction [3]. The reaction is therefore more probable than the case where the reactants must first come together from dilute solution.

The small intramolecular model can imitate the entropic contribution, but it may not measure the full entropic effect since the smaller molecule may not be sufficiently flexible to enable the optimum reacting position to be obtained. In contrast, the widely accepted Koshland model of enzymic catalysis [4] proposes that a (specific) substrate induces the "proper orientation of the catalytic groups required for enzyme action". It is even possible that this "proper orientation" changes as the reaction proceeds.

Importance of the Imidazole Group at the Active Sites of Enzymes

Evidence for the presence of Imidazole groups in the active sites of enzymes has been reviewed by Vallee and Riordan [5]. Methods used

have included (i) X-ray diffraction; (ii) chemical methods and (iii) the dependence on pH of the maximal velocity (an inflection in the region expected for imidazole ionization being used as an indication of an imadazole presence). Jencks [6] has discussed limitations of these criteria, but the extensive occurrence of the imadazole group (usually in the form of a histidine residue) at active sites is well established.

One well defined example is the catalytic site of chymotrypsin which has been described by Blow et al., [7]. The site contains an aspartic acid hydrogen bonded to a histidine which in its turn is hydrogen bonded to a serine. The situation above pH 7 is shown below:

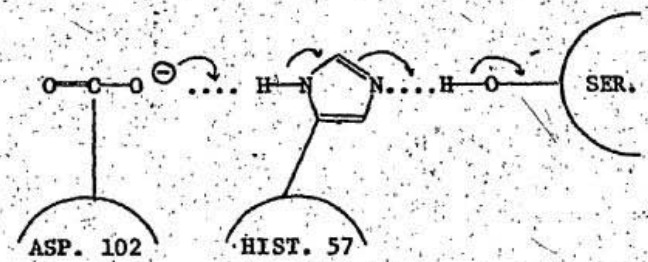

(1.1)

Blow proposed a charge transfer mechanism, as shown, which would result in a negative charge at the surface serine and hence make it strongly nucleophilic and reactive towards amides and esters. Blow's proposal was prompted by Wang [8] who had previously suggested that "facilitated proton transfer along rigidly held hydrogen bonds may play a crucial role in determining the efficiency and specificity of many enzymes".

The Role of Acid-Base Catalysis

That general acid-base catalysis is important in enzyme mechanisms has been repeatedly emphasized [1, 2, 9, 10, 11] and Jencks [6] has shown

that this is certainly true when the catalysing group consists of an imidazole ring. General acid-base catalysis by imidazole is particularly effective as is shown by the following considerations. For any species to act as a general acid-base catalyst, it must undergo a complete protonation-deprotonation cycle in order to regenerate the catalytic species. Since the reaction of protons and of hydroxyl ions with bases and acids respectively are diffusion controlled with rate constants about 10^{10} l.mole.$^{-1}$ sec.$^{-1}$., it follows that the rate of deprotonation of an acid by dissociation is about $10^{10}\ K_A$ sec.$^{-1}$ and the rate of protonation of a base by water is about $\frac{10^{10} K_w}{K_A}$ where K_A is the ionization constant of the conjugate acid to the basic site (i.e. the same K_A as before). At 25° C, $K_W = 10^{-14}$ and the fastest rate determining step in the catalysis cycle will arise when the rate of protonation equals the rate of deprotonation with $K_A = 10^{-7}$. This is the approximate K_A value of imidazole.

An intramolecular proton transfer is sometimes important in acid-base catalysis. Williams and Jencks have recently reported such a case in the synthesis of phenylurea from aniline and cyanic acid by the following mechanism [12]:

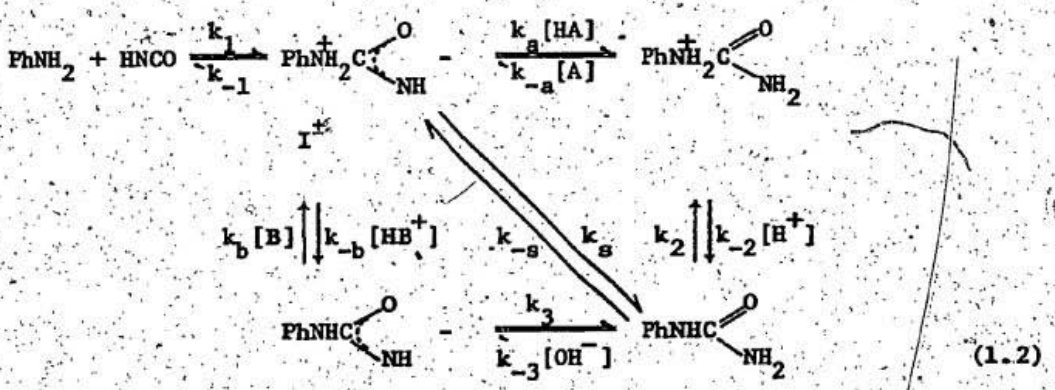

(1.2)

In this mechanism k_a and k_b are the rate constants for simple proton transfer reactions from or to the catalyst, respectively, and are close to the diffusion-controlled limit in the thermodynamically favoured direction. k_s represents an intramolecular reaction in which the initially formed zwitterion ($I^{\pm}$) is converted directly to the uncharged urea. These workers proposed that the intramolecular reaction probably occurs with the aid of water molecules in a stepwise manner, although the participation of water molecules was not proven. The possibility of a concerted mechanism was not excluded.

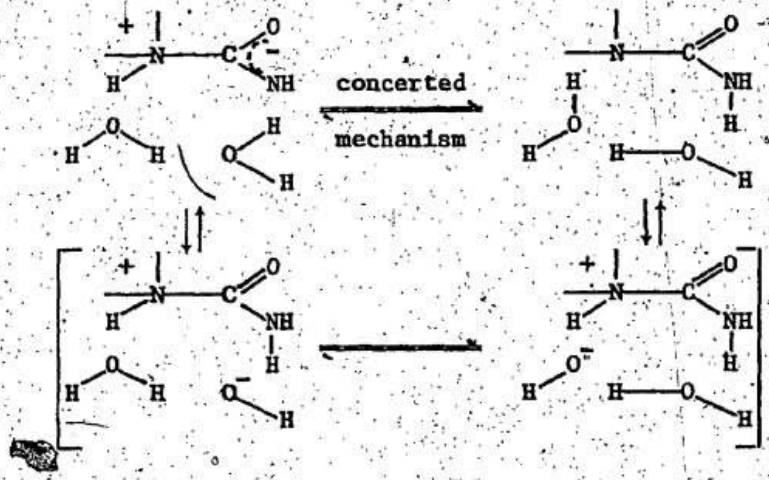

(1.3)

They find a value for k_s of 10^8 sec^{-1} at 25°C.

General Acid-Base Catalysis by Imidazole

Jencks [6] has listed many examples of work on acid-base catalysis by imidazole groups. A few examples of particular interest are given here.

(a) The imidazole catalysed hydration of dichloroacetone in 95% dioxane is unusual in that the rate law contains a term which is second order with respect to imidazole [13]. A mechanism has been proposed in

which one imidazole acts as a general base catalyst of the hydration while a second imidazole acts as a general base catalyst of the general base catalysis.

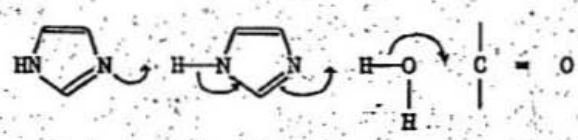

(1.4)

This mechanism is analagous to the action of the aspartate-imidazole couple in the charge transfer process proposed for chymotrypsin by Blow et al., [7].

(b) Overberger and co-workers have prepared a series of polymers based on polyvinylimidazole and investigated their catalytic activity [14]. They found that the rate laws contained all the terms shown by the corresponding monomeric species, but in addition, for each polymer, an additional reaction was observed at high pH with the polymeric species, but not with the monomers. The mechanism for this reaction was a terfunctional process involving neutral and anionic imidazole fractions on the polymer, making possible the reaction with the substrate. The mechanism was thought to consist of general base or acid catalysis of a nucleophilic imidazole attack on the substrate.

(c) Simple 2', 3' - nucleotide cyclic phosphates can serve as substrates of the enzyme ribonuclease. The pH dependence of the hydrolysis of these synthetic nucleotide substrates (as well as of ribonucleic acid)

has a bell shaped profile which is suggestive of a concerted general acid-base catalysed mechanism. Most of the mechanisms which have been suggested for the catalytic action of ribonuclease involve a (possibly concerted) proton removal by imidazole and proton donation by imidazolium [10, 15]. One possible mechanism is shown in equation (1.5) below, with completion of the reaction occurring by the reverse of equation (1.5) after ROH has been replaced by a water molecule:

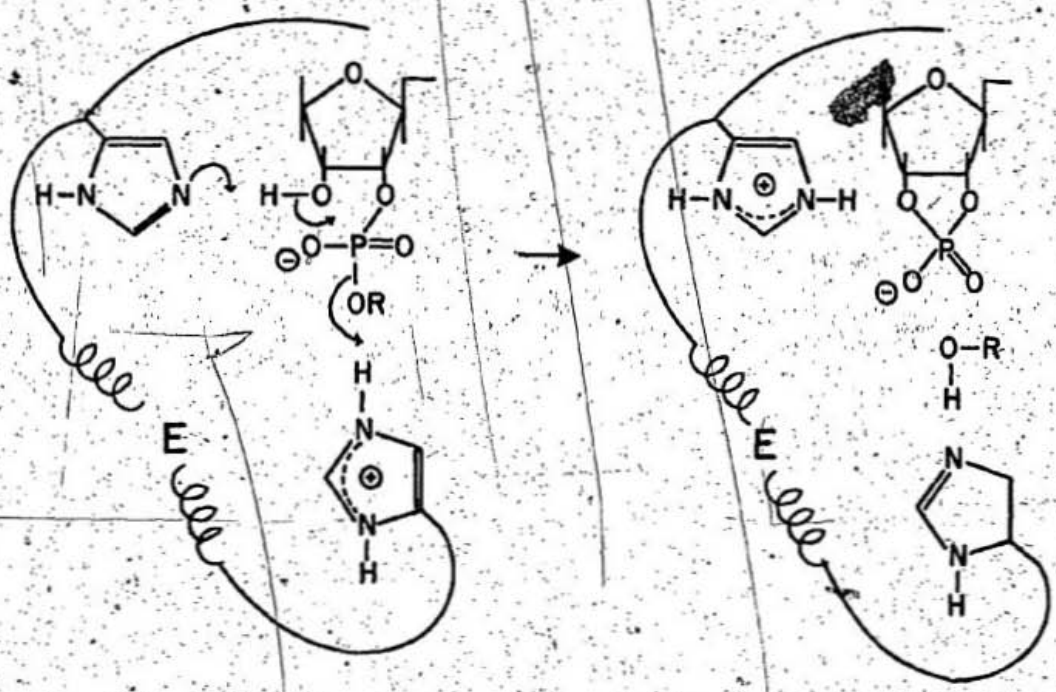

(1.5)

Hydrolysis of the cyclic triester methyl ethylene phosphate was found to be subject to general base catalysis by imidazole [16] in a simple model system for the action of ribonuclease [6].

Proton Transfer Reactions

Acid-base catalysis consists of proton transfer reactions and since this work will largely concern this type of reaction it may be helpful to review some of their basic properties.

(a) It is well known that if a donor group has a lower pK_A than an acceptor group, then the rate of proton transfer may well be diffusion controlled [17]. The rate will then depend largely on the mobilities of the reacting species, but other factors will also influence the rate of reaction. The following considerations [18] may affect the rate of reactions in the present work.

(i) Differences in electrostatic forces depending upon the charge type of the reacting acid or base.

(ii) Configurational influences due to size and shape of the reaction partners.

(iii) Changes in water structure and orientation in the vicinity of the reacting ion or molecule, influencing the rate at which hydrogen bonds are formed. In general, stronger hydrogen bonding will lead to faster rates for reactions in which water participates.

(iv) Intramolecular hydrogen bonds, if present at the reaction site, will have to be broken before the hydrogen bonds necessary for reaction can form.

Cosiderations (iii) and (iv) show the possible importance of solvent effects in the reaction rates and mechanisms of the present work.

(b) Eigen [19] has shown that the magnitude of the isotope effect depends on which step of a proton transfer reaction is rate determining. Thus a "normal isotope effect" (i.e. < 2) is expected for a reaction

in which structural rearrangement of water is rate determining, whereas a somewhat higher isotope effect is expected for reactions in which the actual proton transfer is rate determining. Isotope effects have sometimes been used to elucidate mechanisms in this way.

(c) A final point which may be useful to note concerns work by Alberty and Hammes [20]. These workers applied the theory of diffusion-controlled reactions to enzyme kinetics and showed that the limiting law originally derived by Bronsted [21] was applicable in this case:

$$\log k = \log k_o + Z_1 Z_2 \sqrt{\mu} \qquad (1.6)$$

where k is the rate constant for the reaction when the ionic strength is μ, k_o is the rate constant extrapolated to zero ionic strength, and Z_1 and Z_2 are the number of charges (with signs) on the reacting ions.

Some Intramolecular Rate Constants

Following are some examples of rate constants which have been reported for intramolecular proton transfer reactions. The mechanisms proposed have frequently involved solvent participation and for reactions in aqueous solution the rate constants have been within the range 10^6 to 10^8 $sec.^{-1}$ at temperatures near 25°C.

(a) Eigen has reported the following rate constants (page 1040 of reference 22) which were obtained by sound absorption measurements at 20°C.

$$HSCH_2CH_2NH_2 \rightleftharpoons {}^{-}SCH_2CH_2NH_3^{+} \qquad (1.7)$$

$$k = 2 \times 10^7 \ sec^{-1}.$$

$$H_2NC_6H_4COOH \rightleftharpoons {}^{+}H_3NC_6H_4COO^{-} \qquad (1.8)$$

For o-Aminobenzoic acid, $k = 2.5 \times 10^7$ sec.$^{-1}$

For m-Aminobenzoic acid, $k = 1.7 \times 10^7$ sec.$^{-1}$

For p-Aminobenzoic acid, $k = 2.5 \times 10^7$ sec.$^{-1}$

(b) Luz and Meiboom [23] used nuclear magnetic resonance measurements to determine the rate of proton transfer in a hydrogen bonded complex of one acetic acid molecule and two water molecules in aqueous solutions of acetic acid. Earlier work [24] had indicated that a stepwise ion pair mechanism is more probable than a concerted mechanism:

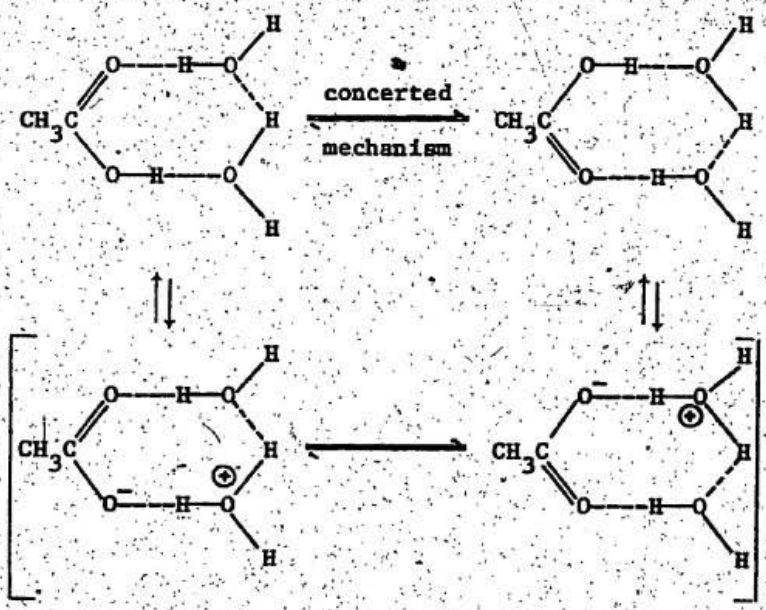

(1.9)

$k = 4.8 \times 10^7$ sec.$^{-1}$ (25°C)

(c) Sheinblatt and Gutowsky [25] made nuclear magnetic resonance measurements on aqueous solutions of glycine. From their data, Grunwald and Ralph [26] were able to determine the following intramolecular rate constant but the data did not allow solvent participation to be determined.

$$H_2NCH_2COOH \rightleftharpoons {}^{+}H_3NCH_2COO^{-} \qquad (1.10)$$

$$k = 7.1 \times 10^{7} \text{ sec.}^{-1} \quad (23°C).$$

(d) The intramolecular proton transfer which occurred in the urea synthesis studied by Williams and Jencks [12] has already been mentioned earlier in this chapter (Equation 1.3).

The Study of Very Rapid Reactions

The methods available for the investigation of the rates and mechanisms of very rapid reactions in solution have been described in detail [22]. Commonly used methods have been classified as relaxation methods or as magnetic resonance methods [22]. The relaxation methods consist of disturbing the chemical equilibrium by either a stepwise pulse (e.g. temperature jump, pressure shock, etc.) or by a periodic perturbation (e.g. by absorption of sound waves). In the case of a method such as temperature jump, the rate at which the system relaxes towards the new equilibrium position is measured. In the case of a periodic perturbation, the chemical concentrations will attempt to follow the periodic perturbation, but there will, of course, be a phase lag. This phase difference will be a measure of the rate of the chemical reactions.

In the temperature jump experiment, the coupling between the

perturbation and the extent of the reaction is given by the equation:

$$\frac{d \ln K}{d T} = \frac{\overline{\Delta H^\circ}}{R T^2} \qquad (1.11)$$

In the present work we will be concerned with some reactions in which a proton is transferred between sites which are chemically similar (e.g. both at nitrogen atoms) or even identical. The value for $\overline{\Delta H^\circ}$ of such reactions will be small or even zero, and the coupling between the perturbation and the extent of the reaction will therefore be poor. The temperature jump method would therefore be difficult to apply to these reactions. Also since only small changes of solvent structure will accompany these reactions, the value of ΔV° will also be small. Therefore other relaxation techniques such as pressure shock will also have poor coupling of the perturbation to the extent of the reaction.

A further disadvantage of the relaxation methods is that they do not measure solvent participation in a reaction whereas the magnetic resonance methods can yield information on this aspect of a reaction. Most work in enzymology has used relaxation techniques and direct information of solvent involvement has not been obtainable. However, the possible involvement of solvent molecules has been proposed [1] and the use of a magnetic resonance method in this work was considered to be advantageous for this reason.

The Effect of Chemical Exchange on Nuclear Magnetic Resonance Spectra

Nuclear magnetic resonance spectral fine structure may result from (i) "chemical shift", which arises by the particular electronic bonding environment causing a change in the resonance frequency, and

(ii) spin-spin interaction with other nuclei in the molecule [27]. This spectral fine structure is strongly modified if the nucleus is subjected to a rapid change in chemical (i.e. electronic) environment. As an example, the proton resonances of pure liquid ammonia and pure water differ by several parts per million at 30 MHz [28]. An equimolar mixture of liquid ammonia and water, however, yields only a single narrow resonance of frequency between those of the pure components. This is due to the fact that the protons are being rapidly transferred by reactions such as

$$H_3N.\underline{H}^+ + OH_2 \rightleftharpoons H_3N + {}^+\underline{H}.OH_2 \qquad (1.12)$$

The result of this rapid process is effectively a new electronic environment corresponding to a weighted average of the H_2O and NH_3 environments. In describing the chemical exchange as rapid, we are comparing it with the reciprocal of the difference between the H_2O and NH_3 resonance frequencies. Thus, in the above example the separation between the two resonances is of the order of 100 Hz. (since one part per million at 30 MHz. corresponds to 30 Hz.) so that the chemical exchange is fast compared with 100 $sec.^{-1}$. Similarly, the spin-spin multiplet structure may vanish if the mean lifetime which a nucleus spends in a given molecule is short in comparison with the reciprocal of the coupling constant (i.e. if the rate of exchange is fast compared with the coupling constant).

For either of the spectral features, if the chemical exchange is very slow compared with the characteristic separation, then no alteration of the spectrum is observed. As the exchange rate increases, however, there will be a corresponding broadening of the component lines of the spectrum until they overlap into a structureless broad single

resonance. As the rate of exchange increases further this broad resonance narrows until a single sharp line is observed at a very rapid rate of exchange [29]. The first stage of broadened individual lines is called "lifetime broadening" because the broadening can be considered as resulting from the finite time a nucleus stays in a definite spin state. The second stage, in which there is a single collapsed line, is referred to as "exchange narrowing". In this stage, the exchange is fast enough for an averaging of the individual resonance frequencies to occur, and the width of the observed line decreases with increasing exchange rate. By analysis of the line shapes in regions where the mean lifetime of the chemical species is the same order of magnitude as the reciprocal of the characteristic frequency of separation, it is possible to obtain lifetimes and hence rates of reaction.

The Case of One Dominant Line

The nuclear magnetic resonance method used in this work was based on measurements of the water resonance. Since changes in the spectrum only arise when a proton experiences a change in magnetic environment, it follows that the only processes detected will involve proton transfer between ^{16}O or ^{18}O water sites and either amino sites or ^{17}O water sites. Exchange between ^{17}O water sites and the other water sites can be detected since the ^{17}O isotope has a different nuclear spin from the other water sites [30]. A direct proton transfer between two amino sites such as in Equation 1.13 will, therefore, not be detected in the present work.

$$H_3N.\underline{H}^+ + NH_3 \longrightarrow H_3N + {}^+\underline{H}.NH_3 \qquad (1.13)$$

If, however, the same result is achieved via a mechanism involving a water molecule, then the process will be detected:

$$H_3N.\underline{H}^+ + \underset{\underset{H}{|}}{O\text{-}H} + NH_3 \rightleftharpoons H_3N + \underline{H}\text{-}\underset{\underset{H}{|}}{O} + {}^{+}H.NH_3 \qquad (1.14)$$

The measurements made on the water resonance were of the longitudinal relaxation time in the rotating frame, designated by $T_{1\rho}$. In the absence of the radiofrequency field, H_1, the $T_{1\rho}$ relaxation is along the same axis as the transverse relaxation time, T_2, and for all the liquids in the present work $T_{1\rho} = T_2$ when $H_1 = 0$. If $T_{1\rho}$ is measured in the presence of chemical exchange and also the longitudinal relaxation time, T_1, is measured for the same solution, then a quantity Δ sec.$^{-1}$ can be calculated from:

$$\Delta = \frac{1}{T_{1\rho}} - \frac{1}{T_1} \qquad (1.15)$$

When $H_1 = 0$, the quantity Δ will measure the broadening of the water line due to exchange (measured as full width at half height), but as H_1 increases the value of Δ will decrease from this value [31]. In the absence of exchange

$\frac{1}{T_{1\rho}}$ equals $\frac{1}{T_1}$ at any value of H_1.

Meiboom [32] has treated the case of two site exchange where the population of one site is dominant. Such a treatment can be applied in the present work provided that the proton fraction in the amino sites is small, i.e. providing the solutions are dilute. In the case of an

aqueous solution of an ammonium salt acidified with hydrochloric acid, the proton fraction in the non-dominant site will be given by:

$$p = \frac{4\left[NH_4^+\right]}{2\left[H_2O\right] + 4\left[NH_4^+\right] + \left[HCl\right]} \qquad (1.16)$$

For the case of one dominant line to be applicable, the value of p should not exceed about 1%. Providing this condition is met, the lifetime (τ sec) of an amino-species undergoing exchange can be calculated from the following equation:

$$\Delta_{NH} = \frac{p\tau}{3}\left[\frac{(\delta - J_e)^2}{1+\left[(\delta-J_e)^2+\omega_1^2\right]\tau^2} + \frac{\delta^2}{1+\left[\delta^2+\omega_1^2\right]\tau^2} + \frac{(\delta + J_e)^2}{1+\left[(\delta+J_e)^2+\omega_1^2\right]\tau^2}\right] \qquad (1.17)$$

where δ radians. sec.$^{-1}$ is the chemical shift between the two sites; $\omega_1 = \gamma H_1$ radians. sec.$^{-1}$ where γ is the gyromagnetic ratio; J_e is an effective N-H coupling constant defined by Meiboom[32] to allow for the fact that quadrupole relaxation of the ^{14}N nuclei will cause broadening of the triplet lines:

$$J_e = J_{NH}\left(\frac{T^1}{T^1 + \tau}\right) \qquad (1.18)$$

In Equation (1.18), J_{NH} sec.$^{-1}$ is the N-H coupling constant and T^1 is the longitudinal relaxation time of the ^{14}N nucleus.

As a first approximation, Equation (1.17) can be greatly simplified by setting $J_e = 0$. Then

$$\frac{\Delta_{NH}}{p} = \frac{\delta^2 \tau}{1 + (\delta^2 + \omega_1^2)\tau^2} \qquad (1.19)$$

Inspection of this equation will show that $(\Delta/p) \longrightarrow 0$ as τ becomes either very small or very large. By differentiating with respect to τ and setting

$$\frac{d\,(\Delta/p)}{d\,\tau} = 0 ,$$

it can be shown that

$$\left(\frac{\Delta_{NH}}{p}\right)_{max} = \frac{\delta^2}{2(\delta^2 + \omega_1^2)^{\frac{1}{2}}} \qquad (1.20)$$

which reduces to $\delta = 2(\Delta/p)_{max}$ as $\omega_1 \longrightarrow 0$. Figure 1-1 shows the general form of the plot of (Δ/p) versus $\log(\delta\tau)$ for various values of ω_1. It can be seen that an increasing radiofrequency field causes the largest reduction of Δ in the lifetime broadening region. The greatest rate of reduction occurs when $\omega_1 = \delta$.

Calculation of Exchange Rates

When values of δ, J_{NH}, T^1 and ω_1 are determined, it is possible to use Equation (1.17) to calculate values of τ from measurements of (Δ/p). Values for the lifetimes of the N–H species can then be used to calculate the rate of breaking of the appropriate bond since

$$\frac{1}{\tau_{NH}} = \text{specific rate} = \frac{v_{NH}}{[BOND]} \qquad (1.21)$$

where the specific rate refers to the breaking of the one particular

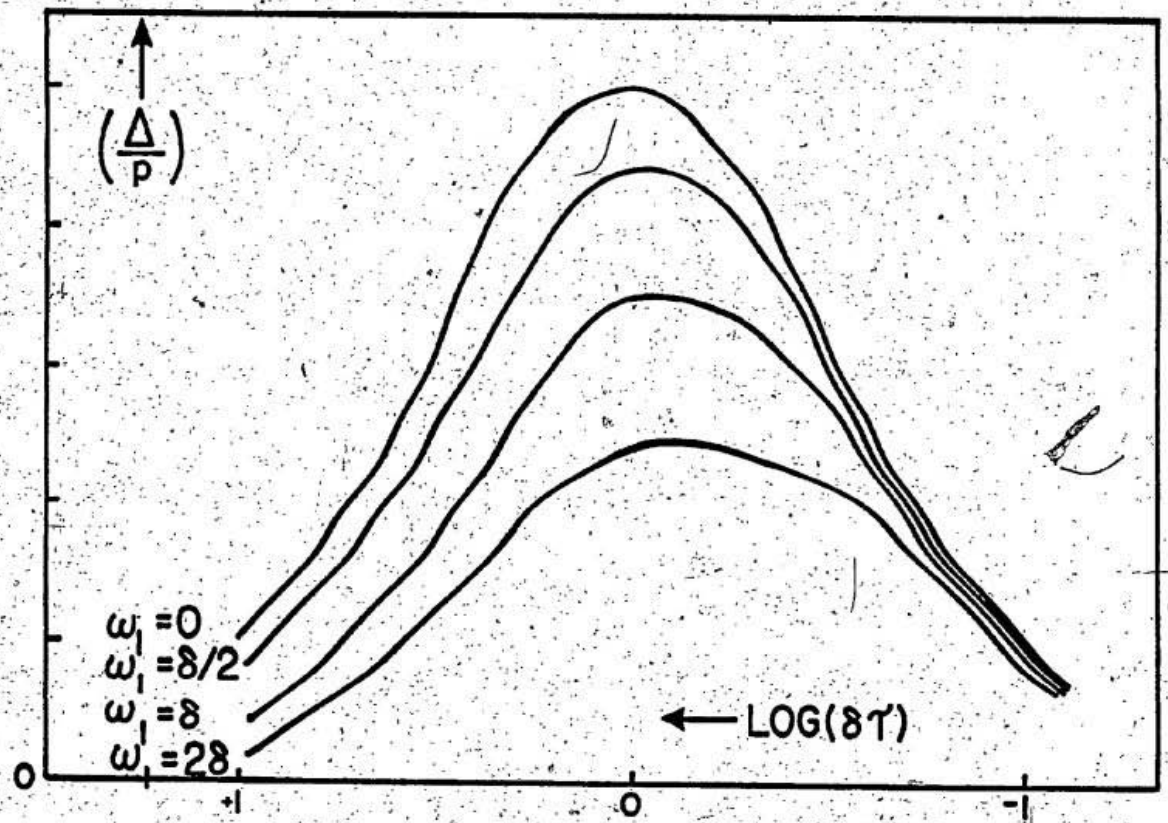

Figure 1.1 Variation of broadening with lifetime at different RF fields

bond and v_{NH} moles. liter.$^{-1}$ sec.$^{-1}$ is the rate of breaking for all bonds of that type.

When there are several equivalent bonds, then the appropriate factor must be used in conjunction with the concentration of the chemical species. For example, if measurements were made on NH_4^+ there would be four bonds which could break and hence

$$\frac{v_{NH}}{[NH_4^+]} = \frac{4}{\tau_{NH}} \tag{1.22}$$

When calculating the rates, it may be noted that the calculations are rather insensitive to the values of J_{NH} and T^1 because $J_{NH} \ll \delta$. Accordingly it is only necessary to have approximate estimates for these parameters. It is also found that values of τ are very sensitive to error in (Δ/p) when near the maximum of the curve. However, the lack of sensitivity to τ in this region implies that (Δ/p) is mainly a function of δ and hence Equation (1.20) provides a rather accurate determination of δ.[†] Grunwald and Price [33] have discussed sensitivities of (Δ_{NH}/p) values to the various parameters.

The Number of Solvent Molecules in a Reaction

It has already been indicated that rates of proton exchange between water molecules can be measured by labelling some of the water molecules with the $^{17}_{8}O$ isotope [30, 34]. The lifetimes in this case can be calculated from the following equation:

$$3\left(\frac{\Delta_{O^{17}}}{p_{O^{17}}}\right) = \frac{\tau\delta_e^2}{(1+x)^2+\tau^2(\delta_e^2+\omega_1^2)} + \frac{9\tau\delta_e^2}{(1+x)^2+\tau^2(9\delta_e^2+\omega_1^2)} + \frac{25\tau\delta_e^2}{(1+x)^2+\tau^2(25\delta_e^2+\omega_1^2)} \tag{1.23}$$

[†]Errors introduced by simplification of Equation (1.17) do not amount to more than 1%.

where p is the atom fraction of $^{17}_{8}O$ sites and

$$x = \frac{\left[{}^{17}_{8}O\right]}{\left[{}^{16}_{8}O\right] + \left[{}^{18}_{8}O\right]}$$

. δ_e is related to the coupling constant between $^{17}_{8}O$ and H($J_{^{17}_{8}O-H}$) by

$$\delta_e = J_{^{17}_{8}O-H}\left(\frac{T^1_{^{17}_{8}O}}{T^1_{^{17}_{8}O} + \tau}\right) \qquad (1.24)$$

where $T^1_{^{17}_{8}O}$ is the longitudinal relaxation time of the $^{17}_{8}O$ nucleus.

The rate of breaking of O-H bonds can now be calculated by a similar equation to (1.22):

$$\frac{v_{O-H}}{[H_2O]} = \frac{2}{\tau_{OH}} \qquad (1.25)$$

If a term of a given kinetic order can now be identified in both the v_{NH} and v_{OH} rate data, then it may be assumed that both of these terms refer to the same process. If we write this process as:

$$A + nS \longrightarrow P \qquad (1.26)$$

then the rate of reaction will be given by

$$-\frac{d[A]}{dt} = -\frac{1}{n}\cdot\frac{d[S]}{dt} \qquad (1.27)$$

If the symbol A represents a species in which an NH bond is broken and the symbol S represents a species in which an OH bond is broken then $-\frac{d[A]}{dt}$ will be determined from the v_{NH} data and $-\frac{d[S]}{dt}$ will be determined from

the ν_{OH} data. The average number of solvent molecules taking part in the process, n, can then be determined from Equation (1.27).

Solutions With More Than One Non-Dominant Site

If a solution contains more than one type of non-dominant reactive site, exchange may occur between any of these sites and water sites. In this case each of the non-dominant sites will provide a contribution to Δ, and the resultant will be equal to the sum of the different contributions, provided that the concentration of each non-dominant site satisfies the requirements for the case of one dominant line. Thus if non-dominant NH sites are labelled 1, 2, ... j, then†

$$\Delta_{NH,\ TOTAL} = \Delta_{NH,1} + \Delta_{NH,2} + \ldots\ldots \Delta_{NH,j} \qquad (1.28)$$

Equation (1.28) applies whether the non-dominant sites are in different molecules or in the same molecule. The same situation exists if both N-H and ^{17}O-H non-dominant sites are present:

$$\Delta_{TOTAL} = \Delta_{NH} + \Delta_{^{17}_{8}OH} \qquad (1.29)$$

Proton Transfer Mechanisms Which Have Been Detected by Nuclear Magnetic Resonance

Examples of the use of nuclear magnetic resonance to investigate rates and mechanisms of reactions in solution are numerous [25, 35]. Few of these applications involve species with two different acid-base

---

†This equation will not be valid if there is a fast direct reaction between the NH sites themselves.

reactive sites [25, 36]. Applications to aqueous solutions of amines with one type of acid–base reactive site, however, have been very common, and since the present work concerns aqueous solutions of amines, the following review will be mainly restricted to these examples.

Reactions Involving One Molecule of Amine

Two different exchange mechanisms involving acid dissociation have been proposed, and one of these proposed mechanisms has been found to occur in most cases of aqueous solutions of amines which have been investigated. This mechanism was first proposed by Swain and co-workers [37] for proton exchange owing to acid dissociation of triethylammonium ion in methanol and first shown to apply to an aqueous amine solution by Grunwald [38].

$$B\underline{H}.^{+}OH_2 \underset{k_{-a}}{\overset{k_a}{\rightleftharpoons}} B.\underline{H}OH + H_3O^{+} \qquad (1.30)$$

$$B.\underline{H}OH + HOH \xrightarrow{k_H} B.HOH + \underline{H}OH \qquad (1.31)$$

$$B.HOH + H_3O^{+} \xrightarrow{k_{-a}} BH.^{+}OH_2 \qquad (1.32)$$

The rate law corresponding to this mechanism is

$$\frac{v}{[BH^{+}]} = \frac{k_a k_H}{k_H + k_{-a}[H^{+}]} \qquad (1.33)$$

or

$$\frac{v}{[BH^{+}]} = \frac{k_a}{1 + Q[H^{+}]} \qquad (1.34)$$

where

$$Q = k_{-a}/k_H \qquad (1.35)$$

In strong acid, $k_{-a}[H^+] \gg k_H$ so that this rate law reduces to

$$\frac{v}{[BH^+]} = \frac{K_A k_H}{[H^+]} \qquad (1.36)$$

where K_A is the usual ionization constant. This rate is repressed as $[H^+]$ increases. When $[H^+]$ becomes very small, then $k_H \gg k_{-a}[H^+]$ and the rate law reduces to

$$\frac{v}{[BH^+]} = k_a \qquad (1.37)$$

which shows a constant first order rate with constant k_a.

The rate constant k_H has been interpreted as measuring the rate of diffusion of the marked water molecule into bulk solvent [39] and it has been shown to be inversely proportional to the viscosity of the solution over a wide viscosity range [39, 40]. The variation of k_H upon substituting non-polar groups into the amine, has been shown to be consistent with the view that this variation in k_H results from changes in the magnitude of the London dispersion forces between amine and the hydrogen bonded water molecule [39, 41]. For substituents with an ionic charge, it has been possible to detect two parallel processes of proton exchange with two different k_H values [35].

The second mechanism proposed for acid dissociation consists of direct transfer of the marked proton to a water molecule:

$$BH^+ + H_2O \longrightarrow B + H_3O^+ \qquad (1.38)$$

The rate law in this case is:

$$\frac{v}{[BH^+]} = k_a \qquad (1.39)$$

Rosenthal and Grunwald have suggested [42] that Cociwera's results for methyl substituted pyridinium salts [43] may be consistent with this mechanism.

Proton Exchange via an Ionized Intermediate

In the case of imidazole [44] The Swain-Grunwald type of mechanism was found to be insufficient to explain the data and an extra process of proton exchange had to be included. This process did not show a strong repression in strong acid and it was proposed that it occurred via an ionized intermediate:

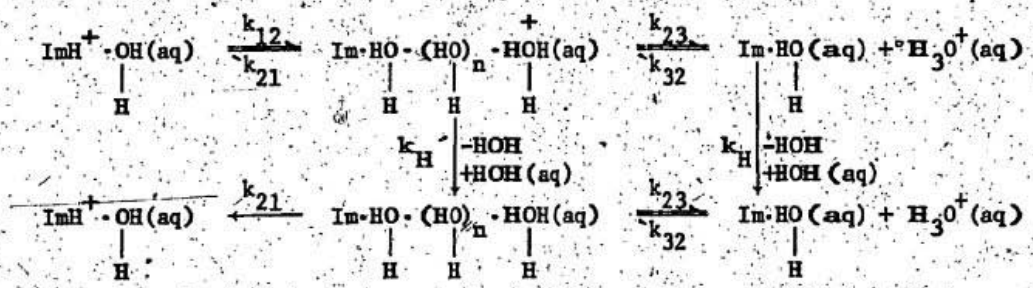

(1.40)

The rate law derived from this mechanism [44] is:

$$\frac{v}{[ImH^+]} = k_{CYCLIC} + \frac{k_a}{1 + Q\,[H^+]} \qquad (1.41)$$

where $k_{CYCLIC} = \frac{k'_H\, k_{12}}{k_{21}}$; $k_a = \frac{k_{23}\, k_{12}}{k_{21}}$; and $Q = \frac{k_{32}}{k_H}$.

Thus the proton exchange occurring in the ionized intermediate (the k'_H process) is given by the rate constant k_{CYCLIC} and in strong acid

this rate will be repressed only by a salt effect. The proton exchange following acid dissociation, however, follows a Grunwald–Swain type rate law and will show a large rate repression with increasing $[H^+]$.

Reactions Involving Two Molecules of Amine

Previous workers have detected two types of mechanism which give rise to rate laws which are second order in amine [30]. The first type of mechanism is a bimolecular process in which the proton is transferred directly from one amine molecule to another [45–49]. The second type of process is termolecular or higher with the third (and any subsequent) molecule consisting of a water molecule which acts as a bridge for transferring the proton from one amine molecule to another amine molecule [39, 42, 44, 50–56].

$$BH^+ \cdots \begin{pmatrix} O\text{–}H \\ | \\ H \end{pmatrix}_n \cdots B \longrightarrow B \cdots \begin{pmatrix} H\text{–}O \\ | \\ H \end{pmatrix}_n \cdots {}^+HB \qquad (1.42)$$

This reaction may occur by a concerted or stepwise mechanism.

Since the present work is exclusively concerned with measurements of the water line, the first type of mechanism will not be detected here. All measurements of rate constants which are second order in amine will, therefore, apply to mechanisms similar to that shown in Equation (1.42).

In cases where the mean number of water molecules has been determined [34, 42, 44, 55, 56] it has been found that $1 \leq n \leq 2$. The higher values of n have been interpreted to indicate stronger hydrogen bonding between amine and water molecules [43, 55]. This deduction follows since the quadrimolecular encounter complex is expected to lose a water molecule (and thus be converted to the termolecular encounter complex) most easily

when the hydrogen bonding is weak:

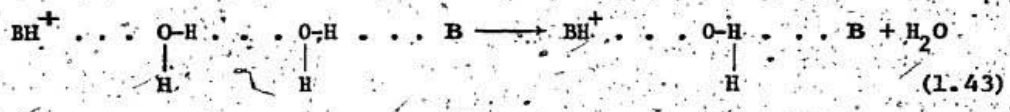

(1.43)

Thus higher values of n would indicate stronger hydrogen bonding which will be expected to lead to higher values for k_2 (since the proton can transfer most readily via a more ordered water chain resulting from stronger hydrogen bonding) and to smaller values for k_H. This argument, of course, depends on the hydrogen bonding being correctly oriented for the proton transfer.

CHAPTER 2

EXPERIMENTAL

Materials

Sodium hydroxide was supplied by Anachemia chemicals and was used to prepare two stock solutions of approximately 1M. and 0.15 M. These solutions were standardized against a primary standard of potassium hydrogen phthalate supplied by the U. S. Department of Commerce National Bureau of Standards. A weight burette and a 2.5 ml. Gilmont micrometer burette were used in a potentiometric titration with the end point determined by the greatest rate of change of pH. The pH meter and electrode are described later. Hydrochloric acid from the McArthur Chemical Co. Limited was used to prepare three stock solutions of approximate molarities 5, 1 and 0.15. These solutions were standardized against the sodium hydroxide solutions by the same technique as above.

All water was doubly distilled. A Corning continuous still was used for the first distillation and an all glass still was used for the second. Potassium hydroxide was added to the water before the second distillation in order to remove dissolved carbon dioxide. A soda lime tube excluded atmospheric carbon dioxide. For experiments in 95% D_2O, D_2O was supplied by Stohler Isotope Chemicals and was redistilled from potassium hydroxide as above. Water enriched with $^{17}_{8}O$ was obtained from Miles Laboratories and small amounts were redistilled on a vacuum line.

N, N - dimethylpiperazine was supplied as the free amine by the Aldrich Chemical Co. and was converted to the dihydrochloride by bubbling

hydrogen chloride gas (Matheson) through an ethanolic solution. Piperazine was obtained as the dihydrochloride from K and K Laboratories and histamine dihydrochloride came from the Nutritional Biochemicals Corporation. All of the dihydrochlorides were purified by two recrystallizations from 95% ethanol and purity was checked by potentiometric titrations and by slow sweep n.m.r. spectra. Solutions were prepared as required from the purified dihydrochlorides.

Instrumentation

All pH measuremehts were made using the Beckman research pH meter with a Beckman 39030 combination electrode. Measurements were made at 25.00 ± 0.01 °C and a Beckman phthalate buffer at pH 4.01 was used for standardisation.

The spectrometer was the Varian HA 100 spectrometer system operating at 100 MHz. For the adiabatic half passage experiments, frequency modulation at about 4000 Hz was provided by a Wavetek Audio Oscillator. Frequency modulation was preferred to field modulation so that the higher frequencies attainable ensured that the side bands were outside the adiabatic sweep width.

Temperature control of the n.m.r. sample was achieved by passing a regulated flow of cooled compressed air through a heater and then through the probe of the spectrometer. A copper-constantan control thermocouple was placed in the air flow between the heater and the probe, and the reference junction maintained at 0°C. by an ice-water slush bath. The output of this thermocouple was balanced against a standard cell by means of a Leeds and Northrup type K5 potentiometer. A Leeds and Northrup null

detector was used to monitor the balance of the potentiometer circuit and to apply necessary corrections to the heater voltage by means of a servo-motor driven Variac. Although the control thermocouple measured the temperature of the air flow immediately before the flow surrounded the sample, it was generally found that the temperature of the sample was slightly different from the temperature of the thermocouple (the difference depending on the operating temperature). The sample was therefore replaced by a probe thermocouple in an n.m.r. tube and the required setting of the potentiometer circuit for the control thermocouple was determined when the probe thermocouple was at the desired operating temperature. The probe thermocouple was then replaced by the sample to be measured. Temperatures adjusted in this manner were accurate to within ± 0.05°C.

For operating temperatures of 20° C. and above, the flowing air was pre-cooled by passing it through a copper coil immersed in an ice bath. For lower operating temperatures it was necessary to cool the coil in solid carbon dioxide or liquid nitrogen. For temperatures near 0°C and below, it was necessary to replace the air by nitrogen gas, since moisture contained in the air leads to the formation of ice in the probe.

Measurement of the RF Field

As indicated in the introduction, the magnitude of the RF field is required when calculating rates of reaction. Two methods were used in the present work. The first method was a long procedure, but it was preferred since it made use of the adiabatic half passage technique, as did the rate measurements. Hence some cancellation of errors might arise when the RF field is measured in this way. Accordingly, the second more rapid method was used for daily monitoring of the RF field with a measure-

ment being made by the first method whenever any irregularity was suspected.

First Method

This procedure used the adiabatic half passage technique to measure $1/T_{1p}$ for a solution of 2, 2', 2" nitriloethanol hydrochloride at various RF fields. This compound was chosen since a reliable value for the chemical shift was available and since 0.17M. solutions were known to show an extensive plateau in the lifetime broadening region of the (Δ/p) versus pH curve.† A fresh solution of 0.17M. triethanolamine hydrochloride at pH ≈ 2 was prepared for each RF determination. Then, recalling Equation (1.19)

$$\frac{\Delta_{NH}}{p} = \frac{\delta^2\tau}{1 + (\delta^2 + \omega_1^2)\,\tau^2} \qquad (1.19)$$

we see that

$$\frac{1}{(\Delta/p)} = \frac{1 + \delta^2\tau^2}{\delta^2\tau} + \frac{\tau\omega_1^2}{\delta^2}$$

If we substitute

$$\omega_1 = F.f \qquad (2.1)$$

where F is the full power of the RF field and f is the fraction to which it is attenuated for a given measurement, then

---

†The information concerning this compound was provided by Dr. E. K. Ralph, unpublished results. As explained previously, $1/T_{1p}$ shows the greatest RF dependence in the lifetime broadening region.

$$\frac{1}{(\Delta/p)} = \frac{1 + \delta^2\tau^2}{\delta^2\tau} + \frac{\tau F^2 f^2}{\delta^2} \qquad (2.2)$$

Thus by plotting values of $1/(\Delta/p)$ against f^2, a straight line graph of slope $\left(\frac{\tau F^2}{\delta^2}\right)$ and intercept $\frac{(1 + \delta^2\tau^2)}{\delta^2\tau}$ can be obtained.

Since the pH of the solution was adjusted to be clearly in the lifetime broadening region however, $\delta\tau >> 1$ so that the intercept is equal to τ. Using this value for τ and the value for δ provided by Dr. E. K. Ralph (3512 rads. sec^{-1} at 100 M.Hz.), the slope of the graph can be used to determine F in radians. sec^{-1}. The standard deviation for different determinations of the RF field by this method was about 10%.

Second Method

This approach used the method of transient nutations as introduced by Torrey [57]. A sample was placed in the probe and the spectrometer was adjusted for resonance. A strong RF field, H_1, was then suddenly applied and the resultant behaviour of the magnetization was recorded on a chart recorder (Texas Instruments Oscillo-riter) while the RF field remained on. Under these conditions, the magnetization precesses about the effective magnetic field in the rotating frame with a precession frequency γH_1 and it decays with a nutation relaxation time, T_n, given by [31].

$$\frac{1}{T_n} = \frac{1}{2}\left(\frac{1}{T_1} + \frac{1}{T_2}\right) \qquad (2.3)$$

A sample of dilute hydrochloric acid was used because $1/T_2$ is smaller than for exchanging solutions and hence the largest possible number of

measurable oscillations could be obtained. γH_1 could then be simply determined by measuring the frequency of the oscillations. Values obtained for the RF field by this method were consistently about 20% lower than values obtained by the first method. For reasons given previously, values obtained by the first method were used in the calculation of rates.

Measurement of $T_{1\rho}$

The use of an adiabatic half passage to measure $T_{1\rho}$ was first described by Solomon [58]. The method has been used by Meiboom [32] to study proton transfer reactions in water, and by Sykes [59] to study biological exchange rates. It was shown by Bloch [60] that the nuclear magnetization can be flipped through 180° by an adiabatic fast passage through the resonance. In Solomon's method, the fast passage is stopped when the centre of the resonance line is reached. The magnetization will therefore be flipped through only 90° and it will be parallel to the RF field after the passage. The magnitude of the magnetization will decay with a characteristic time constant $T_{1\rho}$. Since the magnetization is orientated along H_1 during this decay, the time constant will be related to T_2, but since the RF field remains on throughout the experiment, $T_{1\rho}$ will differ from T_2 as explained in the introduction.

In order to obtain an adiabatic passage, it is necessary to attain a sweep rate which lies between minimum and maximum limits. The maximum rate of the sweep is set by the requirement that the magnetization vector of the sample can remain aligned with the effective magnetic field in the rotating frame of reference. The minimum rate of the sweep is set by the

requirement that there should be no significant relaxation during the sweep.

These conditions are met when

$$\frac{1}{T_2} < \frac{1}{H_1}\left(\frac{d(\Delta f)}{dt}\right) < \frac{\gamma}{H_1^2}\left[(\Delta f)^2 + H_1^2\right]^{3/2} \qquad (2.4)$$

where Δf is the amount the spectrometer is pulsed off resonance. In the present work an exponential sweep was used and the above inequality can then be written as [61]

$$\frac{1}{T_2} < \frac{1}{H_1}\left(\frac{\Delta f}{c}\right) < \frac{\gamma}{H_1^2}\left[(\Delta f)^2 + H_1^2\right]^{3/2} \qquad (2.5)$$

Where c is the time constant characterizing the passage into resonance.

A fast sweep fulfilling these conditions was obtained by the following procedure. Using the linear sweep the proton resonance was centered on the scope to indicate a condition of resonance when the sweep was stopped. The phase was adjusted to the dispersion mode and the modulation coils were then connected to a three volt D.C. power supply via a variable resistor. The resistor was adjusted to attain a position just outside resonance as indicated by the baseline on the scope. The D.C. current was then switched off with the required sweep rate back into the resonance being obtained by the appropriate setting of a variable capacitor shunted across the sweep coils. For the experiment to be acceptable, the exponential decay had to return to the baseline as indicated by the scope, since only then did the adiabatic passage end at the resonance position.

Over the course of this work, two different methods were used to record the decays and calculate values of T_{1p}. The first method consisted of recording the decay on a Texas Instruments 'Oscillo-riter' chart recorder and calculating values of T_{1p} using the keyboard input of a Wang 720B programmable calculator. In the second method, the voltage output from the spectrometer receiver was stored in a Biomation model 610 transient recorder. If the decay was acceptable it was then transferred via a voltage-frequency converter to a Grundig TK.600 tape recorder. In the initial use of this method the decay constant was obtained by playback of the tape recorder directly into a P.D.P 12 computer. For later work a Hewlett Packard frequency counter was used to provide a digital output and this was read into a Wang 720B calculator via a Wang interface unit. The biomation unit truncates the data for storage in a memory of 110 six bit words. The relaxation signal is therefore represented by a histogram with a resolution of 1/64th of full scale. To improve the accuracy of the calculations the data was smoothed by summing the contents of groups of registers. Thus the first point of the smoothed curve was taken to be the sum of the contents of the first ten registers. The second point was the sum of the contents of registers two to eleven and so on. Since there were many points over a period of just two to three half lives, the trapezoidal rule applies and the procedure is essentially a manual integration of the curve which regenerates the original exponential curve with a downward displacement of half a bit. To avoid introducing errors due to truncation of the baseline level, the smoothed data was divided into two equal parts and T_{1p} determined by a Guggenheim calculation.

When using either method of calculation, between 5 and 10 decays were calculated for each solution, with the standard deviation being typically one to two percent. The scatter of results from different solutions run at different times was not more than 3% for low RF measurements. When measurements were made using a high RF field, the scatter was about 10%. The higher uncertainty in this case was caused by greater experimental difficulty, resulting from various factors. For instance, when operating at high RF fields there is a high leakage from the transmitter to the receiver and hence the possibility of receiver overload arises. A second factor was that the stability of the RF amplifier and of the RF attenuator resistors seemed to be poorer at higher RF fields. Furthermore, values of $1/T_{1p}$ are much more sensitive to instability of the RF field when high RF fields are used (see Equation 1.17 and subsequent discussion).

Determination of Ionization Constants

All of the amine salts used in the present work were in the form of the dihydrochloride. The cation of such a salt can undergo two successive ionization steps which can be generally represented by:

$$BH_2^{2+} \rightleftharpoons BH^+ + H^+ \tag{2.6}$$

$$K_{A1} = \frac{[BH^+][H^+]}{[BH_2^{2+}]} \tag{2.7}$$

$$BH^+ \rightleftharpoons B + H^+ \tag{2.8}$$

$$K_{A2} = \frac{[B][H^+]}{[BH^+]} \tag{2.9}$$

In the present work the pH was generally in the range where the first dissociation given by Equation (2.6) was of prime importance. Accordingly the ionization constant given in Equation (2.7) was measured as a function of $[BH_2^{2+}]$ for each of the salts.

The measurements were made as first given by Bacarella et al., [62]. In this method the pH of a solution of known $[BH_2^{2+}]$ is measured first in the presence of a known slight excess of sodium hydroxide and secondly in the presence of a known slight excess of hydrochloric acid. The first pH will depend on the ionization constant in Equation (2.7) but the second pH will depend essentially on the excess of hydrochloric acid since the ionization of $[BH_2^{2+}]$ will be repressed. If a quantity ϵ is defined by

$$\epsilon = \frac{[BH_2^{2+}] + [HCl] - [NaOH]}{[BH_2^{2+}]} \qquad (2.10)$$

then Equation (2.7) can be written as:

$$K_{A1} = \frac{[H^+]([H^+] - (\epsilon - 1)c)}{(\epsilon . c - [H^+])} \qquad (2.11)$$

where

$$c = [BH^{2+}] + [BH^+]$$

upon solving Equation (2.11) for $[H^+]$ and comparing the $[H^+]_1$ from the first measured pH_1 with $[H^+]_2$ from the second measured pH_2 we find

$$\frac{[H^+]_1}{[H^+]_2} = \frac{Z_1}{Z_2} \qquad (2.12)$$

Where Z_1 and Z_2 are the values of Z determined at pH_1 and pH_2

$$-z = (\varepsilon-1)c - K_{A1} + \left\{(\varepsilon-1)^2c^2 + 2K_{A1}.c(1+\varepsilon) + K_{A1}^2\right\} \qquad (2.13)$$

Since $\frac{z_1}{z_2}$ is a function of K_{A1}, the latter can be evaluated.

In the experimental method used here, a solution of the required amine concentration was prepared in a 50 ml. volumetric flask with $\varepsilon \simeq 0.97$. This solution was transferred to a glass cell which was placed in a thermostat bath at 25.00 + 0.01 °C. A 0.25 ml micrometer burette (Gilmont) containing hydrochloric acid was clamped with its tip just below the surface of the liquid. The pH meter, a magnetic stirrer, and a flow of nitrogen gas over the solution were also set up. When the pH was stable (about 30 minutes) a series of small additions of hydrochloric acid were made. A stable pH was measured after each addition with the solution being stirred continuously. The final five or six points were taken in an acid solution and a linear least squares fit of these points was used to determine the pH in acidic solution. Each of the data points with $\varepsilon < 1$ was now compared with this acid point and a series of values for pK_{A1} was calculated from Equations (2.12) and (2.13) using a Wang 720B programmable calculator. Table 2.1 shows typical results obtained for a 95% deuterated solution of histamine, with histamine concentration of 0.05954 M.

For each of the amines, values of pK_{A1} were plotted against $[BH_2^{2+}]$ or ionic strength. In the case of histamine, the thermodynamic value of the ionization constant (K_{A1}°) was required. This value was obtained by fitting data at low ionic strengths to a Debye-Hückel Law of the form

TABLE 2.1

DETERMINATION OF pK_{A1} FOR A 0.05954 M. SOLUTION OF HISTAMINE WHICH WAS 95% DEUTERATED

	mls. of LCl†	pL^{+}†	ε	pK_{A1}
Acid Point	0.1900	3.3820	1.00125	
	0.0100	4.7510	0.96387	6.5653
	0.0150	4.7382	0.96491	6.5657
	0.0200	4.7237	0.96595	6.5640
	0.0250	4.7088	0.96699	6.5623
	0.0300	4.6976	0.96803	6.5670
	0.0350	4.6850	0.96906	6.5703
	0.0400	4.6698	0.97010	6.5702
	0.0450	4.6526	0.97114	6.5678
	0.0500	4.6348	0.97218	6.5652
	0.0550	4.6172	0.97322	6.5639
	0.0600	4.6001	0.97425	6.5644
	0.0650	4.5846	0.97529	6.5685
	0.0700	4.5655	0.97633	6.5681
	0.0750	4.5438	0.97737	6.5648
	0.0800	4.5208	0.97841	6.5608
	0.0850	4.5000	0.97945	6.5618
	0.0900	4.4790	0.98048	6.5641
	0.0950	4.4560	0.98152	6.5651
	0.1000	4.4286	0.98256	6.5611
	0.1050	4.4010	0.98360	6.5589
	0.1100	4.3710	0.98464	6.5555
	0.1150	4.3420	0.98567	6.5565
	0.1200	4.3126	0.98671	6.5601
	0.1250	4.2786	0.98775	6.5600
	0.1300	4.2409	0.98879	6.5581

Hence $pK_{A1} = 6.5636 \pm 0.0040$

†Where $[L^{+}] = [H^{+}] + [D^{+}]$

$$pK_{Al} = pK^{\circ}_{Al} + \frac{1.018\sqrt{\mu}}{1 + A\sqrt{\mu}} \qquad (2.14)$$

and extrapolating to infinite dilution. In Equation (2.14), μ is the ionic strength and A is a constant determined in the curve fitting procedure.

Procedure for the Adiabatic Half Passage Experiments

The solutions

The main data series were obtained at 25°C by making measurements on a series of solutions of constant amine concentration at various pH. A given data series was generally obtained from two separate experiments as follows.

(1) For pH ≥ 2

Two stock solutions were prepared with the same amine concentration but one had a pH of about 6 and the other had a pH of about 1. The solution at pH 6 was used to fill an n.m.r. tube with a small reservoir on top. After standing overnight this tube was mounted in a thermostat bath with the electrode of the pH meter placed in the reservoir part of the tube. Stirring was accomplished by a polyethylene rod which was moved up and down the tube. The pH of this solution could then be adjusted by adding small volumes of the second stock solution of pH ≈ 1. Measurements of $1/T_{1w}$ were generally made at increments of approximately 0.2 units on the pH scale. Calibration of the pH readings was achieved by preparing a third solution with an accurately calculated pH of about 2.5 ($-\log [H^+]$). Standardization of the pH meter was checked with buffer before and after each pH measurement.

(ii) For pH ≤ 2

Individual solutions of the required amine concentration were prepared at pH intervals of about 0.2 units. pH values were calculated stoichiometrically using the p_cH ($-\log [H^+]$) scale. Separate n.m.r. tubes were filled with these solutions and allowed to stand overnight. The following day they were refilled with the same solutions and measurements of $1/T_{1p}$ were made.

Measurement of rates

Adiabatic half passage measurements to determine $1/T_{1p}$ were made at each pH as explained previously. To determine Δ from Equation (1.15) it was also necessary to determine $\left(\frac{1}{T_1}\right)$ or $(1/T_{1p}^{\circ})$. For solutions of low amine concentration, the value of $(1/T_{1p}^{\circ})$ was determined by using an adiabatic half passage to determine $(1/T_{1p})$ for a hydrochloric acid solution of the same pH. For solutions of higher amine concentration, the longitudinal relaxation time of the actual solution was obtained by measuring the time constant for the recovery of the saturated absorption signal.

The value of $\left(\frac{\Delta_{NH}}{p}\right)$† could then be calculated and used to obtain a preliminary estimate of τ using Equation (1.19). This estimate for τ was then used to calculate J_e from Equation (1.18) and an accurate value of τ was then calculated from Equation (1.17). Rates were then obtained

†Since all water contains a small amount of $^{17}_{8}O$, it follows that the measured Δ will contain a contribution due to proton exchange between water molecules. This contribution is only significant above pH ~ 5, but for such cases it must be subtracted from the measured value of Δ before calculating (Δ_{NH}/p).

as explained in the introduction and used to determine the rate law as shown in the results sections. Rate measurements for 95% deuterated solutions will contain a small contribution from the 5% of the $^{1}_{1}H$ isotope. The present work follows the practice of Rosenthal and Grunwald [42] in neglecting this contribution.

Determination of (Δ_{NH}/p) for Histamine

In the case of histamine, two contributions to Δ_{NH} were present. One contribution arises from the exchange of amino protons and the other arises from the exchange of protons from the imidazole ring. Since there are three amine protons which can exchange whereas there are only two imidazole protons which can exchange, it follows that the proton fraction will differ in the two cases:

For amino protons,
$$p = \frac{3[BH_2^{2+}]}{2[H_2O] + [HCl] + 5[BH_2^{2+}]} \qquad (2.15)$$

For imidazole protons,
$$p = \frac{2[BH_2^{2+}]}{2[H_2O] + [HCl] + 5[BH_2^{2+}]} \qquad (2.16)$$

In the initial stages of the histamine data analysis, therefore, it was not possible to calculate values for (Δ_{NH}/p). Accordingly, values of (Δ_{NH}/c) were tabulated where c represents the histamine molarity. As the separation of the two components proceeded, the (Δ_{NH}/c) contributions from each broadening could be converted to (Δ_{NH}/p) values and hence to rates.

To facilitate the repeated calculations above pH ~ 2, a regression analysis was used to fit the (Δ_{NH}/c) data to a curve of the form

$(\Delta_{NH}/c) = c_0 + c_1X + c_2X^2 + \ldots$ where X represents the pH and the c values were the fitting constants. The fitting was done in small segments and generally it was not necessary to use equations higher than third order. Data points could be selected at intervals of 0.2 of a pH unit and this greatly simplified calculations on the Wang 720B. The final rate laws were compared with the original data points.

The Experiments Using a Constant Buffer Ratio

For these experiments, a stock solution of high histamine concentration was prepared at the required buffer ratio. Small amounts of this solution were then added to an n.m.r tube which had originally contained only water. Measures of Δ were then made as described previously. Since these experiments were carried out at relatively high pH, the broadening due to exchange of imidazole protons was small and could, therefore, be calculated from the previously determined rate law and subtracted from the measured Δ. Contributions to Δ from the $^{17}_{8}O$ exchange were also subtracted and the remaining portions of Δ were used to calculate amino proton rates of exchange. The amino proton rate law could then be determined as shown in the results.

Experiments Using Solutions Enriched in $^{17}_{8}O$

These experiments were performed by the constant buffer ratio procedure, using solutions with about 1% $^{17}_{8}O$. To obtain the contribution to Δ from the $^{17}_{8}O$ exchange, it was necessary to subtract the contributions to Δ which were caused by imidazole proton exchange and by amino proton exchange. Since the rate laws were complex, this removal of NH exchange was done by an experimental procedure. To do this, each measurement was

repeated with natural abundance of $^{17}_{8}O$. Both Δ_{O17} and p_{O17} were then determined as the difference between corresponding enriched and natural abundance solutions. The mean lifetime of the $^{17}_{8}O$–H bond could then be determined from Equation (1.23) where

$$T^1_{O17} = 6.5 \times 10^{-3} \text{ secs. and } J_{^{17}O-H} = 613 \text{ rads. sec.}^{-1}$$

The total rate of breaking of the $^{17}_{8}O$–H bond $(1/\tau)_{TOTAL}$ will be determined by the rates at which three different types of reaction are occurring

(i) Exchange between water molecules and H_3O^+

$$^{17}_{8}OH_3^+ + H_2O \longrightarrow {}^{17}_{8}OH_2 + H_3O^+ \qquad (2.17)$$

(ii) Exchange between water molecules and OH^-

$$^{17}_{8}OH_2 + OH^- \longrightarrow {}^{17}_{8}OH^- + H_2O \qquad (2.18)$$

(iii) Exchange between water molecules and amine species. One possible reaction falling into this category is:

$$HBH^{2+} + \left(\begin{matrix}O-H\\|\\H\end{matrix}\right)_n + BH^+ \longrightarrow BH^+ + \left(\begin{matrix}H-O\\|\\H\end{matrix}\right)_n + HBH^{2+} \qquad (2.19)$$

The contribution to the rate of breaking of the $^{17}_{8}O$–H bond by reaction (2.17) is

$$\left(\frac{1}{\tau}\right)_{H^+} = \frac{v}{3[H_2O]} = \frac{k_{H^+}}{3}[H_3O^+] \qquad (2.20)$$

similarly the contribution from reaction (2.18) is

$$\left(\frac{1}{\tau}\right)_{OH^-} = \frac{v}{2[H_2O]} = \frac{k_{OH^-}}{2}[OH^-] = \frac{k_{OH^-}.K_W}{2[H^+]} \qquad (2.21)$$

hence the rate of breaking the $^{17}_{8}O$-H bond due to reactions such as (2.19) can be calculated from

$$\left(\frac{1}{\tau}\right)_{Nett} = \left(\frac{1}{\tau}\right)_{Total} - \left(\frac{1}{\tau}\right)_{H^+} - \left(\frac{1}{\tau}\right)_{OH^-} \qquad (2.22)$$

where $\left(\frac{1}{\tau}\right)_{H^+}$ is calculated from Equation (2.20) using $k_{H^+} = 8.1 \times 10^9$ sec.$^{-1}$ [42] and $\left(\frac{1}{\tau}\right)_{OH^-}$ is calculated from Equation (2.21) using

$k_{OH^-} = 3.8 \times 10^9$ sec.$^{-1}$ [42] and $pK_w = 14.00 - \frac{1.018\sqrt{\mu}}{1+\sqrt{\mu}}$

where μ is the ionic strength.

Rate laws for reactions involving amine species can now be determined from values of $\left(\frac{1}{\tau}\right)_{Nett}$. For example, reaction (2.19) would follow the rate law

$$2\left(\frac{1}{\tau}\right)_{Nett} = \frac{v}{[H_2O]} = \frac{nk[BH_2^{2+}][BH^+]}{[H_2O]}$$

or $$\left(\frac{111}{\tau}\right)_{Nett} = nk\left[BH_2^{2+}\right]\left[BH^+\right] \qquad (2.19)$$

since $[H_2O] \simeq 55.5$ M. in dilute solutions.

Dependence of Chemical Shifts on Acidity

It is well known that the proton resonance for water moves

downfield as $[H^+]$ increases [63, 64]. Hood et al., have tabulated this movement for various concentrations of hydrochloric acid [64]. When this data is plotted, the shift of the water line is seen to vary linearly with the molarity of the hydrochloric acid. A linear least squares fit of the data has, therefore, been made and shows that the downfield shift = 192 ± 4 rads. $sec.^{-1}$ at 100 MHz for each unit increment in the acid molarity. The intercept was zero within the limits of the standard deviation.

Since the chemical shifts of the amino protons with respect to the water line are used in the present rate calculations, it follows that they should be adjusted to allow for the water line shift. This has been done throughout the present work by assuming that any movement of the amino resonances with increasing $[H^+]$ was negligible. Changes of the chemical shifts were, therefore, assumed to be given by the downfield shift of the water line as given above.

CHAPTER 3

N,N'-DIMETHYLPIPERAZINE

Determination of the Ionization Constant

Values of pK_{A1} (defined by equations 2.6 and 2.7) were determined as described previously and listed in Table 3.1. Figure 3.1 shows a plot of this data and it can be seen that above 0.037M, the value of $pK_{A1} = 4.136 \pm 0.001$. Since the present experiments used solutions which were 0.04M and 0.07M in N,N'-dimethylpiperazine, it follows that this value will be used throughout the present work.

Rate Measurements

Measurable broadenings of the dominant water line occurred in solutions which were 0.6M → 8.0M in [HCl] with amine concentrations of 0.04M and 0.07M. Measurements made for 0.0404M solutions are listed in Table 3.2 and measurements for 0.0707M solutions are listed in Table 3.3. The RF field was 330 rads. $sec.^{-1}$ for both series of data. Since amine concentrations were low, estimates of line widths in the absence of exchange were made by measuring $(1/T_{1p})$ values for various concentrations of hydrochloric acid. For solutions less than 4.0M in hydrochloric acid it was found that $(1/T_{1p}) = 0.345 + 0.0067x + 0.0023x^2$ where x = molarity of acid. For higher acid concentrations $(1/T_{1p}) = 0.409 + 0.0243\,(x - 4)$.

For this compound some highly acidic solutions were studied and it was therefore necessary to correct for salt effects. Since a

TABLE 3.1

VALUES OF $pK_{A1} = \frac{[BH^+][H^+]}{[BH_2^{2+}]}$ FOR SOLUTIONS OF N,N'-DIMETHYLPIPERAZINE

[N,N'-dimethylpiperazine]	μ	pK_{A1}
9.870×10^{-3}	2.951×10^{-2}	4.020 ± 0.006
1.456×10^{-2}	4.354×10^{-2}	4.039 ± 0.006
2.585×10^{-2}	7.743×10^{-2}	4.092 ± 0.007
3.715×10^{-2}	1.114×10^{-1}	4.137 ± 0.008
5.121×10^{-2}	1.533×10^{-1}	4.136 ± 0.007
6.827×10^{-2}	2.046×10^{-1}	4.135 ± 0.006

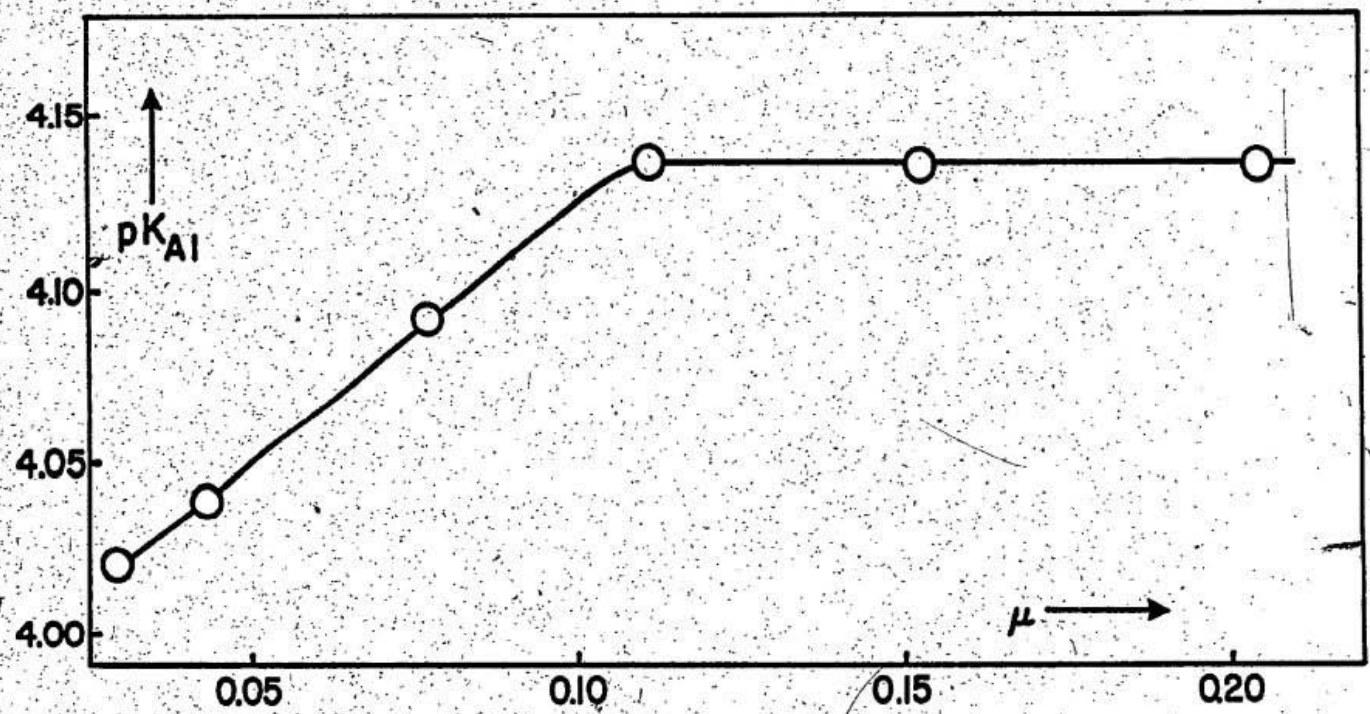

Figure 3.1 pK_{A1} for N,N'-dimethylpiperazine

TABLE 3.2[†]

RATE DATA FOR 0.0404M. SOLUTIONS OF N,N'-DIMETHYLPIPERAZINE

[HCl]	$(1/h_o)$	$(1/T_{1p})$	$10^{-3}(\Delta/p)$	$10^{-4}\left(\frac{\blacktriangledown}{[BH_2^{2+}]}\right)$
1.0002	0.633	0.442	0.118	15.98
1.4023	0.372	0.509	0.200	8.94
1.7708	0.251	0.537	0.230	7.39
2.2888	0.158	0.655	0.375	4.18
2.8602	0.100	0.810	0.560	2.51
3.4388	0.0631	1.005	0.796	1.51
3.9939	0.0398	1.218	1.047	0.889
4.9440	0.0182	1.291	1.098	0.386
5.6590	0.0100	1.117	0.840	0.223
6.1991	0.00664	0.870	0.509	0.1172
6.6303	0.00398	0.690	0.269	0.0592
7.0665	0.00257	0.729	0.303	0.0676
7.5390	0.00158	0.584	0.109	0.0238
7.9981	0.00100	0.623	0.118	0.0262

[†]In this and subsequent tables all of the recorded digits may not be significant.

TABLE 3.3

RATE DATA FOR 0.0707M. SOLUTIONS OF N,N'--DIMETHYLPIPERAZINE

[HCl]	$(1/h_o)$	$(1/T_{1p})$	$10^{-3}(\Delta/_p)$	$10^{-4}\left[\frac{v}{[BH_2^{2+}]}\right]$
1.0071	0.633	0.516	0.124	15.19
1.3445	0.403	0.581	0.169	10.67
1.7692	0.251	0.689	0.246	6.91
2.2978	0.158	0.873	0.377	4.15
2.8625	0.100	1.208	0.614	2.26
3.4414	0.0631	1.555	0.863	1.36
4.0004	0.0398	1.890	1.086	0.821
5.1015	0.0158	1.874	1.048	0.336
5.6581	0.0100	1.499	0.754	0.189
6.1920	0.00638	1.159	0.499	0.114
6.6381	0.00398	0.939	0.330	0.0734
6.9293	0.00296	0.788	0.222	0.0488

suitable H_+ function was not available, data for a Hammett-Deyrup H_o acidity function listed by Paul and Long [65] was tried. The H_o function was thought to be suitable in this instance since a plot of the reciprocal of the specific rate versus h_o (where $H_o = -\log h_o$) showed no systematic deviation from a straight line.

Rates were calculated from (Δ/p) values in the usual way using $J_{NH} = 345$ rads. sec.$^{-1}$, $T^1_{N^{14}} = 0.0025$ secs. and $\delta = 3250$ rads. sec.$^{-1}$. The chemical shift was determined from the maximum broadening and corrected for the concentration of hydrochloric acid as described earlier. Values for the other two constants were assumed to be the same as for trimethylamine [52]. Since the rates are insensitive to these values, these estimates were considered adequate. The value of γH_1 was 590 rads. sec.$^{-1}$.

The specific rates are plotted against $1/h_o$ in Figure 3.2 and no significant difference can be detected between the rates at the two concentrations. It was therefore concluded that the exchange is predominantly first order throughout the pH range. Reduction of the rate with increasing acidity is much greater than would be expected from salt effects alone and therefore proton exchange according to equations (3.1), (3.2) and (3.3) is presumed.

$$^{+}HB\underline{H}^{+}.OH_2 + H_2O \underset{k_{-a}}{\overset{k_a}{\rightleftharpoons}} {}^{+}HB.\underline{H}OH + H_3O^{+} \qquad (3.1)$$

$$^{+}HB.\underline{H}OH + HOH \xrightarrow{k_H} {}^{+}HB.HOH + \underline{H}OH \qquad (3.2)$$

$$^{+}HB.HOH + H_3O^{+} \xrightarrow{k_{-a}} {}^{+}HBH^{+}.OH_2 + H_2O \qquad (3.3)$$

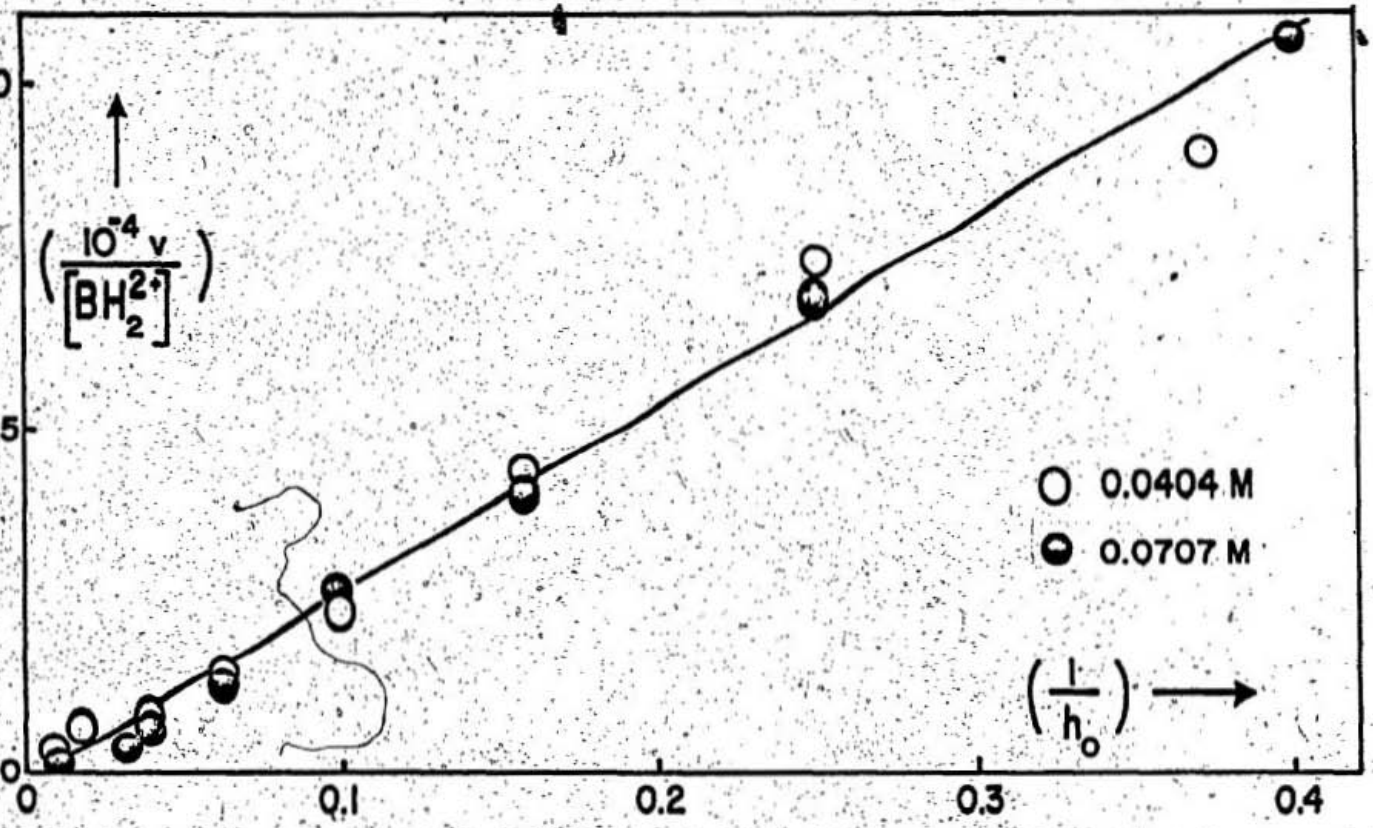

Figure 3.2 Rate data for N,N'-dimethylpiperazine at two concentrations.

The breaking of the B.H hydrogen bond in equation (3.2) may also occur by rotation of the marked water molecule. The rate of breaking of this bond will be given by

$$\frac{v}{[BH_2^{2+}]} = \frac{k_a k_H}{k_H + k_{-a} h_o} \qquad (3.4)$$

where $[H^+]$ has been replaced by the acidity function h_o. Figure 3.2 shows no measurable falling off of the specific rate at least up to $1/h_o = 0.4$ indicating that $k_{-a}.h_o >> k_H$ for [HCl] $\geq$ 1.4M. The gradient of this straight line then provides a value for $\frac{k_a k_H}{k_{-a}} = K_{Al}.k_H$.

A least squares fit of the 0.0404M data provides

$$K_{Al}.k_H = (2.458 \pm 0.052) \times 10^5 \text{ moles.}\ell^{-1}.\text{ sec.}^{-1}$$

and since $K_{Al} = 7.31 \times 10^{-5}$ moles.ℓ^{-1} we have

$$k_H = 3.36 \times 10^9 \text{ sec.}^{-1}.$$

For the 0.0707M. data, the least squares gradient is $(2.498 \pm 0.056) \times 10^5$ and

$$k_H = 3.42 \times 10^9 \text{ sec.}^{-1}.$$

For both of these least squares fits, the intercept was zero within the limits of experimental error. Values for k_H at the two concentrations show good agreement and the mean is $k_H = 3.39 \times 10^9$ sec.$^{-1}$.

Since $k_{-a}h_o > k_H$ over the acidity range where broadening occurred, it was not possible to obtain a value for k_a. However the plot shown does not level off below a specific rate of 1×10^5, sec.$^{-1}$, so it is possible to assert that $k_a > 1 \times 10^5$ sec.$^{-1}$ and that therefore

$k_{-a} > 1.4 \times 10^9$ sec.$^{-1}$ which is reasonable for a process which is likely to be diffusion controlled.

Failure to obtain measurable broadening at lower acidity also prevented any measurements of second order processes in this case.

Comparison With Other Work

Sudmeier and Occupati [66] previously attempted to measure first order rates of proton exchange in N,N'-dimethylpiperazine. However, they arbitrarily assumed that any first order contribution to the rate would be according to mechanism (3.5) with corresponding rate law (3.6).

$$BH_2^{2+} + H_2O \underset{k_{-1}}{\overset{k_1}{\rightleftharpoons}} BH^+ + H_3O^+ \qquad (3.5)$$

$$v = k_1[BH_2^{2+}] \qquad (3.6)$$

This assumption led to the result that $k_1 \leq 1.0 \times 10^{-2}$ sec.$^{-1}$ which leads to the prediction that $k_{-1} < 10^3$ sec.$^{-1}$. Such a low value is quite unrealistic for such a process and the present work has indeed shown that this value is low by at least a factor of 10^6.

PIPERAZINE

Determination of the Ionization Constant

Values of $pK_{A1} = \frac{[BH^+][H^+]}{[BH_2^{2+}]}$ are listed in Table 3.4. Figure 3.3 shows a plot of this data.

TABLE 3.4

VALUES OF $pK_{A1} = \frac{[BH^+][H^+]}{[BH_2^{2+}]}$ FOR SOLUTIONS OF PIPERAZINE

[Piperazine]	μ	pK_{A1}
1.126×10^{-2}	3.412×10^{-2}	5.5278 ± 0.0049
2.178×10^{-2}	6.599×10^{-2}	5.5875 ± 0.0011
3.291×10^{-2}	9.972×10^{-2}	5.6125 ± 0.0023
5.486×10^{-2}	1.662×10^{-1}	5.6530 ± 0.0031
7.656×10^{-2}	2.320×10^{-1}	5.6978 ± 0.0021

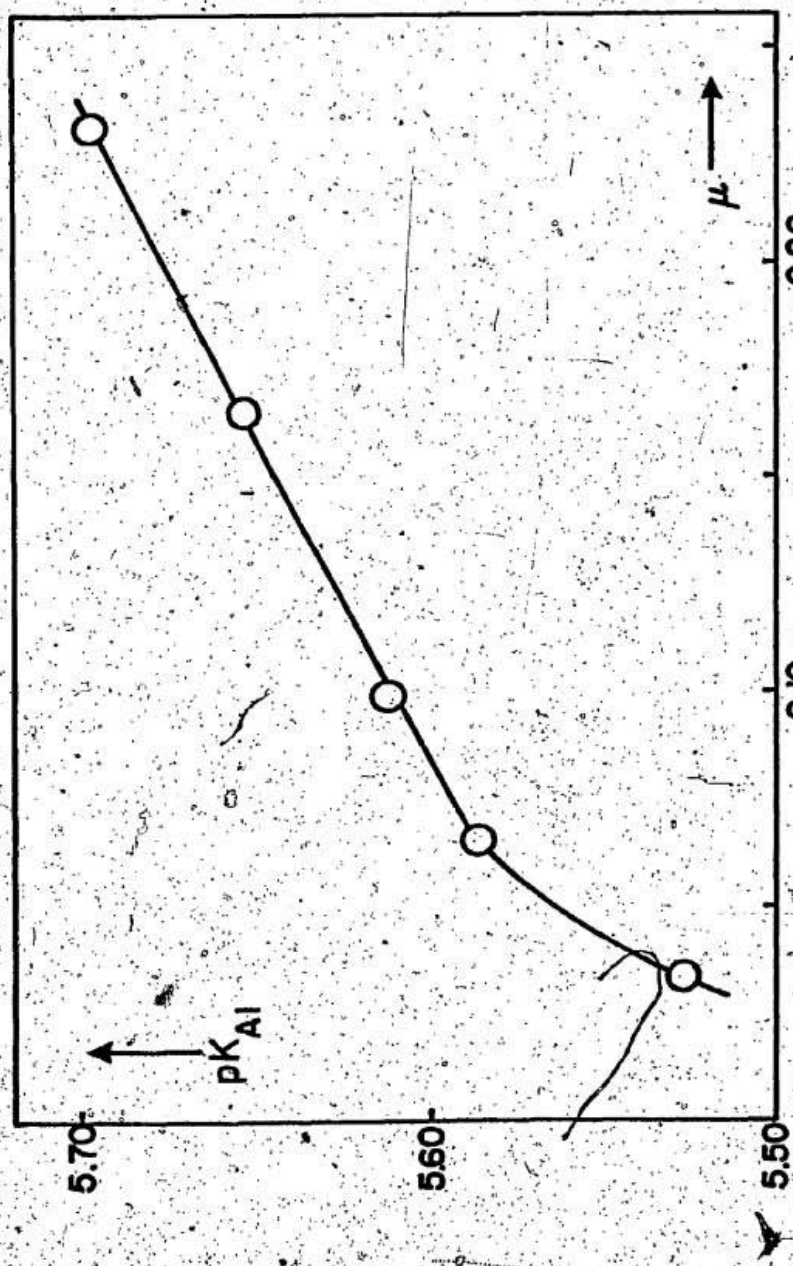

Figure 3.3 pK$_{A1}$ for piperazine.

Rate Measurements

Two series of measurements were made across the full range of acid concentrations for which measurable broadening of the water line occurred. Tables 3.5 and 3.6 show results for solutions which were about 0.03M in piperazine and Tables 3.7 and 3.8 show results for solutions which were about 0.05M in piperazine. Values of (Δ/p) from Tables 3.5 and 3.6 are plotted in Figure 3.4 and (Δ/p) values from Tables 3.7 and 3.8 are plotted in Figure 3.5. The discrepancy where the two series of data overlap is about 3% of the measured value in each figure and this was considered to be within the limits of experimental error.

The broadenings below about pH2 (i.e. below $H_o \simeq 2$) showed no significant difference between the two concentration series and exchange in this region was therefore judged to be predominantly first order in amine. For lower acid concentrations, however, the rates at higher piperazine concentration became appreciably faster than the rates at the lower piperazine concentration. It was therefore deduced that second order processes were prominant in this region of acidity.

Calculation of Rates and Determination of Rate Laws

Rates were calculated from the broadenings in the usual way. The chemical shift was determined as 2290 rads. $sec.^{-1}$ (corrected to low acid concentration) from the maximum broadening. Line widths in the absence of exchange were determined by using different concentrations of hydrochloric acid as before. The same H_o function as used previously was found to be satisfactory. The same estimates of J_{NH} and T'_{N14} as used for N,N'-dimethylpiperazine were considered to be adequate here.

TABLE 3.5

RATE DATA FOR 0.0296M. SOLUTIONS OF PIPERAZINE

$pH(H_o)$	$(1/[H^+])$	$(1/T_{1p})$	(Δ/p)	$10^{-4}\left(\frac{v}{[BH_2^{2+}]}\right)$
4.339	21827	0.578	219	9.616
4.147	14028	0.656	291	7.176
3.980	9550	0.725	355	5.826
3.798	6281	0.811	435	4.683
3.584	3837	0.855	504	3.776
3.376	2377	0.962	576	3.408
3.208	1614	1.009	619	3.128
3.006	1014	1.054	661	2.884
2.866	734.5	1.075	681	2.776
2.675	473.2	1.111	714	2.612
2.510	323.6	1.102	706	2.650
2.298	198.6	1.128	730	2.536
2.096	124.7	1.128	730	2.536
1.759	57.41	1.137	739	2.494
1.549	35.40	1.139	740	2.489
1.243	17.50	1.136	738	2.498

TABLE 3.6

RATE DATA FOR 0.0299M. SOLUTIONS OF PIPERAZINE

H_o	[HCl]	h_o	$(1/T_{1p})$	(Δ/p)	$10^4\left[\frac{[BH_2^{2+}]}{v}\right]$
1.598	0.02512	0.02519	1.112	709	0.3796
1.026	0.09019	0.09398	1.127	721	0.3949
0.703	0.1816	0.1980	1.192	778	0.4471
0.503	0.2753	0.3137	1.236	799	0.4775
0.343	0.3789	0.4535	1.267	818	0.5030
0.269	0.4375	0.5382	1.289	852	0.5447
0.196	0.5022	0.6369	1.331	865	0.5678
0.099	0.5996	0.7955	1.409	902	0.6291
0.007	0.7057	0.9833	1.430	971	0.7699
-0.115	0.8703	1.306	1.460	988	0.8690
-0.339	1.2386	2.183	1.442	1005	1.164
-0.453	1.4652	2.843	1.299	982	1.377
-0.605	1.8064	4.029	1.220	848	1.932
-0.711	2.0512	5.147	1.129	769	2.294
-0.810	2.3317	6.470	0.968	678	2.767
-0.963	2.7633	9.202	0.815	524	3.853
-1.104	3.1612	12.73	0.731	380	5.553
-1.241	3.5459	17.43	0.619	296	7.213
-1.456	4.1540	28.64	1.236	181	11.84

TABLE 3.7

RATE DATA FOR 0.0502M. SOLUTIONS OF PIPERAZINE

$pH(H_o)$	$(1/[H^+])$	$(1/T_{1p})$	(Δ/p)	$10^{-4}\left(\frac{v}{[BH_2^{2+}]}\right)$
4.182	15191	0.696	193	10.94
3.893	7811	0.908	310	6.724
3.601	3990	1.115	423	4.836
3.258	1811	1.371	564	3.504
2.988	972	1.510	640	3.016
2.784	608.3	1.588	683	2.780
2.421	264.1	1.670	727	2.566
2.255	180.2	1.705	747	2.474
2.027	106.6	1.720	755	2.440
1.801	63.27	1.747	769	2.379
1.582	38.22	1.702	745	2.484
1.276	18.91	1.703	745	2.484

TABLE 3.8

RATE DATA FOR 0.0503M. SOLUTIONS OF PIPERAZINE

H_o	[HCl]	h_o	$(1/T_{1p})$	(Δ/p)	$10^4\left(\frac{[BH_2^{2+}]}{v}\right)$
2.010	0.00976	0.00976	1.662	721	0.3887
1.793	0.01613	0.01611	1.657	719	0.3877
1.599	0.02506	0.02513	1.663	722	0.3906
1.391	0.04011	0.04062	1.668	727	0.3953
1.191	0.06263	0.06429	1.636	706	0.3819
1.027	0.09010	0.09388	1.661	721	0.3949
0.496	0.2793	0.3190	1.788	790	0.4667
0.192	0.5053	0.6418	1.966	883	0.5895
0.006	0.7074	0.9862	2.126	966	0.7595
−0.229	1.0463	1.6970	2.207	1004	1.164
−0.432	1.4211	2.7068	2.111	949	1.482
−0.593	1.7786	3.9231	1.891	805	2.348
−0.799	2.3005	6.3072	1.562	639	3.030
−1.206	3.4488	16.1032	0.939	287	7.483
−1.404	4.0061	25.3778	0.756	178	13.23
−1.604	4.5717	40.2698	0.625	103	22.91

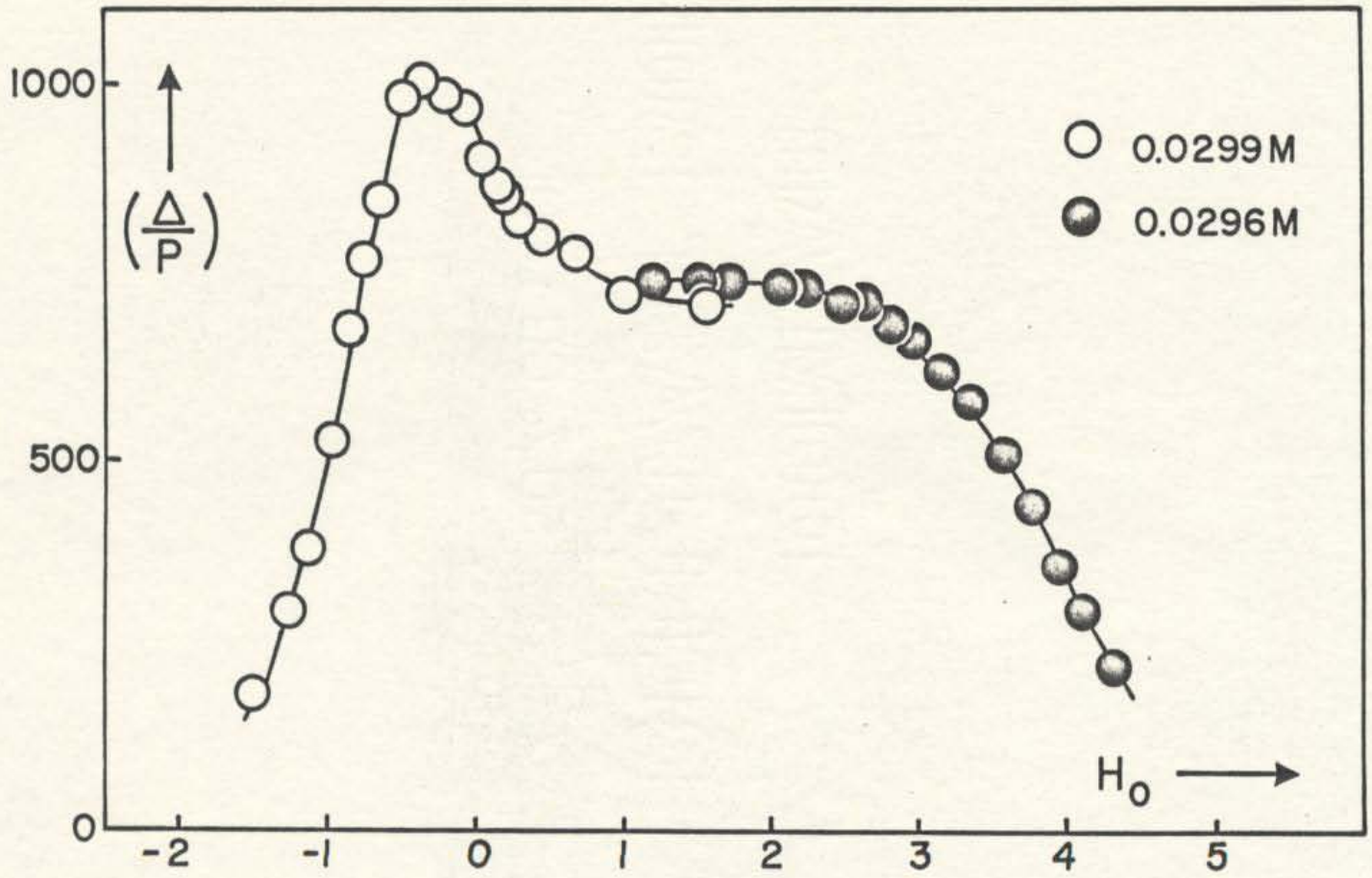

Figure 3.4 Measurable broadenings for solutions of piperazine.

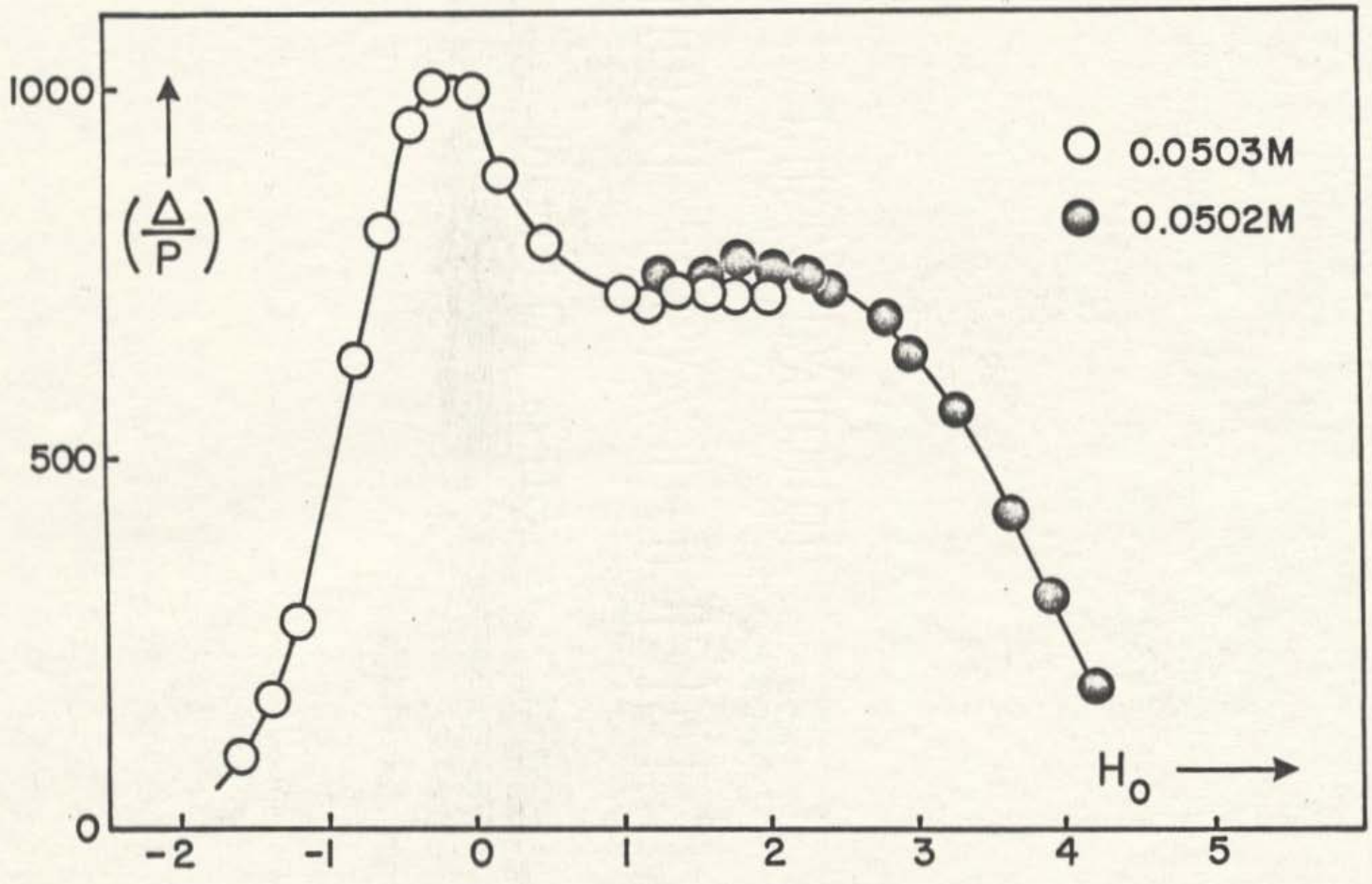

Figure 3.5 Measurable broadenings for solutions of piperazine.

The value of γH_1 was 590 rads. sec.$^{-1}$.

The Rate Law for Reactions Which are First Order in Amine

As in the case of N,N'- dimethylpiperazine the acid repression of the first order rate was again too large to be explained by salt effects alone. Consequently the mechanism for proton exchange was considered to be given by equations (3.1), (3.2), and (3.3) with the rate of exchange given by equation (3.4).

$$\frac{v}{[BH_2^{2+}]} = \frac{k_a k_H h_o}{k_H + k_{-a} h_o} \qquad (3.4)$$

Plots of the specific rate versus $(1/h_o)$ were made for the sets of the data shown in Tables 3.6 and 3.8. Both plots were curved even from the slowest rates and they levelled off from $1/h_o \simeq 20$. This indicated that k_H was not negligible compared with $k_{-a} h_o$. To determine k_H, a plot of $\left(\frac{[BH_2^{2+}]}{v}\right)$ versus h_o was made for each data series and found to be linear in each case: Figure 3.6 shows part of the plot for the data from Table 3.6 and a least squares fit of this data gave

$$\text{gradient} = \frac{1}{K_{A1} \cdot k_H} = (3.985 \pm 0.030) \times 10^{-5} \text{ mole.}^{-1} \ell. \text{ sec.}$$

$$\text{and intercept} = \frac{1}{k_a} = (3.25 \pm 0.32) \times 10^{-5} \text{ sec.}$$

Since $K_{A1} = 2.49 \times 10^{-6}$ mole. ℓ^{-1} in this case,

$$k_H = (1.09 \pm 0.03) \times 10^{10} \text{ sec.}^{-1}$$

and $$k_a = (3.08 \pm 0.30) \times 10^{4} \text{ sec.}^{-1}$$

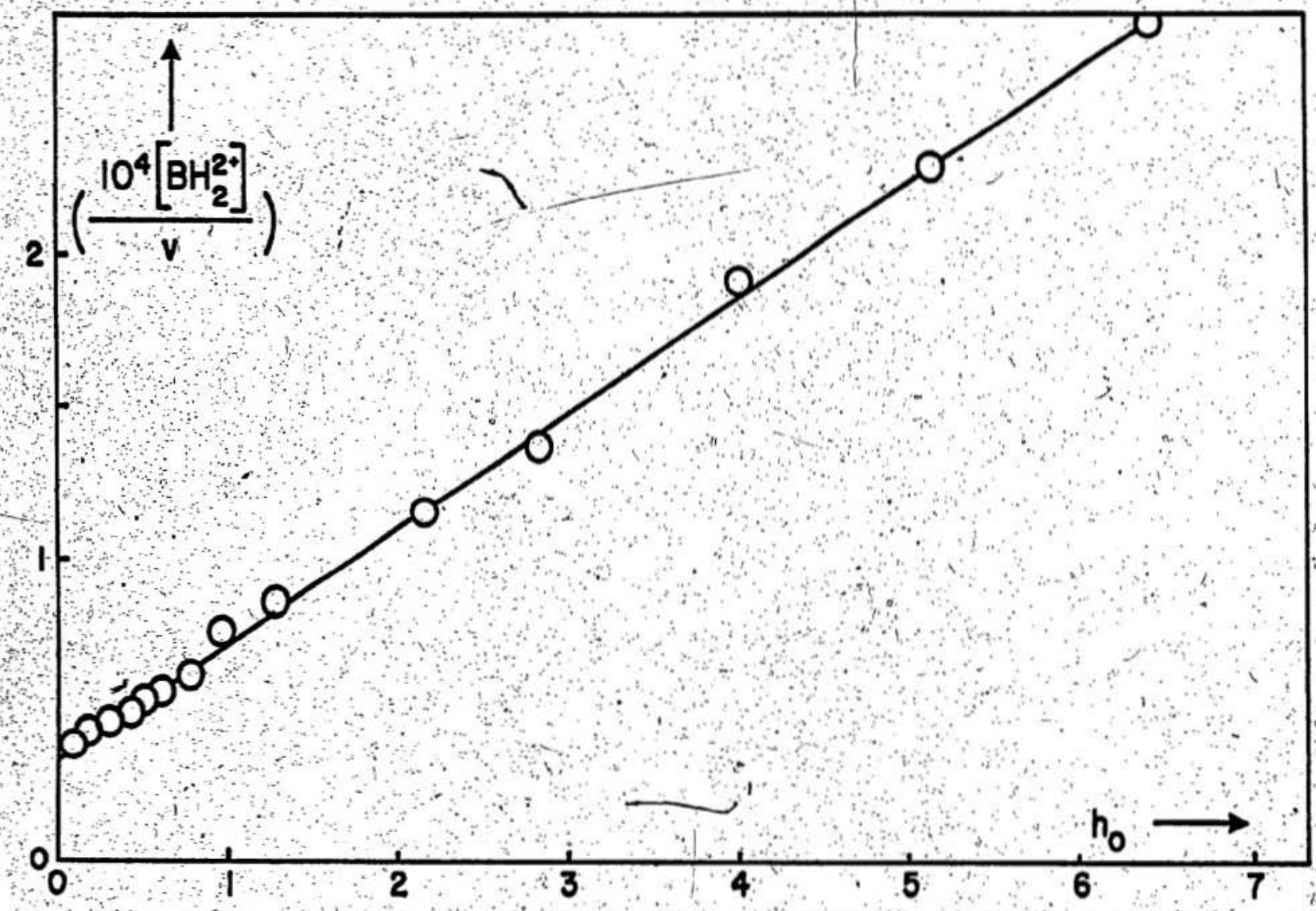

Figure 3.6 First order rate law for 0.0299M piperazine.

Similarly for the data from Table 3.8,

gradient = $(4.431 \pm 0.043) \times 10^{-5}$ mole.$^{-1}$ l. sec.

and intercept = $(3.19 \pm 0.29) \times 10^{-5}$ sec.

and since $K_{A1} = 2.26 \times 10^{-6}$ moles. l.$^{-1}$ here,

$k_H = (0.97 \pm 0.03) \times 10^{10}$ sec.$^{-1}$

and $k_a = (3.14 \pm 0.29) \times 10^{4}$ sec.$^{-1}$.

To obtain a more accurate value for k, the mean of all the specific rates which were on the plateau for all four series of experiments was taken.

at 0.03M, $k_a = (2.594 \pm 0.039) \times 10^{4}$ sec.$^{-1}$

at 0.05M, $k_a = (2.489 \pm 0.030) \times 10^{4}$ sec.$^{-1}$

and hence

at 0.03M, $k_{-a} = \frac{k_a}{K_{A1}} = (1.04 \pm 0.03) \times 10^{10}$ sec.$^{-1}$

and at 0.05M, $k_{-a} = \frac{k_a}{K_{A1}} = (1.10 \pm 0.03) \times 10^{10}$ sec.$^{-1}$

The Second Order Rate Law

The data listed in Tables 3.5 and 3.7 can now be used to determine the second order rate law. It has been shown that above pH ~ 1, $k_H >> k_{-a}[H^+]$ so that the first order contribution to the rate has become equal to $k_a [BH_2^{2+}]$. The rate law including the second order component will therefore be

$$\frac{v}{[BH_2^{2+}]} = k_a + k_2 [BH^+]$$

or

$$\frac{v}{[BH_2^{2+}]} = k_a + \frac{k_2 . K_{A1} [BH_2^{2+}]}{H^+}$$

and a plot of the specific rate versus $(1/[H^+])$ should be a straight line with gradient $k_2 K_{A1} . [BH_2^{2+}]$ and intercept k_a. Figure 3.7 shows such a plot for the 0.0296M piperazine data from Table 3.5 and a linear least squares fit gives

$$k_2 . K_{A1} . [BH_2^{2+}] = 3.234 \pm 0.039 \text{ moles. } \ell.^{-1} \text{ sec.}^{-1}$$

and $k_a = (2.629 \pm 0.037) \times 10^4 \text{ sec}^{-1}$

hence

$$k_2 = (4.38 \pm 0.08) \times 10^7 \ \ell. \text{ mole.}^{-1} \text{ sec.}^{-1} \text{ (at } \sqrt{\mu} = 0.298)$$

A similar procedure for the data at 0.0502M (Table 3.7) gives:

$$k_a = (2.47 \pm 0.05) \times 10^4 \text{ sec.}^{-1}$$

and $k_2 = (4.91 \pm 0.12) \times 10^7 \ \ell. \text{ mole.}^{-1} \text{ sec.}^{-1} \text{ (at } \sqrt{\mu} = 0.388)$

The values for k_a are in excellent agreement with the previous values. Assuming a primary kinetic salt effect on k_2 such that

$$\log k_2 = \log k_2^\circ + m \sqrt{\mu} \qquad (3.5)$$

where μ is the ionic strength and m is a constant, we find that

$$m = 0.552$$

and $k_2^\circ = (3.00 \pm 0.46) \times 10^7 \ \ell. \text{ mole.}^{-1} \text{ sec.}^{-1}$

Summary of Rate Constants Determined for Piperazine

The rate constants determined from the present work are listed below.

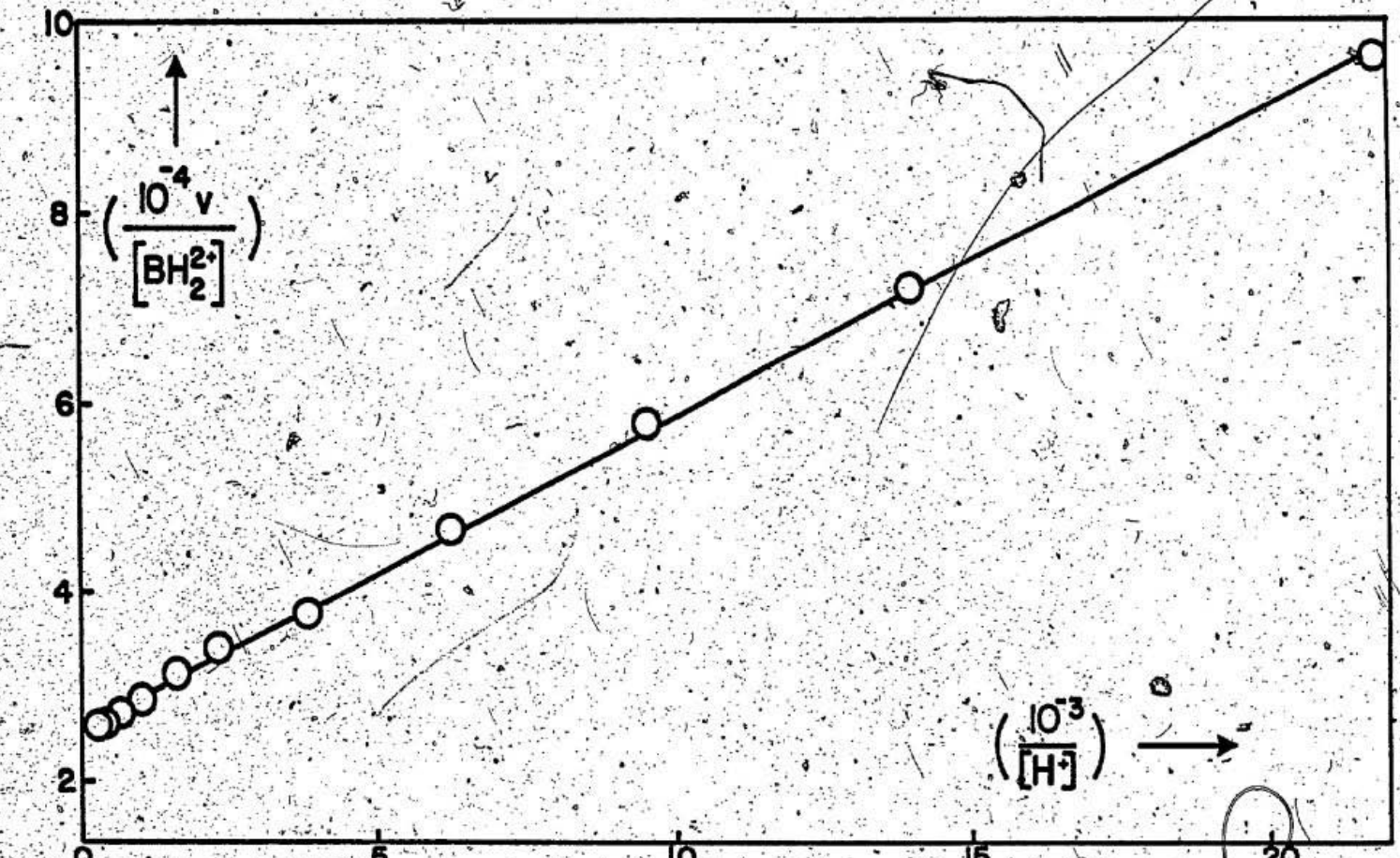

Figure 3.7 Second order rate law from data in Table 3.5.

CHAPTER 4

HISTAMINE RESULTS

Ionization Constants of Histamine

In the present work, the first ionization of histamine was of prime importance, and as explained previously, K_{A1} was defined in terms of concentrations:

$$BH_2^{2+} = BH^+ + H^+ \qquad (4.1)$$

$$K_{A1} = \frac{[BH^+][H^+]}{[BH_2^{2+}]}$$

Values of pK_{A1} (= - log K_{A1}) were determined at different ionic strengths and the results are listed in Table 4.1 and plotted in Figure 4.1. Although it is customary to plot pK_A against the square root of ionic strength, a plot against the first power of the ionic strength is used here since it is more convenient for subsequent calculations. The first three points listed in Table 4.1 were fitted in Equation (2.14), and by extrapolating to zero ionic strength it was determined that pK_{A1}° = 5.85 ± 0.01 with the constant A = 2.58. As expected from the Debye-Hückel limiting law, the points at higher concentrations do not lie on the curve defined by Equation (2.14) with constant A = 2.58.

Several determinations of pK_{A1}° have been reported but the values show considerable variation possibly due to difficulty in extrapolating to zero ionic strength. In some cases a simplified equation

$k_a^\circ = (3.17 \pm 0.05) \times 10^4$ sec.$^{-1}$

$k_{-a} = (1.07 \pm 0.03) \times 10^{10}$ sec.$^{-1}$

$k_H = (1.03 \pm 0.06) \times 10^{10}$ sec.$^{-1}$

$k_2^\circ = (3.00 \pm 0.46) \times 10^7$ ℓ. mole.$^{-1}$ sec.$^{-1}$

The value of k_a appeared to show a significant increase as the ionic strength decreased. Such a change in k_a with ionic strength (according to an equation similar to 3.5) has been found for trimethylammonium ion by Grunwald [49]. If it be assumed that the present data shows a real measure of such an effect, then the above value for k_a° will apply at zero ionic strength.

Consideration of The k_H Values

Since the k_H process consists of a water molecule departing from the reacting species, it might be thought that a more basic species would be associated with a slower k_H. However, in the present work, piperazine is more basic than N,N'-dimethylpiperazine but nevertheless is associated with a faster k_H. This result supports the argument of Ralph and Grunwald that basicity has little (if any) effect on k_H [35]. According to these workers the slower k_H for N,N'-dimethylpiperazine is explained by the larger dispersion interactions between the amine and the departing water molecule in that case.

TABLE 4.1

VALUES OF pK_{A1} FOR SOLUTIONS OF HISTAMINE.

[Histamine]	μ	pK_{A1}
4.315×10^{-3}	1.295×10^{-2}	5.936 ± .005
9.963×10^{-3}	2.989×10^{-2}	5.969 ± .004
2.992×10^{-2}	8.976×10^{-2}	6.042 ± .002
4.587×10^{-2}	1.376×10^{-1}	6.066 ± .003
4.640×10^{-2}	1.392×10^{-1}	6.074 ± .004
5.760×10^{-2}	1.728×10^{-1}	6.113 ± .002
6.997×10^{-2}	2.099×10^{-1}	6.128 ± .013
1.053×10^{-1}	3.159×10^{-1}	6.153 ± .004
1.507×10^{-1}	4.521×10^{-1}	6.205 ± .006
2.432×10^{-1}	7.296×10^{-1}	6.268 ± .002
3.216×10^{-1}	9.648×10^{-1}	6.326 ± .005

And in a solution prepared in 95% D_2O and 5% H_2O.

5.95×10^{-2}	1.785×10^{-1}	6.564 ± .004

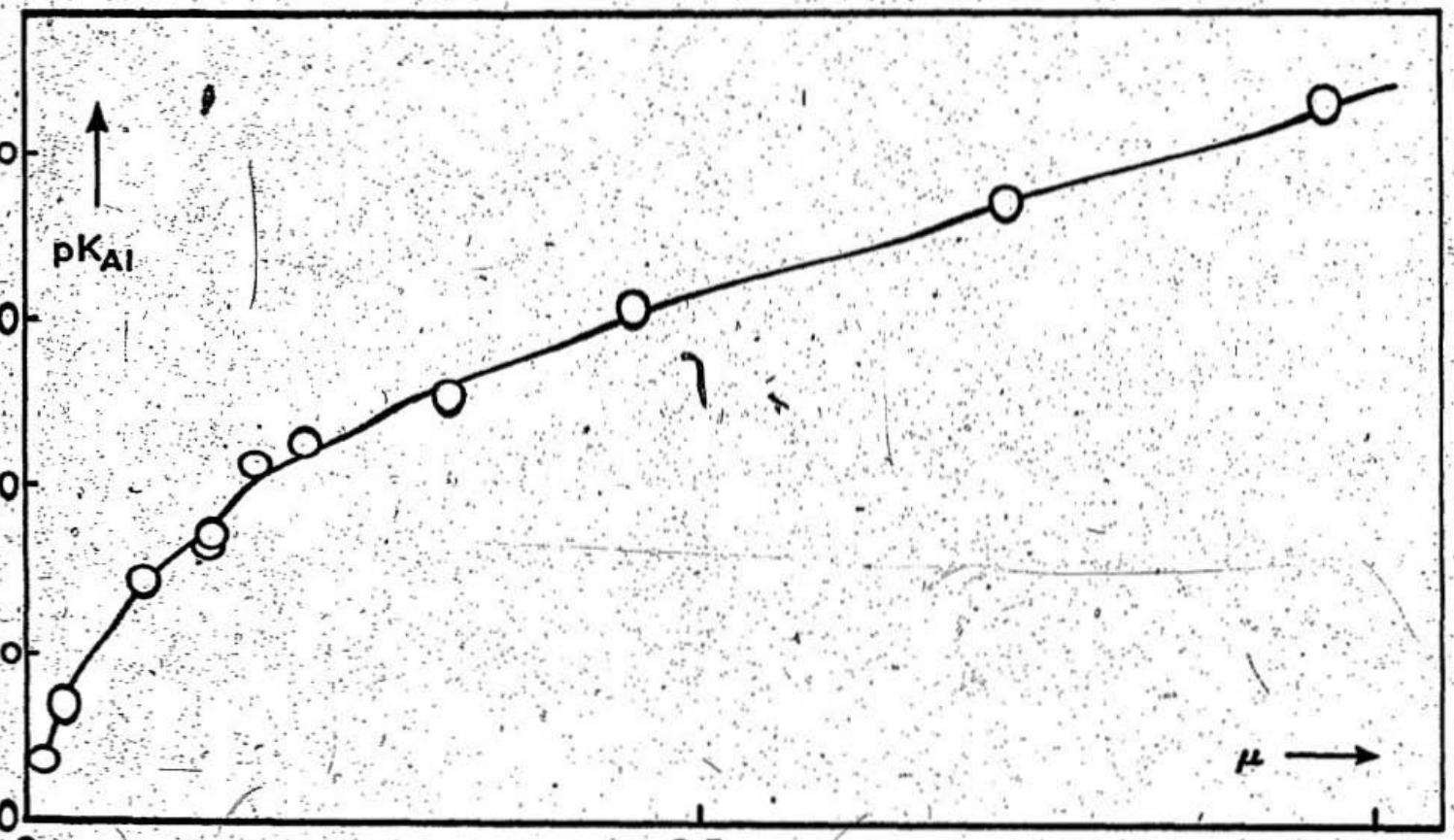

Figure 4.1 pK_{A1} for Histamine

was used for the extrapolation and, in addition, the extrapolation was made from high ionic strengths. Values for pK_{A1}^{o} at 25°C include 5.788 [67], 6.04 [68], and 6.12 [69]. Channing et al., [70] do not report a value at 25°C but give $pK_{A1}^{o} = 6.05$ at 20°C and 5.87 at 30°C.

The ratio

$$K' = \frac{K_{A2}^{o}}{K_{A1}^{o}} \qquad (4.2)$$

is required in the discussion of the present results. No determination of K_{A2}^{o} was made here since two values reported in the literature were in good agreement.† Randolf V. Schalien [67] reported $K_{A2}^{o} = 1.75 \times 10^{-10}$ while Paiva et al., [68] reported $K_{A2}^{o} = 1.78 \times 10^{-10}$. Using the mean of these two values together with the value of K_{A1}^{o} determined in the present work, we obtain $K' = 1.25 \times 10^{-4}$.

n.m.r. Results for Series with Fixed Histamine Concentration—The Data

The histamine molecule (B, Fig. 4.2), can be protonated in two positions (BH_2^{2+}, Fig. 4.3). The three hydrogen atoms which are now at the ammonium site are magnetically equivalent, and the two hydrogen atoms at imidazolium sites, although not magnetically equivalent, will be expected to have the same chemical shift within the limits of the line widths of the NH resonances. Provided the rates are of a suitable magnitude, an n.m.r. experiment will be able to detect proton exchange between each of these two types of site and water sites. Thus examination

†K_{A2} is expected to show less variation with ionic strength than does K_{A1}.

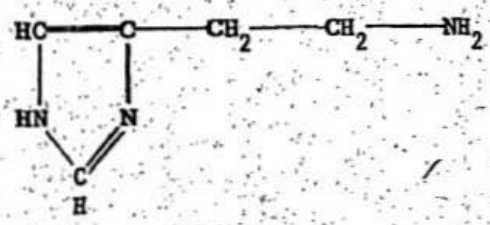

Figure 4.2

The histamine molecule, B.

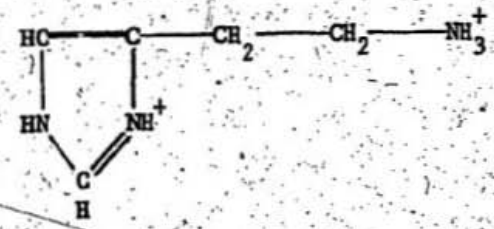

Figure 4.3

The doubly protonated histamine molecule, BH_2^{2+}.

of the water line at various hydrogen ion concentrations will be expected to show two separate broadening components.

To attempt to detect these two components, preliminary ($1/T_{1p}$) measurements were made at low RF for the water line of 0.03 M histamine solutions ranging from approximately 100% BH_2^{2+} to approximately 100% BH^+. Viewing the broadening of water versus pH as a spectrum which reflects exchange, one might expect that with magnetically and probably chemically different sites, several peaks would be observed. If this were true, the exchange broadenings for each NH could be separated by inspection and the rates of reaction determined in a very straightforward manner. Since only one continuous broadening curve was found it was suspected that the two components overlapped at this histamine concentration. In attempting to separate the two components, further low RF ($1/T_{1p}$) measurements were made in the regions of broadening for histamine solutions of approximately 0.006 M., 0.03 M., 0.06 M., and 0.27 M. These measurements are listed in Tables 4.2 to 4.5 and (Δ/c) values are plotted in Figures 4.4 to 4.7. The curves show least square fits of the data for use in the subsequent analysis. Low RF ($1/T_{1p}$) measurements were also made for approximately 0.06 M. histamine solutions in 95% D_2O and 5% H_2O. These are listed in Table 4.6 and the (Δ/c) values are plotted in Figure 4.8. The estimated uncertainties in the low RF (Δ/c) values are generally less than one (Δ/c) unit. It will be noted, however, that the series at 6.00×10^{-3} M. histamine has subtraction terms ranging from approximately 50% to approximately 80% of the total ($1/T_{1p}$) measurement so that the (Δ/c) uncertainties throughout this series will be somewhat

TABLE 4.2[†]

6.00×10^{-3} M. HISTAMINE SOLUTIONS WITH RF FIELD AT 251 RADS. $SEC.^{-1}$

pH	$1/T_{1p}$	$1/T_1$	Δ	$(\Delta/c)_e$
5.580	0.475	0.330	0.101	16.8
5.267	0.505	0.330	0.155	25.8
4.806	0.614	0.330	0.277	46.1
4.490	0.682	0.330	0.349	58.1
4.248	0.704	0.330	0.374	62.3
4.120	0.683	0.330	0.353	58.8
4.088	0.681	0.330	0.351	58.5
3.932	0.666	0.330	0.336	56.0
3.788	0.653	0.330	0.323	53.9
3.224	0.609	0.330	0.279	46.4
2.921	0.579	0.330	0.267	44.5
2.643	0.581	0.330	0.251	41.9

[†]All digits shown in this and subsequent tables are not necessarily significant. Assessment of errors is made at the completion of the numerical analysis.

TABLE 4.3

2.98×10^{-2} M. HISTAMINE SOLUTIONS WITH RF FIELD AT 500 RADS. $SEC.^{-1}$

pH	$1/T_{1p}$	$1/T_1$	Δ	$(\Delta/c)_e$
5.602	0.567	0.333	0.190	6.40
5.401	0.622	0.333	0.262	8.82
5.197	0.769	0.333	0.418	14.0
4.990	0.918	0.333	0.573	19.3
4.785	1.114	0.333	0.774	26.0
4.683	1.312	0.333	0.974	32.7
4.554	1.397	0.333	1.064	35.8
4.410	1.654	0.333	1.321	44.3
4.286	1.792	0.333	1.459	47.5
4.119	1.847	0.333	1.514	50.9
3.863	1.884	0.333	1.551	52.2
3.424	1.809	0.333	1.473	49.5
2.970	1.655	0.333	1.322	44.4
2.404	1.567	0.333	1.234	41.5
2.260	1.544	0.333	1.211	40.6
1.993	1.437	0.333	1.104	36.8
1.874	1.388	0.333	1.055	35.5
1.624	1.433	0.333	1.100	36.9
1.320	1.450	0.333	1.117	37.5
1.059	1.402	0.333	1.069	35.9
0.658	1.388	0.333	1.055	35.5
0.502	1.389	0.333	1.056	35.5
0.275	1.402	0.348	1.054	35.4
0.020	1.370	0.359	1.010	33.9
-0.326	1.138	0.368	0.770	25.8
-0.469	0.896	0.385	0.511	17.1
-0.573	0.691	0.400	0.291	9.7
-0.599	0.666	0.408	0.258	8.7
-0.666	0.592	0.424	0.168	5.6
-0.747	0.547	0.447	0.100	3.4

TABLE 4.4

5.96×10^{-2} M HISTAMINE SOLUTIONS WITH RF FIELD AT 200 RADS. $SEC.^{-1}$

pH	$1/T_{1p}$	$1/T_1$	Δ	$(\Delta/c)_e$
5.553	0.668	0.343	0.286	4.80
5.535	0.700	0.340	0.324	5.45
5.468	0.758	0.344	0.381	6.46
5.334	0.804	0.340	0.456	7.65
5.240	0.890	0.340	0.530	8.91
5.138	1.017	0.343	0.658	11.0
4.997	1.151	0.340	0.800	13.5
4.887	1.366	0.343	1.014	17.0
4.764	1.623	0.344	1.272	21.6
4.660	1.986	0.343	1.638	27.5
4.453	2.515	0.340	2.173	36.5
4.298	2.839	0.343	2.496	41.9
4.201	2.986	0.340	2.646	44.5
4.020	3.195	0.340	2.855	48.0
3.978	3.235	0.343	2.892	48.5
3.730	3.340	0.343	2.997	47.9
3.566	3.313	0.343	2.970	48.1
3.385	3.185	0.343	2.842	47.7
3.150	3.133	0.343	2.790	46.8
3.135	3.137	0.340	2.800	47.0
2.907	3.002	0.343	2.659	44.6
2.624	3.021	0.343	2.678	44.9
2.480	2.880	0.340	2.543	43.5
2.289	2.904	0.343	2.561	43.0
1.926	2.685	0.343	2.342	39.2
1.910	2.815	0.343	2.472	41.5
1.695	2.685	0.343	2.342	39.3
1.389	2.667	0.343	2.324	39.0
1.081	2.630	0.343	2.287	38.3

TABLE 4.4 (CONTINUED)

pH	$1/T_{1p}$	$1/T_1$	Δ	$(\Delta/c)_e$
0.744	2.723	0.344	2.379	39.9
0.498	2.686	0.345	2.341	39.2
0.300	2.650	0.346	2.304	38.6
0.073	2.603	0.350	2.253	37.7
-0.134	2.368	0.356	2.012	33.8
-0.309	1.936	0.366	1.570	26.3
-0.472	1.360	0.383	0.977	16.4
-0.572	0.973	0.400	0.573	9.6
-0.685	0.704	0.429	0.275	4.6

TABLE 4.5

2.70×10^{-1} M HISTAMINE SOLUTIONS WITH RF FIELD AT 355 RADS. SEC^{-1}

pH	$1/T_{1p}$	$1/T_1$	Δ	$(\Delta/c)_e$
5.403	1.023	0.350	0.645	2.40
5.213	1.818	0.350	1.449	5.41
5.154	1.528	0.350	1.162	4.33
4.853	2.400	0.350	2.042	7.60
4.640	4.680	0.350	4.325	16.1
4.562	4.171	0.350	3.818	14.2
4.460	5.814	0.350	5.464	20.4
4.339	7.366	0.350	7.015	26.2
4.273	7.866	0.350	7.516	28.1
4.186	8.338	0.350	7.988	29.9
4.113	9.429	0.350	9.079	33.9
4.063	9.218	0.350	8.868	33.2
3.963	9.903	0.350	9.553	35.7
3.855	10.067	0.350	9.717	36.2
3.843	10.542	0.350	10.192	38.0
3.825	10.230	0.350	9.880	36.9
3.773	10.364	0.350	10.014	37.4
3.709	9.984	0.350	9.634	36.0
3.688	10.430	0.350	10.080	37.7
3.572	10.021	0.350	9.671	36.2
3.400	10.443	0.350	10.093	37.7
3.381	10.828	0.350	10.478	39.2
3.365	11.129	0.350	10.779	40.3
3.108	12.458	0.350	12.108	45.3
2.960	12.539	0.350	12.189	45.4
2.637	12.567	0.350	12.217	45.4
2.293	12.458	0.350	12.108	45.1
2.279	11.991	0.350	11.641	43.4
1.882	11.015	0.350	10.665	39.7

TABLE 4.5 (CONTINUED)

pH	$1/T_{1p}$	$1/T_1$	Δ	$(\Delta/c)_e$
1.774	10.817	0.342	10.475	38.8
1.493	10.303	0.350	9.953	37.1
1.346	10.243	0.342	9.901	36.6
1.282	10.796	0.342	10.454	38.6
0.881	10.545	0.345	10.200	37.7
0.585	10.330	0.349	9.981	36.8
0.260	10.249	0.362	9.887	36.5
0.069	10.116	0.371	9.745	36.0
-0.154	9.037	0.382	8.655	32.0
-0.159	8.538	0.382	8.156	30.1
-0.350	6.849	0.394	6.455	23.9
-0.560	3.508	0.408	3.100	11.5
-0.680	2.130	0.421	1.709	6.3
-0.735	1.516	0.435	1.081	4.0

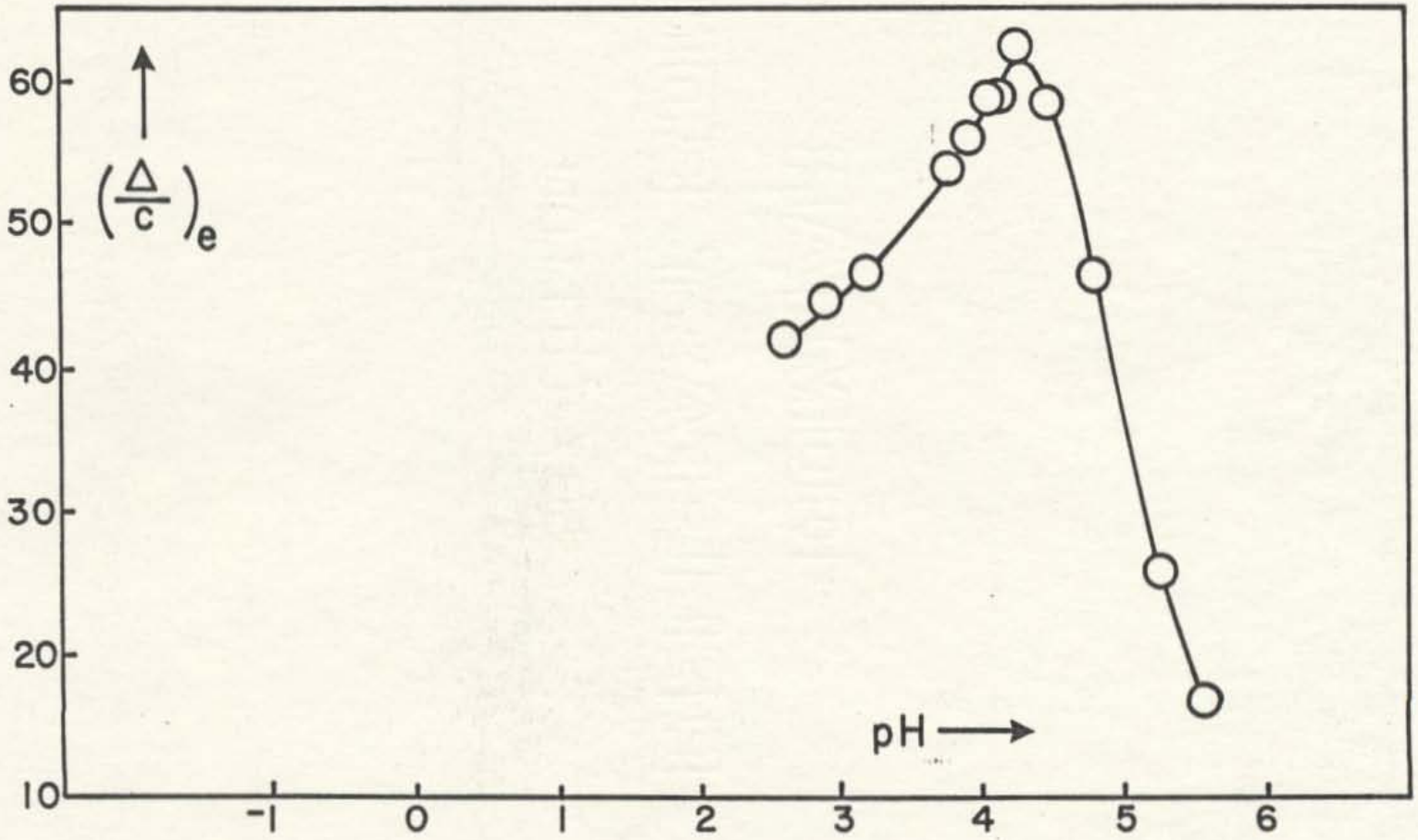

Figure 4.4 Experimental broadenings for 6.00×10^{-3}M. histamine solutions

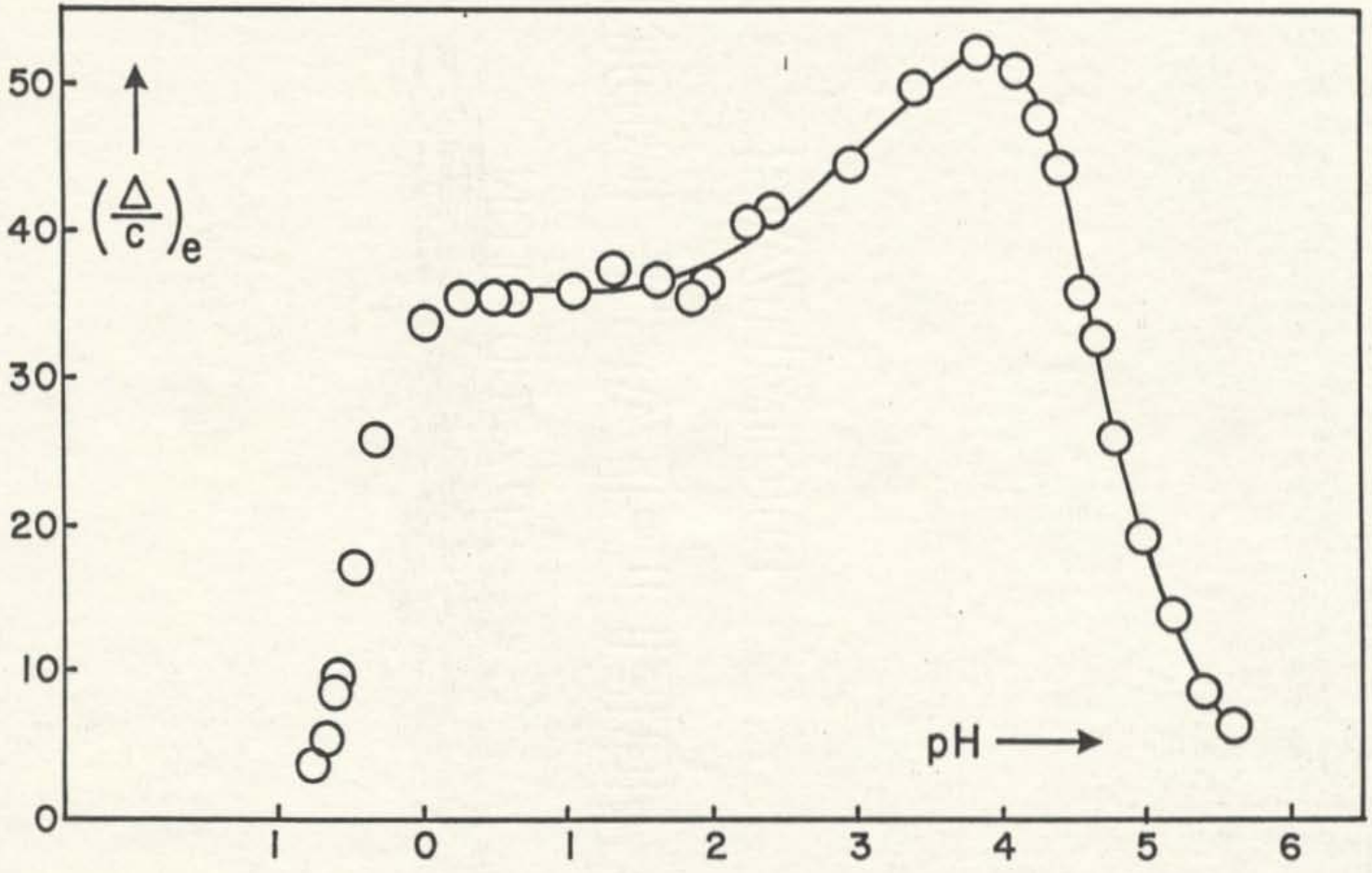

Figure 4.5 Experimental broadenings for 2.98×10^{-2}M. histamine solutions

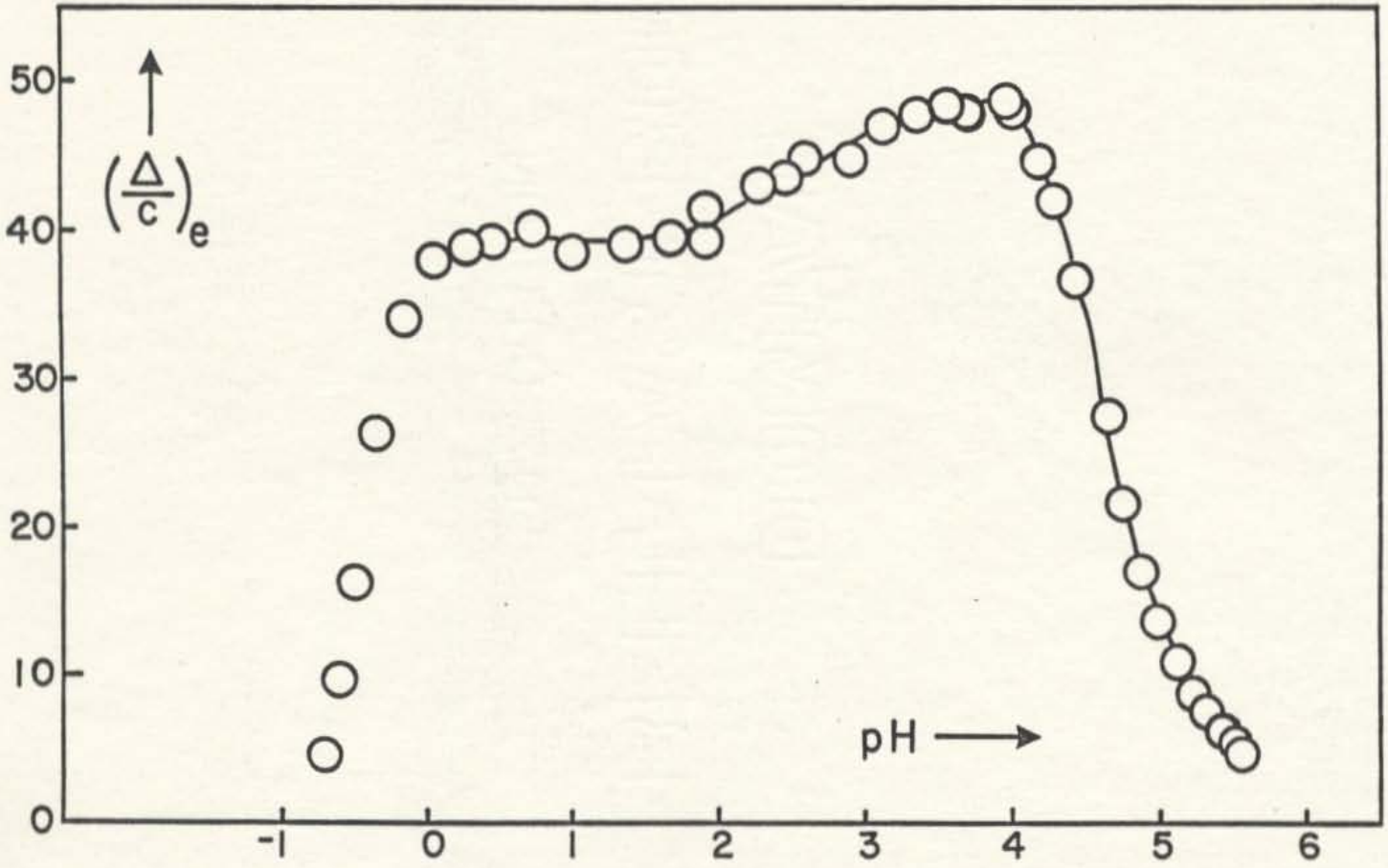

Figure 4.6 Experimental broadenings for 5.96×10^{-2}M. histamine solutions

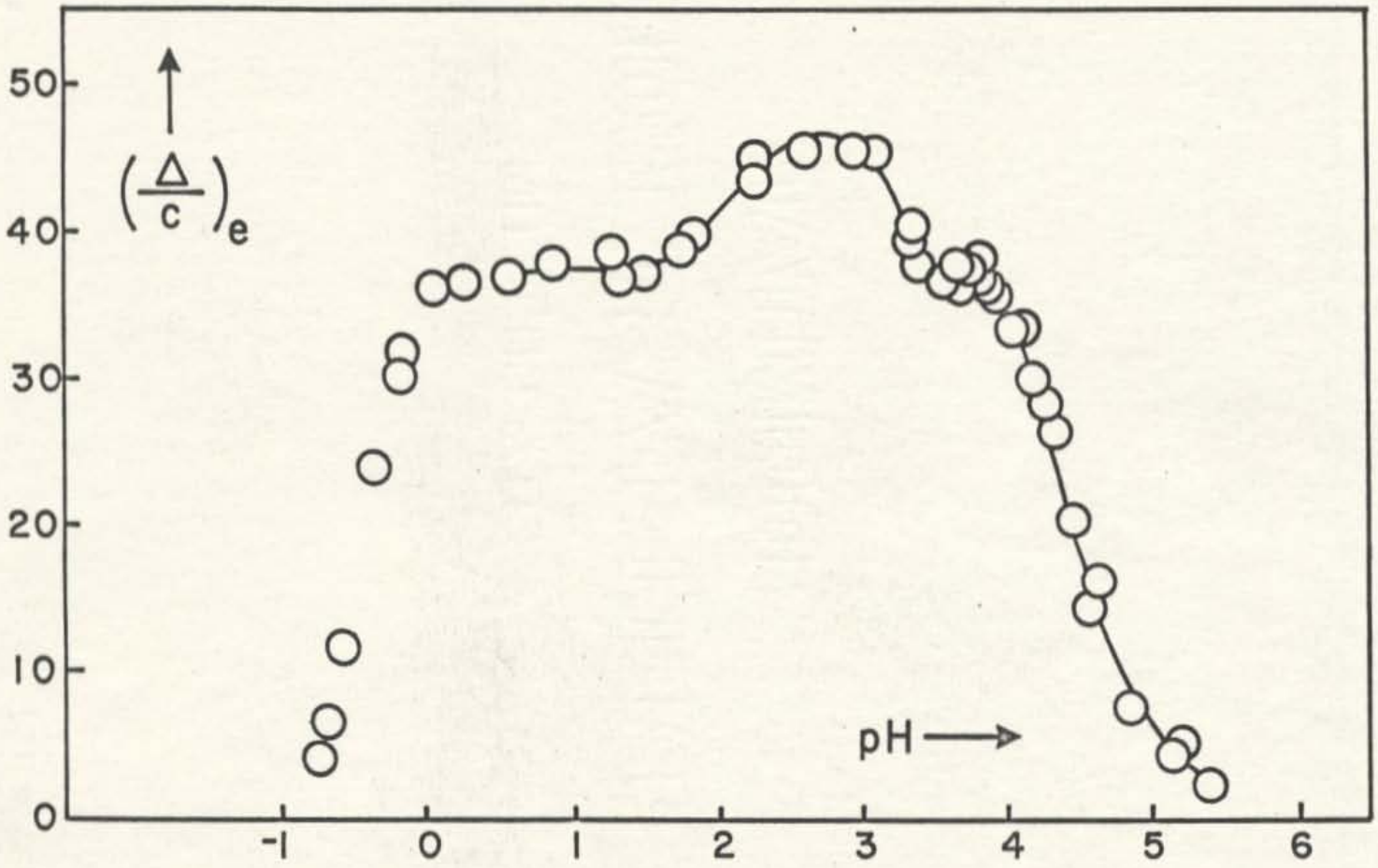

Figure 4.7 Experimental broadenings for 2.70×10^{-1} M. histamine solutions

TABLE 4.6

95% DEUTERATED SOLUTIONS 5.95 X 10^{-2} M. IN HISTAMINE
WITH RF FIELD AT 632 RADS. $SEC.^{-1}$

pH	$1/T_{1p}$	$1/T_1$	Δ	$(\Delta/c)_e$
6.200	.800	.095	.570	9.6
5.953	1.030	.097	.839	14.1
5.707	1.463	.098	1.310	22.0
5.473	1.949	.099	1.817	30.6
5.214	2.556	.101	2.436	40.9
4.989	3.020	.102	2.907	48.9
4.796	3.162	.103	3.052	51.3
4.576	3.260	.104	3.152	53.0
4.333	3.096	.105	2.990	50.3
4.134	2.948	.107	2.841	47.8
3.891	2.640	.108	2.532	42.6
3.691	2.469	.109	2.360	39.7
3.418	2.259	.111	2.148	36.2
3.186	2.208	.112	2.096	35.2
2.967	2.105	.113	1.992	33.5
2.736	2.027	.114	1.913	32.2
2.492	2.053	.116	1.937	32.6
2.202	2.065	.117	1.948	32.7
1.818	2.039	.122	1.917	32.2
1.808	2.002	.119	1.883	31.7
1.307	1.977	.126	1.851	31.1
1.102	1.935	.128	1.807	30.4
0.839	1.854	.130	1.724	29.0
0.599	1.785	.132	1.653	27.8
0.370	1.608	.134	1.474	24.8
0.127	1.461	.136	1.325	22.3
- .064	1.118	.137	.981	16.5
- .242	0.867	.139	.728	12.2

TABLE 4.6 (CONTINUED)

pH	$1/T_{1p}$	$1/T_1$	Δ	$(\Delta/c)_e$
- .401	0.572	.140	.432	7.27
- .596	0.273	.142	.131	2.19
- .772	0.168	.143	.025	0.41

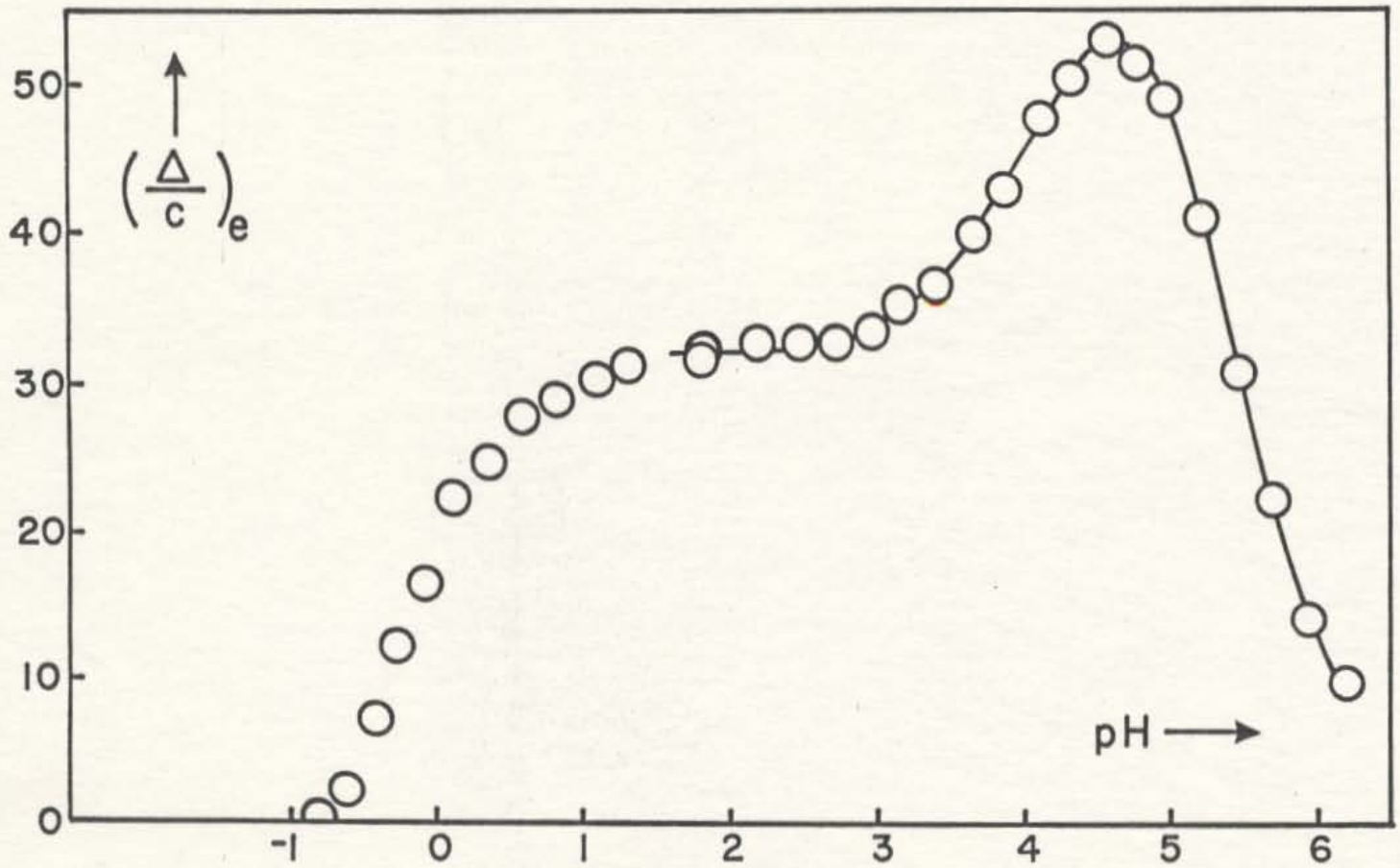

Figure 4.8 Experimental broadenings for deuterated histamine solutions

higher.† High RF ($1/T_{1p}$) measurements for histamine solutions at 0.03 M, 0.06 M, 0.27 M are listed in Tables 4.7 to 4.9. The high RF measurements showed considerably greater scatter than the low RF measurements and the uncertainties are estimated to be about 2 or 3 (Δ/c) units.

It can be seen that the two components are not separated in any of this data, but a shoulder does appear at the right hand side of the 0.27 M curve (Fig. 4.7). Inspection of the curves in Figs. 4.4 to 4.7 will also show that $(\Delta/c)_{max}$ decreases systematically from about 62 to 46 units as the concentration increases. Since a single broadening component would show no change in $(\Delta/c)_{max}$ with concentration, there seems to be little doubt that more than one component is present. To assist in the separation of the two components, a plot showing the % reduction in (Δ/c) as the RF field increased is shown in Fig. 4.9. Data used for this plot is taken from Tables 4.5 and 4.9 and, for reasons given in the introduction, a maximum in (Δ/c) difference is expected to occur in the lifetime broadening region of each component. If only one component were present, the maximum of the difference plot would therefore appear towards the left hand side of the single component. Since there are two maxima in the difference plot, it follows that the exchange broadening cannot be a single component resulting from proton exchange between a single average NH resonance and the water resonance.

Parameters Required for the Kinetic Analysis

For each of the two types of NH bond being broken, three

---

†For similar reasons there will also be high uncertainties at the extremes of pH in the series at other concentrations.

TABLE 4.7

2.98×10^{-2} M. HISTAMINE SOLUTIONS WITH RF FIELD AT 2513 RADS. $SEC.^{-1}$

pH	$1/T_{1p}$	$1/T_1$	Δ	$(\Delta/c)_e$
5.586	0.600	0.307	0.251	8.4
4.682	1.220	0.365	0.849	28.5
4.410	1.526	0.365	1.161	39.0
4.344	1.442	0.320	1.122	37.7
4.119	1.542	0.365	1.177	39.5
3.927	1.482	0.365	1.117	37.5
3.863	1.450	0.320	1.130	37.9
3.725	1.483	0.365	1.118	37.5
3.424	1.537	0.320	1.217	40.8
2.970	1.577	0.320	1.257	42.2
2.404	1.552	0.320	1.232	41.4

TABLE 4.8

5.90×10^{-2} M. HISTAMINE SOLUTIONS WITH RF FIELD AT 2513 RADS. SEC^{-1}.

pH	$1/T_{1p}$	$1/T_1$	Δ	$(\Delta/c)_e$
5.809	0.613	0.392	0.150	2.54
5.468	0.714	0.392	0.289	4.90
5.113	1.070	0.392	0.663	11.24
4.764	1.420	0.392	1.021	17.3
4.384	2.131	0.392	1.739	29.5
3.985	2.498	0.392	2.106	35.7
3.562	2.844	0.392	2.452	41.6
3.140	2.871	0.392	2.479	42.0

TABLE 4.9

2.70×10^{-1} M. HISTAMINE SOLUTIONS WITH RF FIELD AT 2819 RADS. SEC^{-1}.

pH	$1/T_{1p}$	$1/T_1$	Δ	$(\Delta/c)_e$	Percent Reduction†
5.403	1.193	0.350	0.815	3.03	
5.154	1.396	0.350	1.030	3.83	
4.853	2.358	0.350	2.000	7.44	
4.562	4.074	0.350	3.721	13.9	2.1
4.334	5.807	0.350	5.457	20.3	16.5
4.038	6.183	0.350	5.833	21.7	36.2
3.855	6.965	0.350	6.615	24.6	32.1
3.647	7.851	0.350	7.501	27.9	25.1
3.234	8.842	0.350	8.492	31.5	25.7
2.960	9.326	0.350	8.976	33.3	26.7
2.637	9.698	0.350	9.348	34.8	23.4
2.293	8.952	0.350	8.602	32.0	25.6
1.979	8.319	0.342	7.977	29.5	27.7
1.882	8.187	0.350	7.837	29.2	24.2
1.637	8.560	0.342	8.218	30.4	20.0
1.493	8.084	0.350	7.734	28.8	22.4
1.346	8.276	0.342	7.934	29.3	20.0
1.093	8.064	0.342	7.722	28.6	23.1
0.668	8.179	0.347	7.832	28.9	22.3
0.289	7.921	0.361	7.560	28.0	23.3
0.069	7.985	0.371	7.614	28.2	21.7
-0.154	6.664	0.382	6.282	23.2	27.5
-0.350	5.190	0.394	4.796	17.8	25.5
-0.560	3.066	0.408	2.658	9.8	14.8
-0.588	2.742	0.411	2.331	8.6	15.7
-0.680	1.920	0.421	1.499	5.5	12.7
-0.735	1.211	0.435	0.776	2.9	

†This column shows the percent reduction in $(\Delta/c)_e$ due to measurements being made with the high RF field compared with the low RF field used for the data in Table 4.5. Where no corresponding data point is listed in Table 4.5, the smoothed curve value is used.

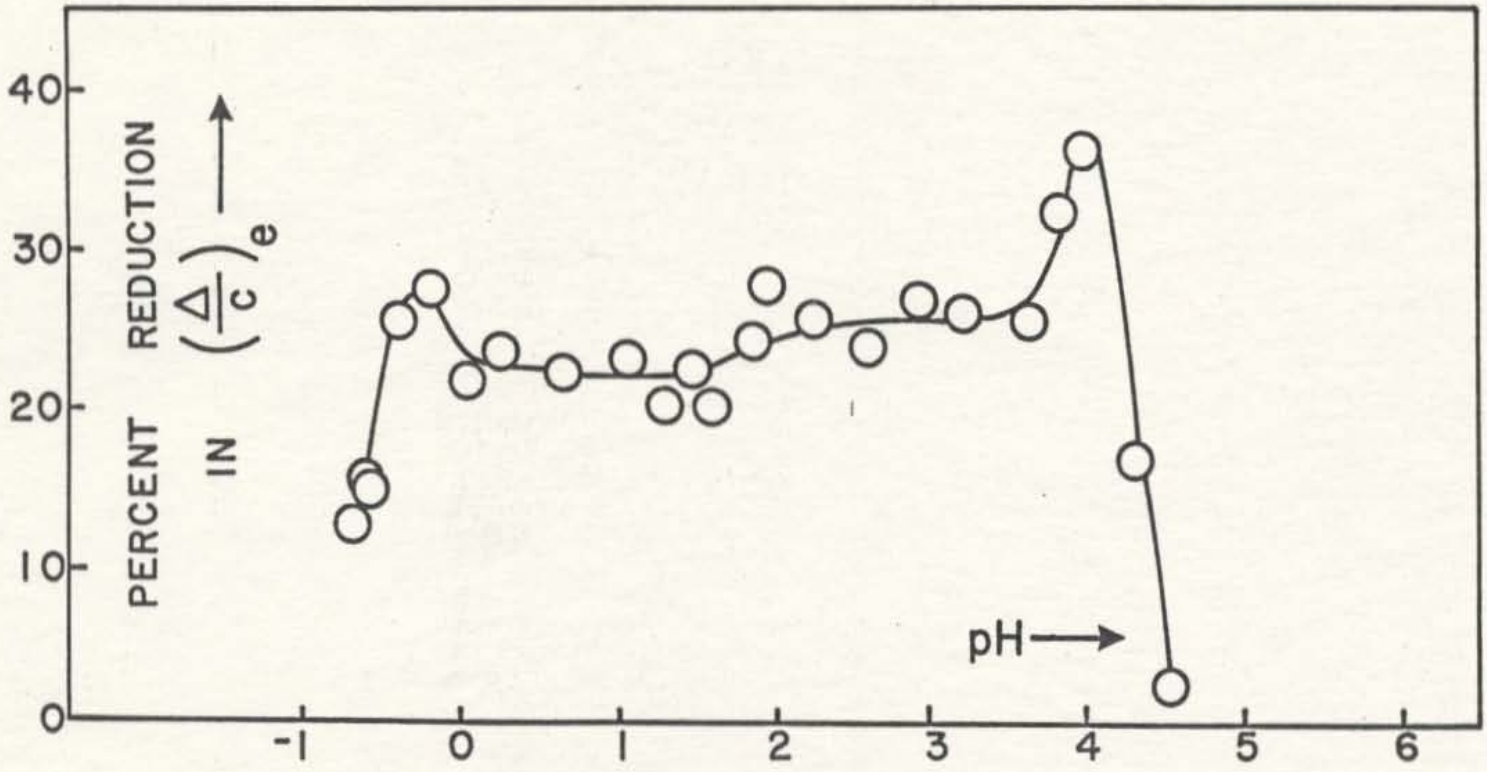

Figure 4.9 Percent reduction in $(\Delta/c)_e$ due to increased RF field

parameters are needed to convert the experimental exchange broadening to the rate of proton exchange. These are: (i) the NH to HOH chemical shift (δ), (ii) the longitudinal relaxation time of the ^{14}N nucleus ($T^1_{N^{14}}$), and (iii) the N-H coupling constant (J_{NH}).

(i) The Chemical Shift Values

As explained earlier the rate calculations are very sensitive to δ in the region of maximum broadening and in the region of exchange narrowing. Estimates are therefore inadequate and attempts to obtain more accurate values are explained later.

(ii) Longitudinal Relaxation Time for ^{14}N

The rate calculations are insensitive to this value throughout the full broadening region. Accordingly an estimate of $T^1 = 0.005$ secs. was considered adequate for both NH sites. For the ammonium protons this estimate is based on data for methylammonium chloride [71]. For the imidazolium protons the estimate is based on data for imidazolium chloride [44].

(iii) The N-H Coupling Constants

Since the coupling constant is considerably smaller than the chemical shift for both NH sites, it follows that the rates are much less dependant on the coupling constants than on the chemical shifts. Grunwald and Price [33] have noted that J is quite insensitive to change of solvent and to alkyl substitution on nitrogen, and a value of J = 327 rads. $sec.^{-1}$ has accordingly been used for the ammonium protons. Similarly a value of J = 452 rads. $sec.^{-1}$ (the NH coupling constant for

imidazolium chloride found by Ralph and Grunwald [44]) was considered adequate for the imidazolium protons.

Chemical Shifts by Slow Sweep

To analyze the data, it was necessary to know the chemical shifts of both types of NH proton with reference to the water line. Due to the overlap it was not possible to obtain these shifts from the broadening measurements. It was therefore necessary to obtain the values from slow sweep spectra of acidic histamine solutions in which the rates of exchange were so slow that no appreciable exchange broadening occurred. Under these conditions it was possible to obtain fairly precise values of the shifts despite the broadenings caused by the electric quadrupole moments of the nitrogen atoms. However, considerable corrections had to be made due to the shift of the water line in the strongly acidic solutions (see experimental section).

To minimize errors, the corrections were made as small as possible by using the highest pH solutions which did not cause significant exchange broadening. Resonance I could be observed in approximately 0.1 M acid (Fig. 4.10) whereas resonance II required about 6 M acid. The large shift of the water line in 6 M acid causes a larger uncertainty in the chemical shift of resonance II. Table 4.10 lists the mean results of several measurements.

Ralph and Grunwald [44] found the NH shift in imidazolium ion at 9.00 ppm. while Meyer, Saika and Gutowsky [72] list ammonium resonances of various alkylammonium ions between 3.1 ppm and 4.2 ppm. There is, therefore, little doubt that resonance I should be assigned to the histamine ammonium resonance, and resonance II should be assigned to the

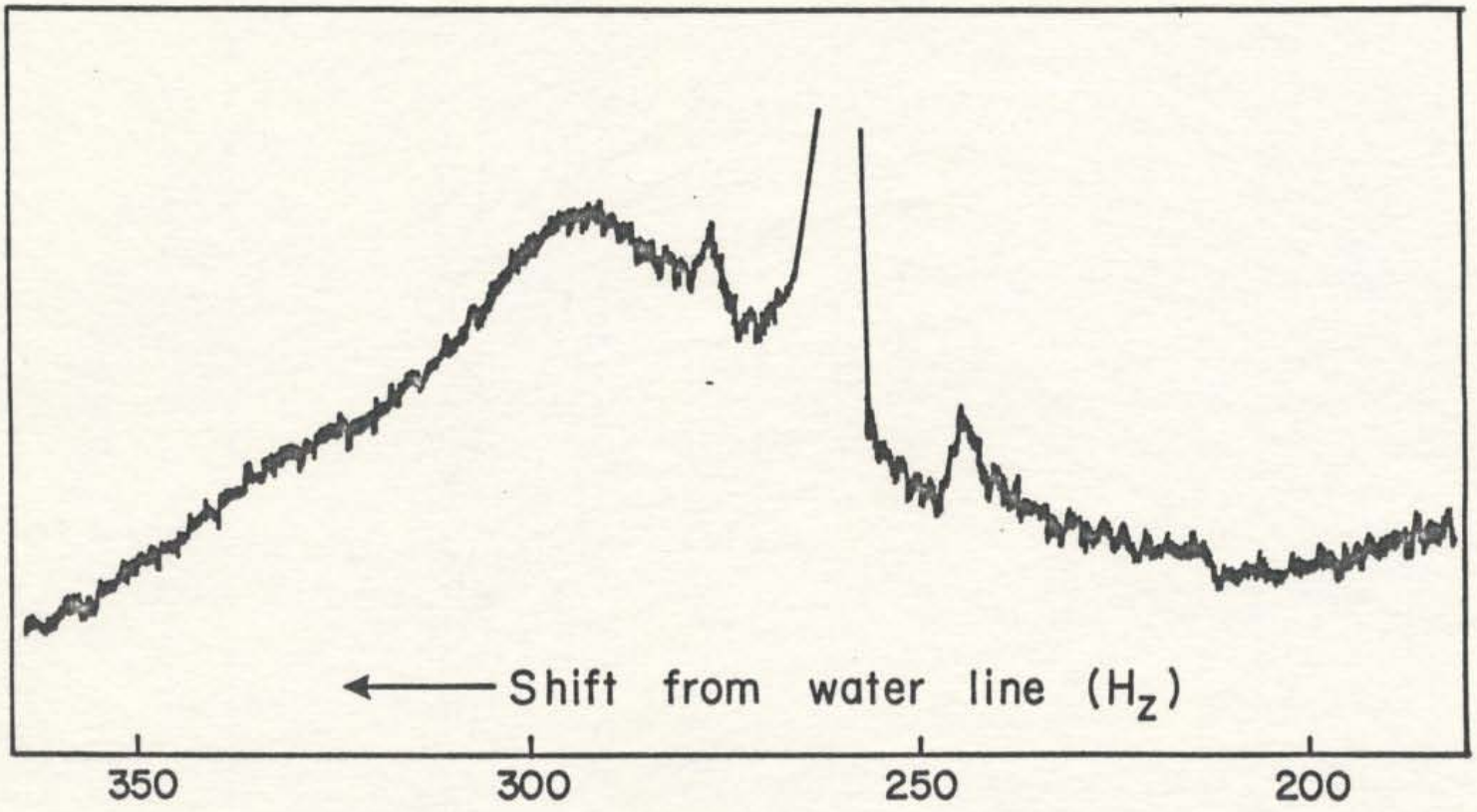

Figure 4.10 Slow sweep spectrum of resonance attributed to protons in amine sites

TABLE 4.10

AMMONIUM PROTON SHIFTS IN HISTAMINE SOLUTIONS

(REFERRED TO THE WATER LINE)

Resonance	[Histamine]	[HCl]	Uncorrected Shift (Rads. $sec.^{-1}$)	Corrected Shift (Rads. $sec.^{-1}$)	Corrected Shift ppm.
I	1.5 M	0.1 M	1830 ± 20	1850 ± 30	3.12±.09
II	0.5 M	6.1 M	3755 ± 100	4925 ± 200	8.32±.34

TABLE 4.11

RESULTS OF DOUBLE IRRADIATION EXPERIMENTS

$[BH_2^{2+}]$	[HCl]	$1/\tau$ for NH_3^+ ($sec.^{-1}$)	$v / [BH_2^{2+}]$
.326	0.50	5.5 ± 0.2	16.5 ± 0.6
.326	0.10	8.6 ± 0.8	25.8 ± 2.4

histamine imidazolium resonances.

Having made these assignments it is noted that the ammonium resonance could be observed at a higher pH than could the imidazolium resonance so that exchange of ammonium protons must have been slower than exchange of imidazolium protons as expected on the basis that the stronger acid will exchange faster. Therefore the amino component will be at a higher pH than the imidazole component in the (Δ/c) data. With the present chemical shift assignments, the (Δ/c) difference plot (Fig. 4.9) confirms that this is the case.

Measurement of the First Order Component of the Side Chain Exchange

Due to the greater basicity of the side chain amino group [67, 68], it was expected that the acid dissociation and hence the pseudo first order rate contribution at this site (when protonated) would be very small. To check this reasoning, Dr. E. K. Ralph [73] conducted double irradiation experiments as devised by Forsen and Hoffman [74]. His results are shown in Table 4.11 (the chemical shift for ammonium protons agreed with the previous value).

It will be seen that fairly high acid concentrations were necessary in these experiments, and as a result acid repression of the pseudo first order rate may be present. At this point however it is not possible to allow for acid repression, so as a first approximation the psuedo first order contribution is taken as constant in these experiments.

Accordingly:

$$v = j_1 [BH_2^{2+}] + j_2' [BH_2^{2+}] [BH^+]$$

where j_1 and j_2' are rate constants.

$$\therefore \quad \frac{v}{[BH_2^{2+}]} = j_1 + j_2' [BH^+]$$

$$\therefore \quad \frac{v}{[BH_2^{2+}]} = j_1 + j_2' K_{A1} \frac{[BH_2^{2+}]}{[H^+]} \qquad (4.3)$$

substitution of the data provides two simultaneous equations which can be solved to give

$$j_1 = 14.2 \pm 1.4 \text{ sec.}^{-1}$$

and

$$j_2' = (7.6 \pm 2.6) \times 10^6 \text{ l.mole.}^{-1} \text{ sec}^{-1}.$$

Experiments in Which the Temperature was Varied

Each of the data series at fixed histamine concentrations shows a plateau in the pH region approximately 0.5 to 2. Since the ammonium resonance showed no significant exchange broadening at pH ≃ 1 (in the slow sweep spectra) it would appear that the broadening at the plateau is due to exchange of imidazolium protons.† A series was therefore run using a solution from this plateau at various temperatures. This was expected to show the temperature dependance of the imidazolium proton

†Since the largest reduction of (Δ/c) with increasing RF field occurred at about pH 3 to 4, it follows that the lifetime broadening region for side chain exchange was in this pH region. This is further evidence that the significant broadening due to ammonium proton exchange occurs somewhat above pH = 1.

exchange rate in this solution, with the maximum broadening depending on the chemical shift of the imidazolium protons. Table 4.12 lists such results for a solution which was 0.0595 M in histamine with a calculated pH of 1.467 at 25°C. Assuming that all exchange broadening is due to imidazolium proton exchange it was possible to calculate (Δ/p) values and hence to determine the imidazolium proton chemical shift, (δ_r), as 4790 rads sec.$^{-1}$ from $(\Delta/p)_{max}$. Rates were then calculated in the usual way.

Assuming the Arrhenius equation for the rate constant,

$$\text{ln. } (k_1) = \frac{E_a}{RT} + \text{ln } A$$

we can use calculated values of $\frac{v}{[BH_2^{2+}]}$ to substitute for k_1 and hence plot ln (k_1) against 1/T (Fig. 4.11). A least squares fit to a straight line gives

Activation energy (E_a) = 9.2 ± 0.6 kcal. mole^{-1} and

ln A = 24.7 ± 0.9

This experiment was repeated using a 95% deuterated (i.e. 95% D_2O and 5% H_2O) solution which was 0.0595 M. in histamine with a calculated pH of 1.94 at 25° (Table 4.13). Results obtained were

$$\delta_r^* = 4795 \text{ rads. sec.}^{-1}$$

$$E_a^* = 10.2 \pm 0.7 \text{ kcal. mole}^{-1}$$

$$\text{ln } A^* = 25.7 \pm 0.8$$

TABLE 4.12

5.95×10^{-2} M. HISTAMINE SOLUTIONS AT pH 1.467 RUN AT VARIOUS TEMPERATURES WITH RF FIELD AT 632 RADS. SEC.$^{-1}$†

$1/T_{1p}$	$1/T_1$	Δ	Δ/p	$\ln(k_1)$	$10^3/T$
2.830	0.390	2.440	2261	8.863	3.415
2.885	0.353	2.532	2350	9.389	3.356
2.845	0.331	2.514	2333	9.351	3.300
2.723	0.301	2.422	2244	9.567	3.247
2.654	0.302	2.352	2178	9.510	3.247
2.126	0.287	1.839	1704	10.034	3.195
2.370	0.267	2.103	1949	9.864	3.177
1.927	0.251	1.676	1555	10.160	3.146
1.741	0.227	1.514	1401	10.295	3.101
1.560	0.200	1.360	1263	10.421	3.050

†The chemical shift (δ_r) which fitted this data was 4790 rads.sec^{-1}.

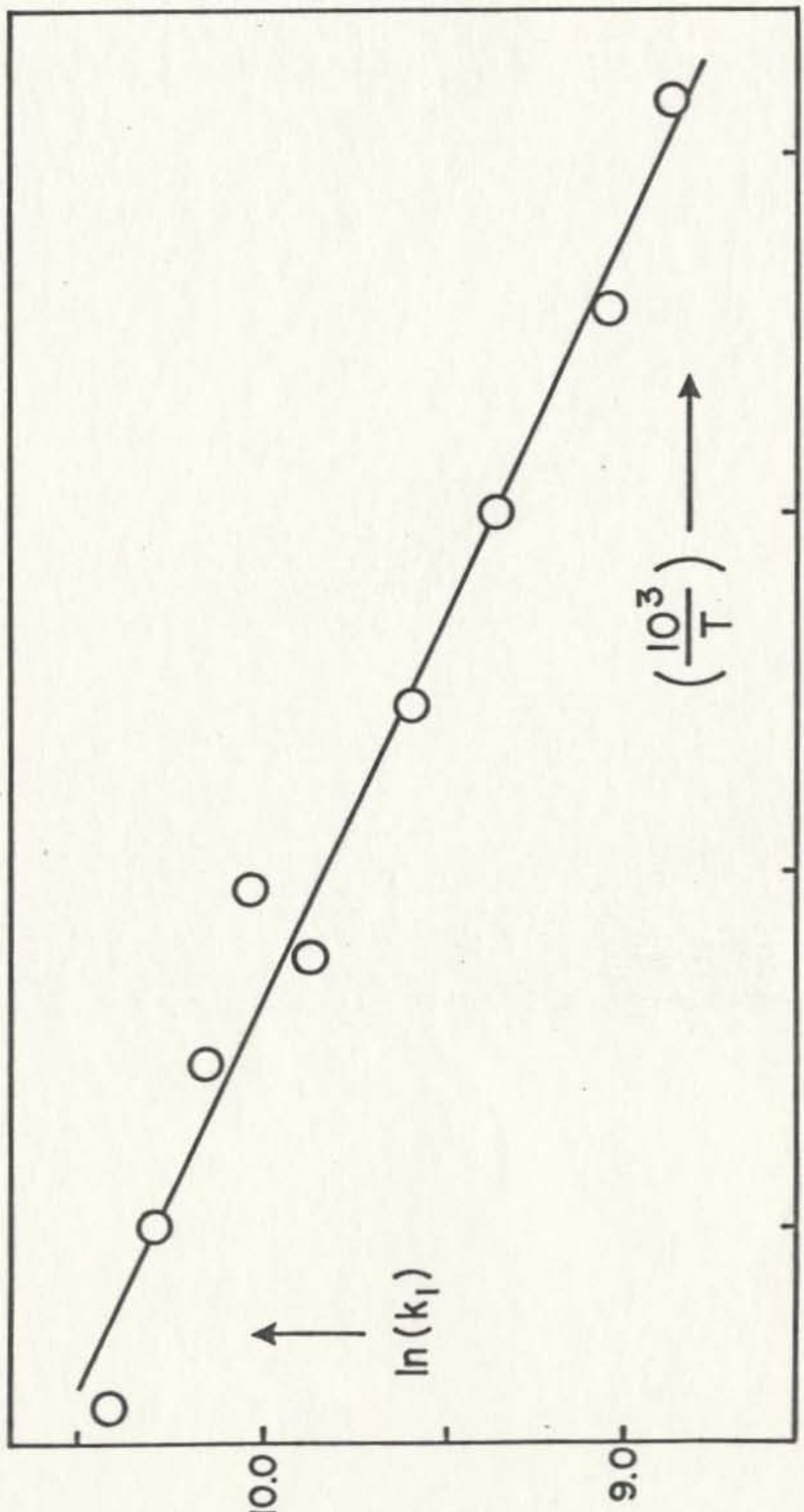

Figure 4.11 Temperature dependence of first order imidazole rate constant

TABLE 4.13

SOLUTION IN 95% D_2O, 5.95×10^{-2} M. IN HISTAMINE AT pH 1.941
RUN AT VARIOUS TEMPERATURES WITH RF FIELD
AT 632 RADS. SEC.$^{-1}$†

$1/T_{1p}$	$1/T_1$	Δ	Δ/p	$\ln(k_1)$	$10^3/T$
1.514	0.104	1.410	1307	7.971	3.445
1.731	0.101	1.630	1511	8.151	3.386
1.998	0.096	1.902	1765	8.365	3.355
2.145	0.090	2.055	1903	8.483	3.300
2.521	0.087	2.434	2256	8.849	3.246
2.641	0.082	2.559	2372	9.175	3.195
2.396	0.069	2.327	2156	9.623	3.146
2.333	0.094††	2.239	2074	9.710	3.101
2.112	0.133††	1.979	1836	9.927	3.050

†The chemical shift (δ_r) which fitted this data was 4795 rads.sec^{-1}.

††Values of $1/T_1$ at the two highest temperatures show an unexpected increase. If the first seven points in this table are fitted to an Arrhenius equation of the form $\ln (1/T_1) = E_a/RT + \ln A$ and values of $1/T_1$ at the two highest temperatures obtained by extrapolation, only small differences result. In this case $E_a^* = 10.3 \pm 0.6$ kcal. mole^{-1} and $\ln A^* = 25.9 \pm 0.9$.

Kinetic Analysis of the Data at Fixed Histamine Concentrations above pH Approximately 1.0

Chemical Shift Used

The slow sweep value of $\delta_s = 1850 \pm 30$ rads. sec.$^{-1}$ was used for the side chain N-H to HOH chemical shift. Two values were available for the ring NH to HOH chemical shift (one from the slow sweep experiments and one from the experiment in which the temperature was varied). The mean of these values, viz. $\delta_r = 4860$ rads. sec.$^{-1}$, was used in the following analysis with the maximum uncertainty estimated at $\pm$ 150 rads. sec.$^{-1}$.

Attempts to Fit the Data with Simple Rate Laws

The first calculations were carried out using two rate laws each consisting of a first order term and a second order term in histamine. Viz. for exchange of imidazolium protons,

$$\frac{v_r}{[BH_2^{2+}]} = k_1 + k_2 [BH^+] \qquad (4.4)$$

and for exchange of ammonium protons

$$\frac{v_s}{[BH_2^{2+}]} = j_1 + j_2' [BH^+] \qquad (4.5)$$

For exchange of ammonium protons, j_1 was fixed at 14.2 sec.$^{-1}$ as determined by the double irradiation experiments. The value of k_1 was set by the plateau of the (Δ/c) versus pH plot for each series of data. The second order term (k_2) of the rate law for imidazole exchange was then fixed by subtracting the maximum broadening due to ammonium exchange,

and this in turn was fixed by the chemical shift of the ammonium protons. Rates of imidazolium exchange (v_r) were then calculated over the full concentration range using Equation (4.4). Equations (1.21) and (1.17) could then be used to calculate the theoretical contribution to the broadening which was caused by imidazolium exchange. Subtraction of these imidazolium contributions from the total experimental exchange broadenings provided the contributions to the broadenings which were caused by ammonium exchange. The ammonium broadenings were used to calculate ammonium exchange rates using Equations (1.17) and (1.21) and the second order rate constant of the ammonium rate law (j_2') was obtained by a linear least squares fit of these rates versus $[BH^+]$.

During the above numerical analysis, the chemical shifts were allowed to move within their maximum estimated error limits in order to obtain the best fits between calculated and experimental exchange broadenings. In some cases, however, the minimum discrepancy between theoretical and experimental (Δ/c) values could not be reduced below the estimated error limits for extended pH ranges (see dotted plots in Figs. 4.12 and 4.13). Also when the ammonium rates were plotted against $[BH^+]$, considerable deviations from straight lines were obtained. With this failure to obtain a satisfactory fit, it was considered necessary to introduce a further first order term into the theoretical rate laws.

More Complex Rate Laws

Since the ammonium rate law has a very small pseudo first order component, it is not clear how any change in this law could cause a significant improvement in the fit. In contrast, the first order term

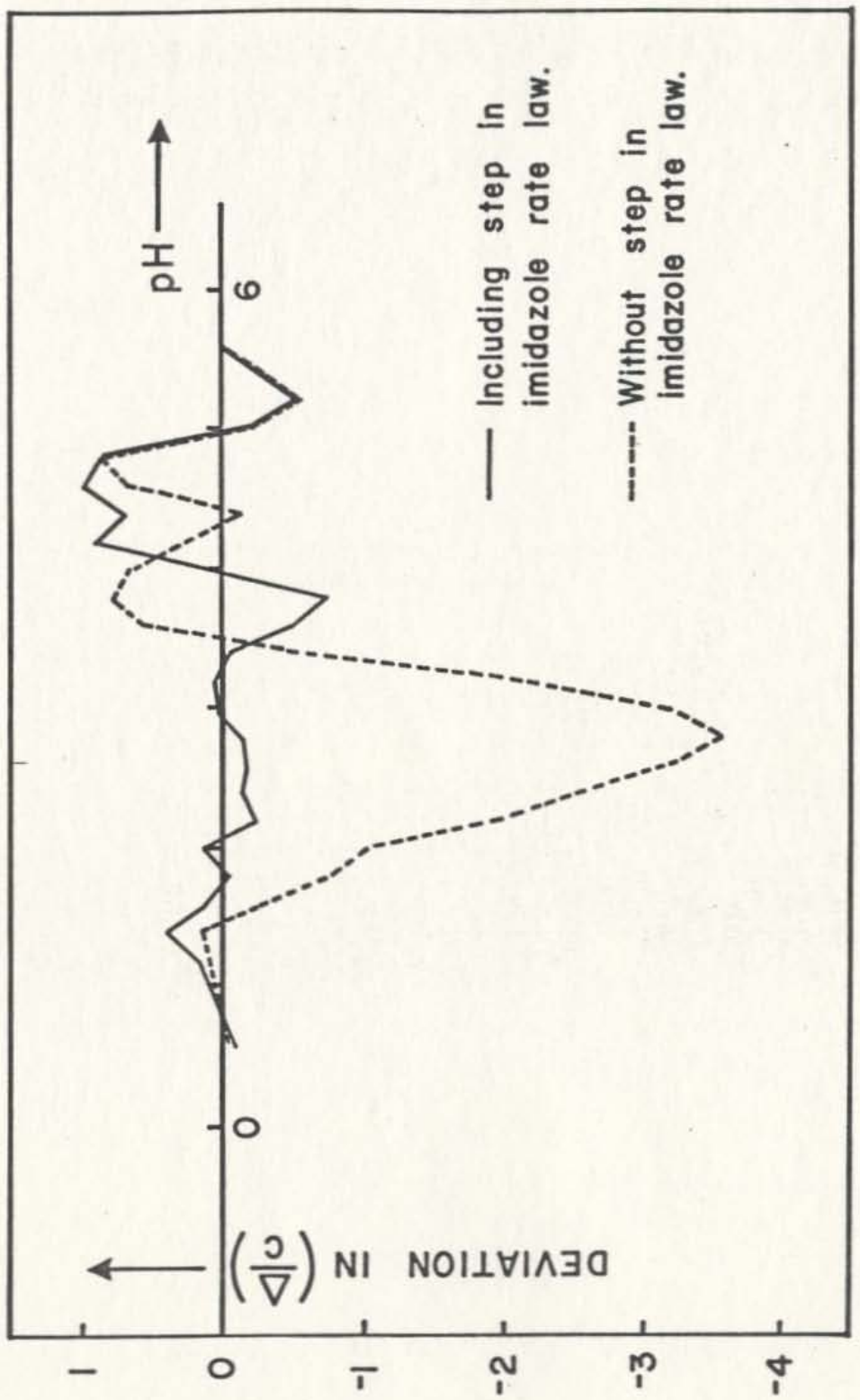

Figure 4.12 Fitting of 2.98×10^{-2}M. smoothed data

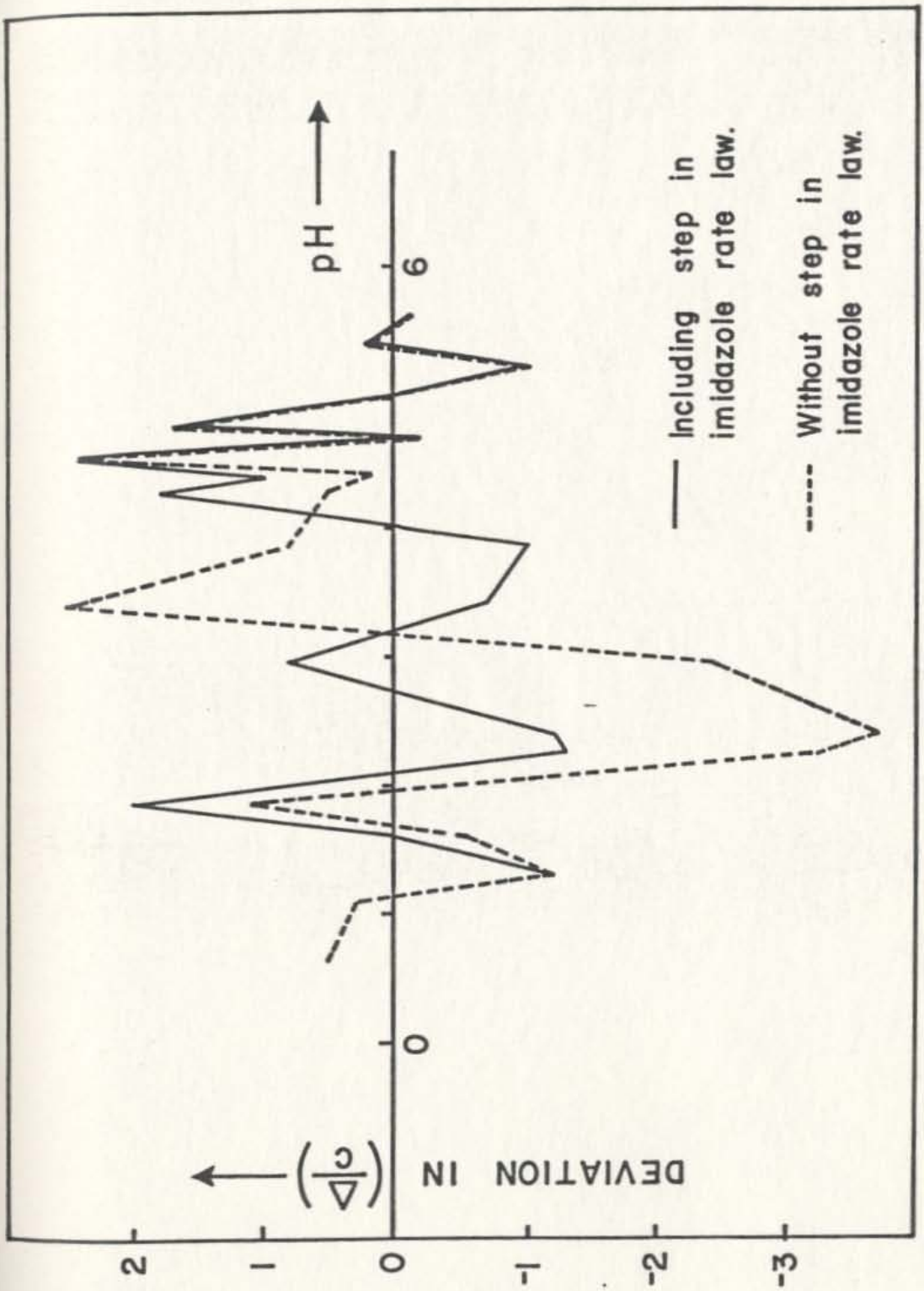

Figure 4.12a Fitting of 2.98×10^{-2}M. original data

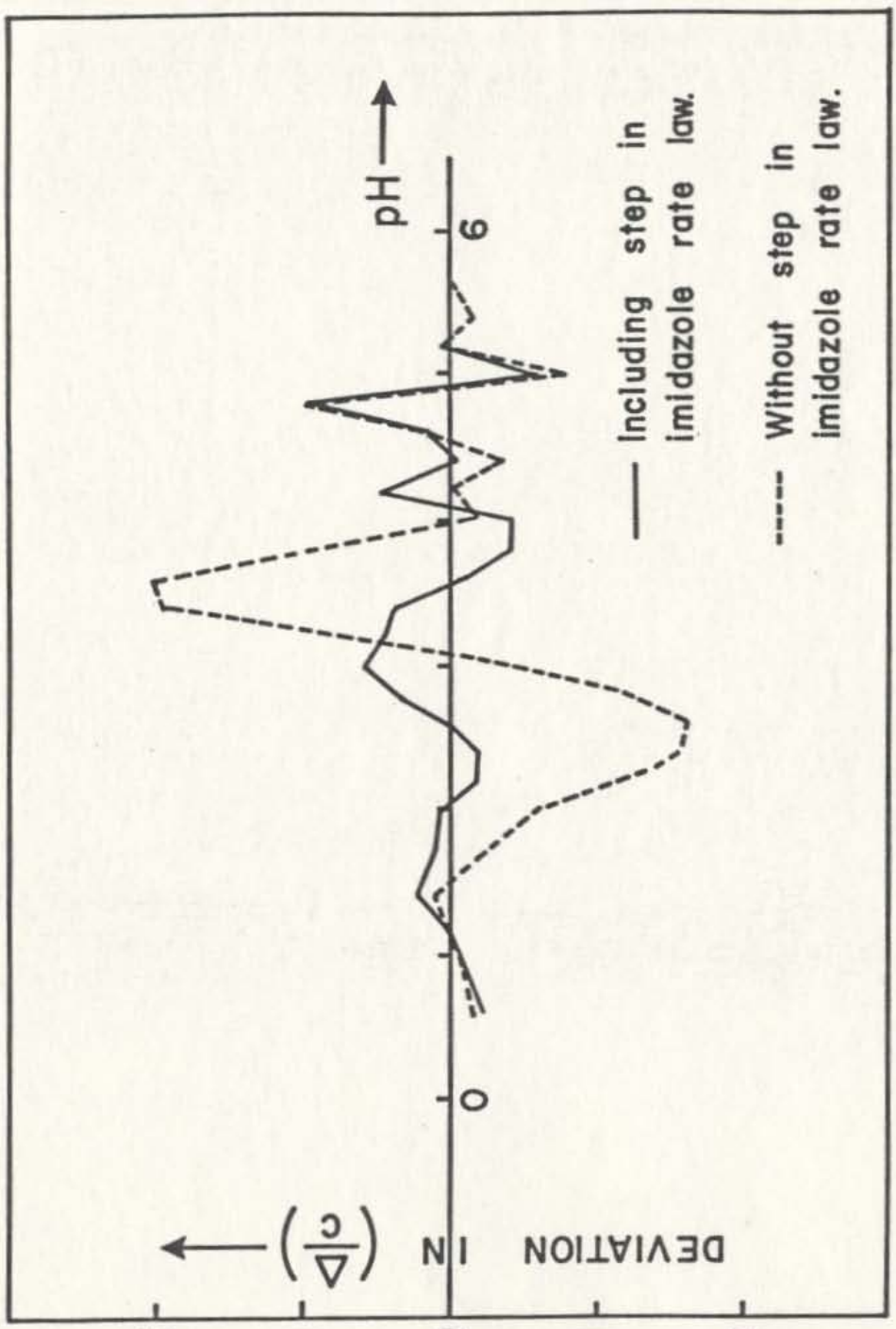

Figure 4.13 Fitting of 5.96×10^{-2}M smoothed data

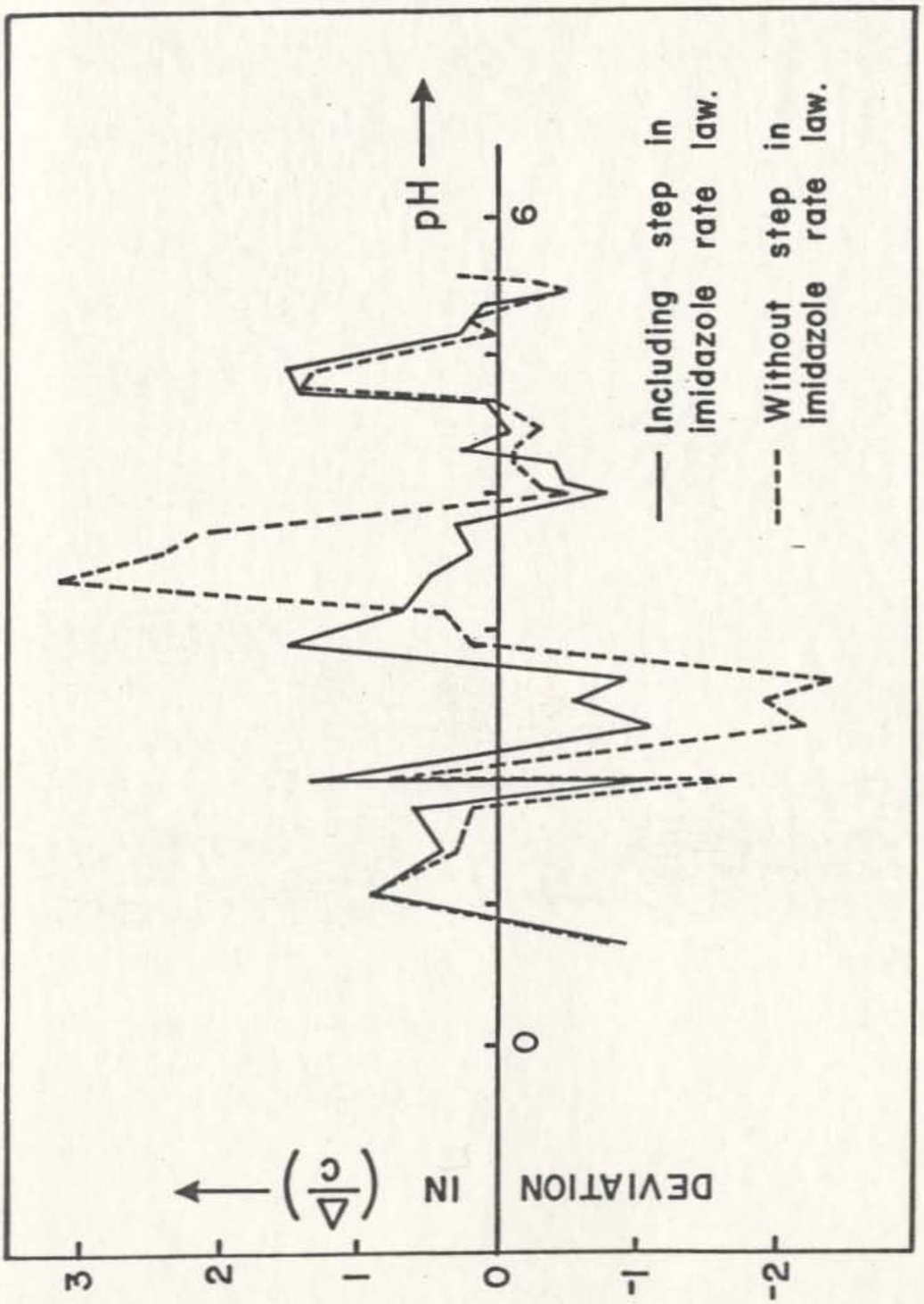

Figure 4.13a Fitting of 5.96×10^{-2}M. original data

in the rate law for imidazolium exchange may very possibly show significant "steps" for two different reasons.† (i) Ralph and Grunwald [44] found two parallel first order proton exchange processes in their work on imidazole. They attributed one process to exchange following acid dissociation and the other process to exchange occurring in an ionized state. (ii) Previous work on amines with an ionic charge [35] has shown two parallel first order processes of proton exchange. These two processes have been ascribed to exchange occurring in the trans and gauche isomers respectively.

A parallel first order process due to either of these two reasons would result in the same rate expression for the exchange of imidazolium protons:

$$\frac{v_r}{[BH_2^{2+}]} = k_1 + \frac{k_1'}{1+Q_1[H^+]} + k_2\,[BH^+] \qquad (4.6)$$

where $\frac{k_1}{1+Q_1[H^+]}$ is the new term defining the step in the first order law which would be caused by a parallel first order process due to either of the above reasons.

The ammonium exchange will be governed by the previous simple law

$$\frac{v_s}{[BH_2^{2+}]} = j_1 + j_2'\,[BH^+] \qquad (4.5)$$

---

†The word "step" in this discussion is used to indicate that the first order term is pH dependent. See, for example, Equations (1.30) to (1.37) in the introduction which shows one mechanism by which a pH dependence can arise.

Procedure for Fitting the Data Using the New Rate Law for Imidazolium Proton Exchange

After various trials, the following procedure was found to be the most successful method for obtaining a satisfactory fit with the rate laws given by Equations (4.5) and (4.6).

(i) The chemical shifts were fixed at the previously determined values, δ_r = 4860 rads. sec.$^{-1}$ and δ_s = 1850 rads. sec.$^{-1}$.

(ii) j_1 was fixed at 14.2 sec.$^{-1}$.

(iii) k_1 was initially set by the plateau of the (Δ/c) versus pH plot.

(iv) k_1' was initially set at zero.

(v) k_2 was selected so that the maximum broadening due to ammonium exchange was in agreement with δ_s = 1850 rads. sec.$^{-1}$.

(vi) j_2' was chosen to give the correct rate at the maximum ammonium broadening.

(vii) The rate law for ammonium exchange was now used to calculate broadenings ($(\Delta/c)_s$ values).

(viii) The $(\Delta/c)_s$ values were subtracted from the experimental $(\Delta/c)_e$ values and the results used to calculate rates of imidazolium exchange. When these rates were plotted as ordinate against $[BH^+]$, a straight line was obtained for points arising from pH $\geq$ 4.4, and the least squares gradient of this line was used to set a new value for k_2. Below pH $\simeq$ 4.4, the rates were found to fall off below the straight line, and this fall off was interpreted as a step in the first order component. Accordingly the rates below pH = 4.4 were treated by subtracting k_1 and also subtracting the calculated second order rate. The residual rates (v') were the contributions from the k_1' term

i.e. $$\frac{v'}{[BH_2^{2+}]} = \frac{k_1'}{1 + Q_1[H^+]}$$

$$\therefore \quad \frac{[BH_2^{2+}]}{v'} = \frac{1}{k_1'} + \frac{Q_1[H^+]}{k_1'} \qquad (4.6a)$$

A plot of $\frac{[BH_2^{2+}]}{v'}$ as ordinate against $[H^+]$ produced a straight line graph which could be used to determine values for k_1' and Q_1.

(ix) The values obtained for k_1, k_1', Q_1 and k_2 were now used to calculate theoretical $(\Delta/c)_r$ broadenings due to imidazolium exchange. Small adjustments were made in k_1 in order to maintain good agreement with the plateau of the experimental $(\Delta/c)_e$ curve--i.e. $(\Delta/c)_e = (\Delta/c)_r + (\Delta/c)_s$. Small adjustments were also made in k_2 in order to keep the maximum broadening due to ammonium exchange in agreement with $\delta_s = 1850$ rads. sec.$^{-1}$.

(x) The $(\Delta/c)_r$ calculated values were now subtracted from the $(\Delta/c)_e$ values and the residual broadenings used to calculate ammonium exchange rates. A plot of these rates against $[BH^+]$ gave a straight line, and a least squares fit of the data points in the exchange narrowing region was used to determine a new value for j_2' while j_1 remained fixed at 14.2 sec.$^{-1}$. The exchange narrowing region was used to determine j_2' since (a) the side chain broadening was a larger fraction of the total broadening in this region, and (b) the k_1' term was still only very approximately determined, and it strongly affected the ammonium lifetime broadening region, but only slightly affected the

exchange narrowing region.

(xi) The new ammonium rate law was now used as in step (vii) and the whole process repeated as many times as necessary in order to obtain reproducible parameters across the full pH range under consideration. Checks were then made to assure (a) that the calculated (Δ/c) values agreed with the original experimental data within the limits of experimental error, and (b) that the rate law plots were linear.

Results from the Above Fitting Procedure

The above method was used to obtain rate constants from each of the five series of measurements made at low RF fields and the constants are listed in Table 4.14. The fitted data in Table 4.15 is used to demonstrate the determination of the rate laws. After several calculation cycles as described above, the parameters for the imidazole rate law were set at the following values.

$\delta_r = 4850$ rads. sec.$^{-1}$

$k_1 = 6120$ sec.$^{-1}$

$k_1' = 8885$ sec.$^{-1}$

$Q_1 = 4810$

$k_2 = 3.01 \times 10^7$ ℓ.mole.$^{-1}$ sec.$^{-1}$.

Equation (4.6) was used to calculate the specific imidazole exchange rate $\left(\frac{v_r}{[BH_2^{2+}]} \right)$ at intervals of 0.2 pH units. By use of Equation (1.21) followed by Equation (1.17) and (1.16), corresponding exchange broadenings, $(\Delta/c)_r$, could be calculated. The exchange broadenings are listed in Table 4.15 and they are subtracted from the total experimental broadenings

TABLE 4.14

PARAMETERS OBTAINED FROM THE SERIES OF DATA AT FIXED HISTAMINE CONCENTRATIONS[†]

Histamine Molarity	.00600	.0298	.0596	.270	.0595[††]
RF Field	251	500	200	355	632
δ_r	4850	4860	4860	4860	4860
k_1	6120	5120	5880	5050	4230
k_1'	8885 (13%)	5705 (7%)	5397 (12%)	5879 (50%)	828 (30%)
Q_1	4810 (20%)	1404 (10%)	1556 (15%)	2242 (60%)	6525 (43%)
$k_H \times 10^{-6}$	1.6	4.4	4.4	5.1	0.47
$10^{-7} \times k_2$	3.01 (2%)	3.90 (4%)	3.90 (3%)	5.85 (4%)	1.42 (3%)
δ_s	1840	1850	1850	1850	1840
j_1	14.2	14.2	14.2	14.2	4[†††]
$10^{-6} \times j_2'$	32.5 (1%)	9.7 (2%)	6.45 (1%)	4.02 (.5%)	2.4 (2%)

[†]Percentages in brackets show the standard deviations of linear least squares fits as described in the text.

[††]This column refers to 95% deuterated solutions.

[†††]Calculated from an estimated isotope effect on j_1. Since j_1 is so small, the analysis is very insensitive to this value.

TABLE 4.15

COMPARISON OF THEORETICAL BROADENINGS WITH SMOOTHED EXPERIMENTAL BROADENINGS FOR 6.00×10^{-3} M. HISTAMINE SOLUTIONS

pH	$(\Delta/c)_s$	$(\Delta/c)_r$	$(\Delta/c)_{s+r}$	$(\Delta/c)_e$
2.400	.6	40.5	41.2	41.3
2.600	.9	41.0	41.9	41.7
2.800	1.4	41.7	43.1	43.0
3.000	2.1	42.5	44.6	44.7
3.200	3.2	43.2	46.4	46.3
3.400	5.0	43.5	48.5	48.5
3.600	7.6	43.2	50.8	51.1
3.800	11.6	42.2	53.8	53.8
4.000	16.7	40.7	57.4	57.4
4.200	21.9	38.6	60.5	60.4
4.400	24.4	35.9	60.3	60.1
4.600	22.6	32.5	55.1	54.5
4.800	18.0	28.4	46.4	46.4
5.000	13.0	23.8	36.8	37.3
5.200	9.1	19.2	28.3	28.5
5.400	6.4	15.1	21.5	21.1
5.600	4.6	11.8	16.4	16.5

in the second column of Table 4.15a. These residual experimental broadenings were attributed to ammonium exchange and Equation (1.16) could therefore be used to convert them to the $(\Delta/p)_s$ values listed in the third column of Table 4.15a. The specific rates, $\left(\frac{v_s}{[BH_2^{2+}]}\right)$, were obtained in the usual way by means of Equations (1.17) and (1.21). The linear plot in Figure (4.14) is consistent with the amine rate law (4.5) and a least squares fit of this data gives

$$j_1 = -14 \pm 235 \text{ sec.}^{-1}$$

and $$j_2' = (32.5 \pm 0.4) \times 10^6 \text{ ℓ.mole.}^{-1} \text{ sec.}^{-1}.$$

The value of j_1 is in good agreement with the results of the double irradiation experiments (+ 14 sec.^{-1}). This latter value for j_1 was now used with the value for j_2' to calculate the $(\Delta/c)_s$ values which are listed in Table 4.15 and which are used in Table 4.15b . The first five columns of Table 4.15b are similar to Table 4.15a. The plot of specific rate versus $[BH^+]$ is linear above pH 4.6, but falls below this straight line at lower pH (Figure 4.15). The non-linearity results from the pH dependence of the first order component of the rate law and has been referred to as a 'step' in the rate law. To determine the parameters of the imidazolium rate law, the least squares gradient of the linear portion of the plot determined k_2. This constant could then be used to calculate the second order contributions to the specific rate in the pH region 3.0 to 4.4. The pH independent part of the first order law has already been set at 6120 sec.^{-1}. The second order contributions and the pH independent first order contributions can now be subtracted from the specific rates in the pH range 3.0 to 4.4. The residual parts of the specific rate are used to calculate the reciprocal rates listed in the

TABLE 4.15a

CALCULATION OF THE AMINO RATE LAW FOR 6.00×10^{-3} M HISTAMINE SOLUTIONS

pH	$\left(\frac{\Delta}{c}\right)_e - \left(\frac{\Delta}{c}\right)_r$	$(\Delta/p)_s$	$\left(\frac{v_s}{[BH_2^{2+}]}\right)$	$10^5[BH^+]$
2.400	0.8	30	94	0.170
2.600	0.7	24	75	0.270
2.800	1.3	46	142	0.427
3.000	2.2	81	250	0.677
3.200	3.1	116	356	1.072
3.400	5.0	183	565	1.698
3.600	7.9	290	909	2.687
3.800	11.6	429	1390	4.247
4.000	16.7	618	2169	6.703
4.200	21.8	808	3350	10.55
4.400	24.2	898	4647	16.56
4.600	22.0	814	9015	25.83
4.800	18.0	666	12893	39.93
5.000	13.5	500	18838	60.91
5.200	9.3	344	28833	91.12
5.400	6.0	224	45395	132.6
5.600	4.7	174	58966	186.1

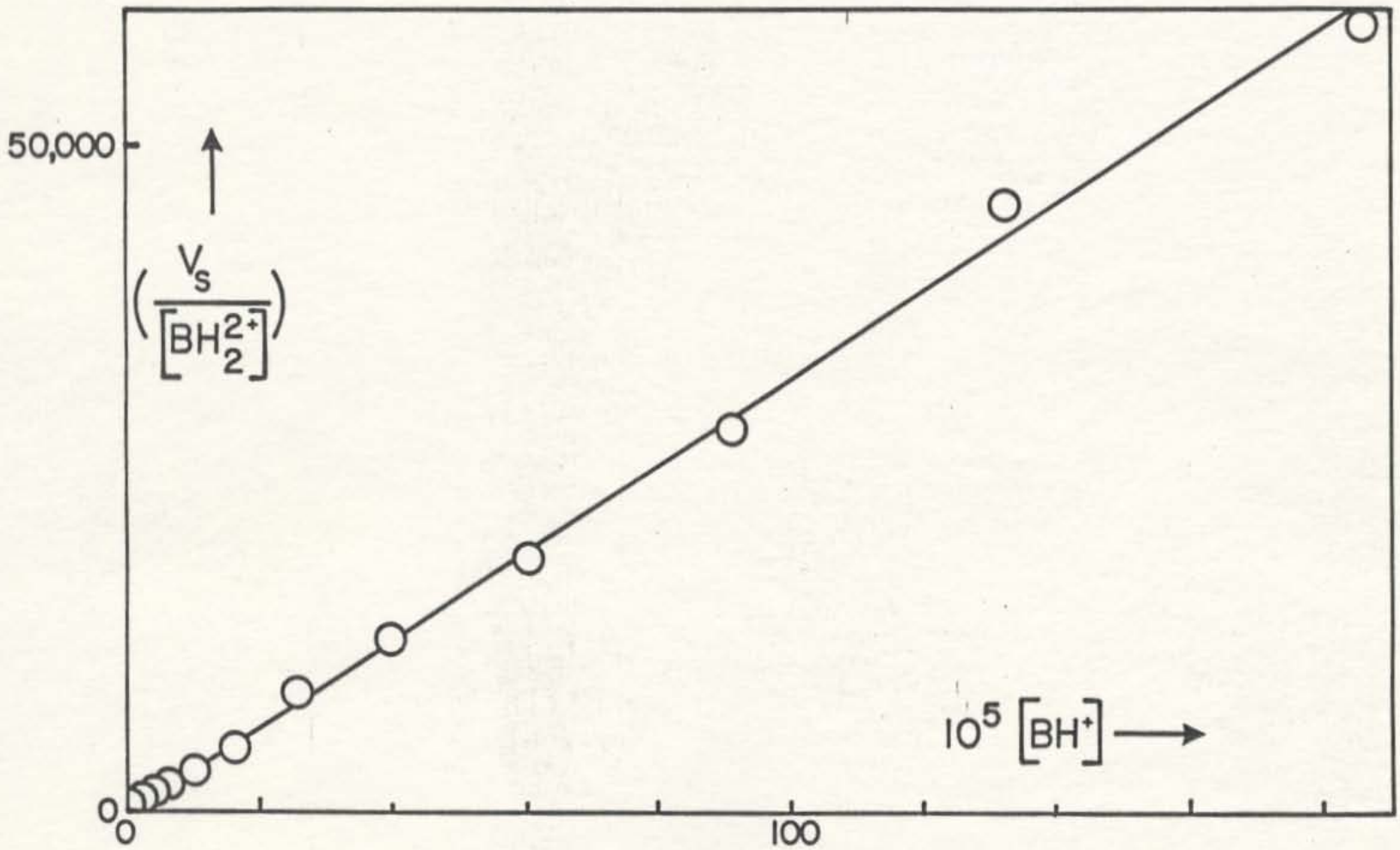

Figure 4.14 Amino rate law for 6.00×10^{-3} M. histamine solutions

TABLE 4.15b

CALCULATION OF THE IMIDAZOLE RATE LAW FOR 6.00×10^{-3} M. HISTAMINE SOLUTIONS

pH	$\left(\frac{\Delta}{c}\right)_e - \left(\frac{\Delta}{c}\right)_s$	$\left(\frac{\Delta}{p}\right)_r$	$\left(\frac{v_r}{[BH_2^{2+}]}\right)$	$10^5\ [BH^+]$	$\frac{10^4\ [BH_2^{2+}]}{v'}$	$10^5\ [H^+]$
2.400	40.7	2258	6639	0.170		
2.600	40.8	2264	6691	0.270		
2.800	41.6	2312	7127	0.427		
3.000	42.6	2369	7846	0.677	6.58	100.0
3.200	43.1	2395	8351	1.072	5.25	63.1
3.400	43.5	2415	9700	1.698	3.26	39.8
3.600	43.5	2409	10706	2.687	2.66	25.1
3.800	42.2	2346	12486	4.247	1.97	15.85
4.000	40.7	2258	14157	6.703	1.67	10.00
4.200	38.5	2140	16131	10.55	1.47	6.31
4.400	35.7	1983	18678	16.56	1.33	3.98
4.600	31.9	1769	22426	25.83		
4.800	28.4	1576	26306	39.93		
5.000	24.3	1348	32050	60.91		
5.200	19.4	1076	41618	91.12		
5.400	14.7	819	55979	132.6		
5.600	11.9	660	70196	186.1		

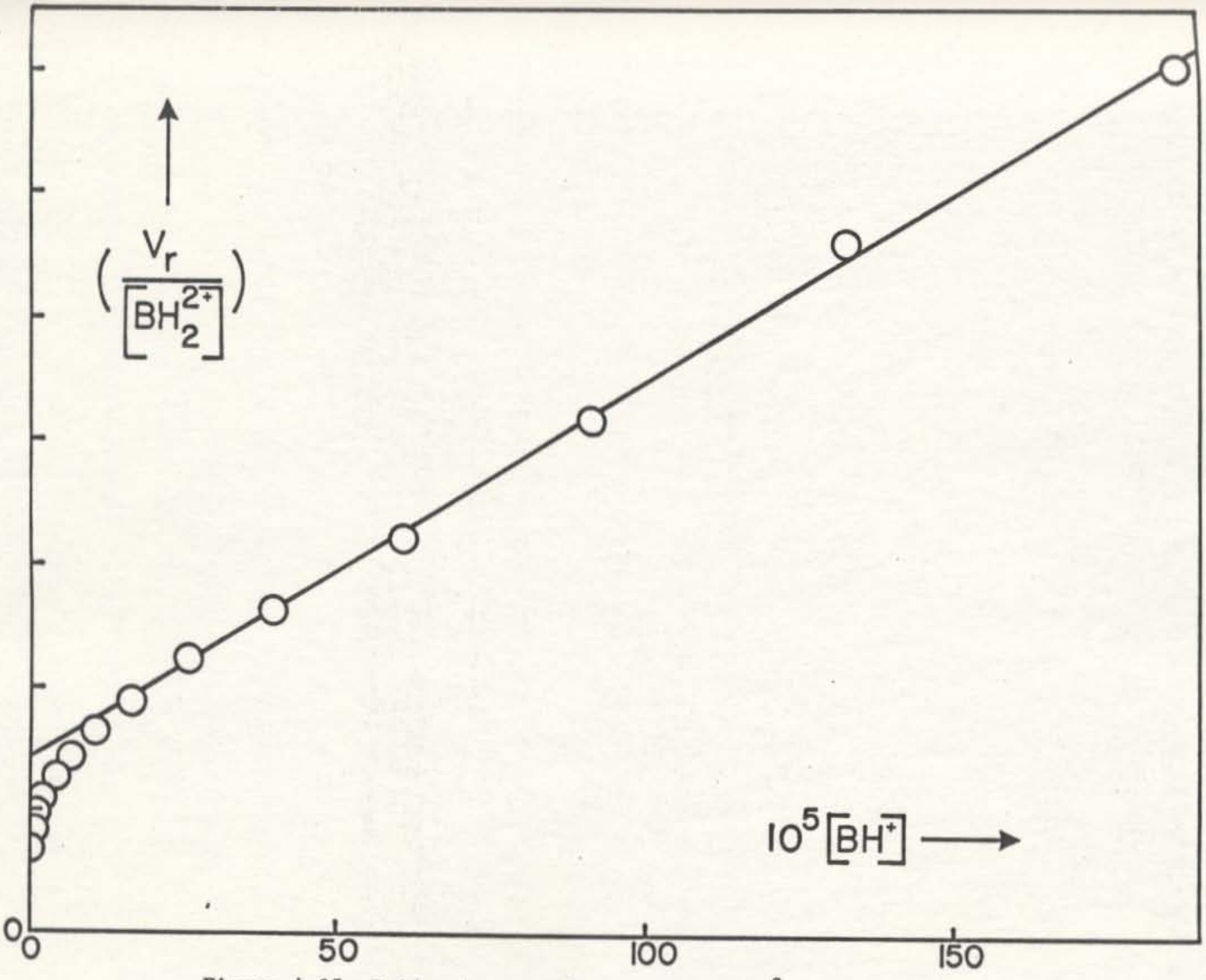

Figure 4.15 Imidazole rate law for 6.00×10^{-3} M. histamine solutions

sixth column of Table 4.15b and the plot of these reciprocal rates versus $[H^+]$ is shown in Figure (4.15a). The plot is linear and a least squares fit with Equation (4.6a) provides values for k_1' and Q_1. The newly determined parameters for the imidazolium rate law are

$$\delta_r = 4850 \text{ rads. sec.}^{-1}$$

$$k_1 = 6120 \text{ sec.}^{-1}$$

$$k_1' = 8850 \pm 160 \text{ sec.}^{-1}$$

$$Q_1 = 5085 \pm 1160$$

$$k_2 = (3.04 \pm 0.06) \times 10^7 \text{ ℓ.mole.}^{-1} \text{ sec.}^{-1}.$$

Since all of these parameters are in good agreement with the values obtained previously, a further cycle of calculations was not necessary.

Similar cyclic calculations were carried out on the other series of data and similar rate law plots were obtained. The ammonium rate law was always linear and the imidazolium rate law always fell away at lower pH. As expected, the non-linearity became less pronounced as $[BH_2^{2+}]$ increased. The calculated broadenings for the different $[BH_2^{2+}]$ series are compared with the smoothed experimental broadenings in Tables 4.15 to 4.19. Agreement is seen to be well within the limits of experimental error. Deviations between the calculated and experimental broadenings are shown by the continuous lines in Figures 4.12 and 4.13. Figures 4.12 and 4.12a show deviations for 2.98×10^{-2} M solutions while Figures 4.13 and 4.13a show deviations for 5.95×10^{-2} M solutions. For comparison, each of these figures also shows the deviations which were obtained using the simple rate laws 4.4 and 4.5. The theoretical components of the total experimental broadenings are illustrated in Figure 4.16, using the 2.7×10^{-1} M histamine series data.

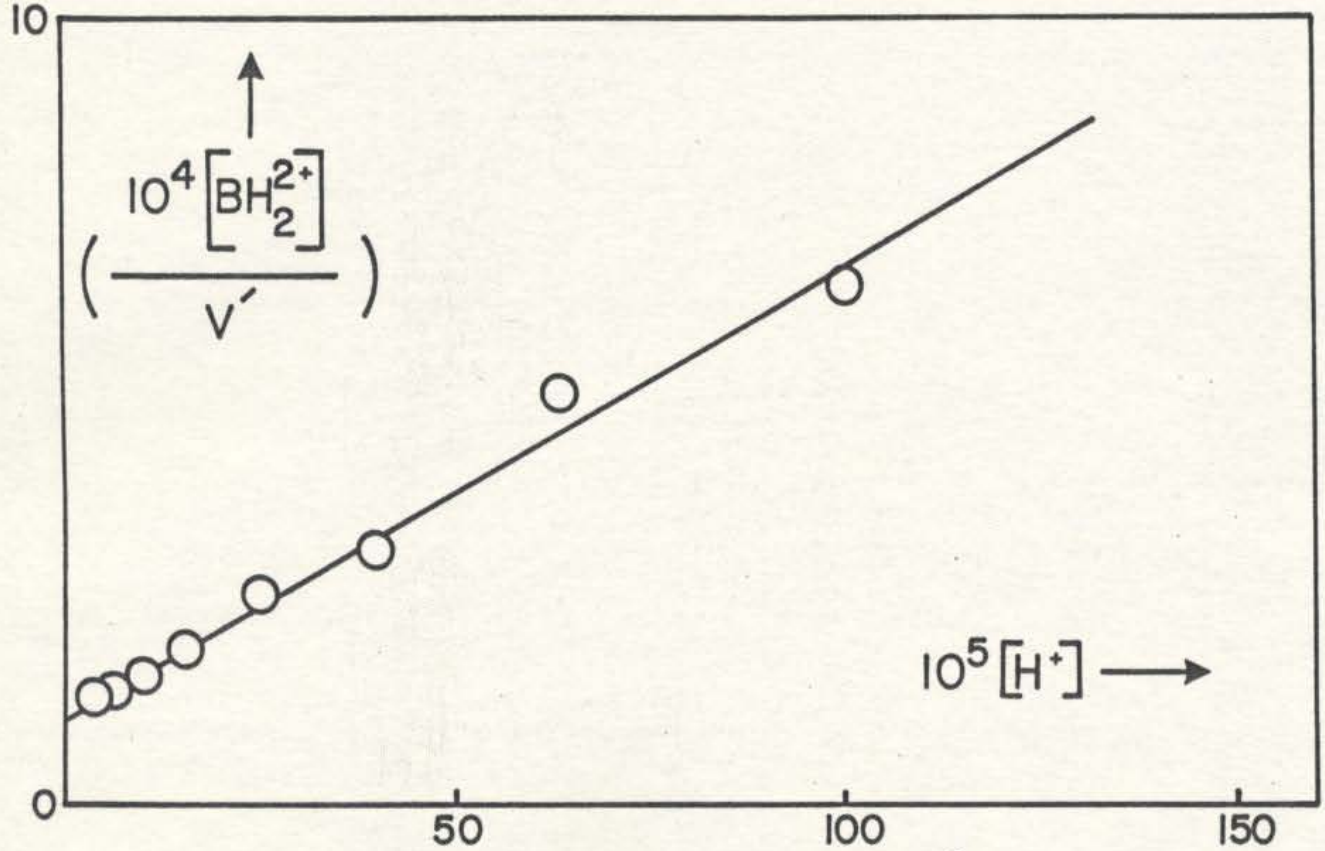

Figure 4.15a Determination of k_1' and Q for 6.00×10^{-3} M. histamine solutions

TABLE 4.16

COMPARISON OF THEORETICAL BROADENINGS WITH SMOOTHED EXPERIMENTAL BROADENINGS FOR 2.98×10^{-2} M HISTAMINE SOLUTIONS

pH	$(\Delta/c)_s$	$(\Delta/c)_r$	$(\Delta/c)_{s+r}$	$(\Delta/c)_e$
.600	.1	35.8	36.0	36.1
.800	.1	35.9	36.0	36.1
1.000	.1	36.0	36.1	36.1
1.200	.2	36.1	36.3	36.1
1.400	.2	36.3	36.5	36.1
1.600	.2	36.6	36.8	36.7
1.800	.3	37.0	37.2	37.3
2.000	.3	37.6	37.9	37.8
2.200	.5	38.4	38.9	39.1
2.400	.7	39.5	40.2	40.4
2.600	1.0	40.8	41.8	42.0
2.800	1.5	42.1	43.7	43.8
3.000	2.3	43.1	45.5	45.5
3.200	3.6	43.5	47.2	47.1
3.400	5.6	43.0	48.6	48.7
3.600	8.6	41.4	50.0	50.5
3.800	12.9	38.3	51.3	52.0
4.000	18.2	33.8	52.0	51.9
4.200	22.7	28.1	50.8	49.9
4.400	23.9	21.8	45.7	45.0
4.600	20.8	16.1	36.9	35.9
4.800	15.7	11.4	27.1	26.2
5.000	11.0	7.9	18.9	19.1
5.200	7.6	5.4	12.0	13.5
5.400	5.2	3.8	9.0	9.3
5.600	3.7	2.7	6.3	6.3

TABLE 4.17

COMPARISON OF THEORETICAL BROADENINGS WITH SMOOTHED EXPERIMENTAL BROADENINGS FOR 5.96×10^{-2} M. HISTAMINE SOLUTIONS

pH	$(\Delta/c)_s$	$(\Delta/c)_r$	$(\Delta/c)_{s+r}$	$(\Delta/c)_e$
.600	.1	38.8	39.0	39.2
.800	.1	38.9	39.1	39.2
1.000	.2	39.0	39.1	39.2
1.200	.2	39.1	39.3	39.2
1.400	.2	39.2	39.4	39.2
1.600	.2	39.5	39.7	39.5
1.800	.3	39.8	40.1	40.0
2.000	.4	40.3	40.7	40.6
2.200	.6	40.9	41.5	41.7
2.400	.8	41.8	42.6	42.8
2.600	1.2	42.7	43.9	43.9
2.800	1.8	43.5	45.4	45.0
3.000	2.8	43.9	46.2	46.2
3.200	4.4	43.3	47.7	47.3
3.400	6.8	41.4	48.1	47.8
3.600	10.4	37.9	48.3	48.4
3.800	15.3	32.9	48.2	48.6
4.000	20.8	26.8	47.6	48.0
4.200	24.5	20.5	45.0	44.5
4.400	23.8	14.9	38.7	38.8
4.600	19.5	10.4	29.8	29.7
4.800	14.1	7.0	21.2	20.3
5.000	9.7	4.7	14.4	15.0
5.200	6.5	3.2	9.7	9.7
5.400	4.4	2.2	6.6	6.8
5.600	3.1	1.5	4.6	4.6

TABLE 4.18

COMPARISON OF THEORETICAL BROADENINGS WITH SMOOTHED EXPERIMENTAL BROADENINGS FOR 2.70×10^{-1} M. HISTAMINE SOLUTIONS

pH	$(\Delta/c)_s$	$(\Delta/c)_r$	$(\Delta/c)_{s+r}$	$(\Delta/c)_e$
.400	.1	37.0	37.1	37.2
.600	.1	37.0	37.2	37.2
.800	.2	37.2	37.3	37.3
1.000	.2	37.3	37.5	37.3
1.200	.2	37.6	37.8	37.4
1.400	.3	38.0	38.2	37.5
1.600	.3	38.5	38.9	38.0
1.800	.4	39.4	39.9	39.1
2.000	.6	40.6	41.2	41.1
2.200	.9	42.1	43.0	43.2
2.400	1.4	43.7	45.1	45.1
2.600	2.1	44.8	47.0	46.1
2.800	3.3	44.3	47.6	46.5
3.000	5.1	41.1	46.2	45.6
3.200	7.9	35.1	43.0	42.8
3.400	11.9	27.6	39.5	38.7
3.600	17.2	20.3	37.6	37.5
3.800	22.5	14.2	36.8	36.9
4.000	25.1	9.6	34.7	34.6
4.200	22.9	6.4	29.3	29.7
4.400	17.7	4.2	21.9	21.8
4.600	12.4	2.7	15.1	15.2
4.800	8.2	1.7	10.0	10.1
5.000	5.4	1.1	6.5	6.7
5.200	3.5	.7	4.3	4.3
5.400	2.3	.5	2.8	2.8

TABLE 4.19

COMPARISON OF THEORETICAL BROADENINGS WITH SMOOTHED EXPERIMENTAL BROADENINGS FOR 95% DEUTERATED HISTAMINE SOLUTIONS AT 5.95×10^{-2} M

pH	$(\Delta/c)_s$	$(\Delta/c)_r$	$(\Delta/c)_{s+r}$	$(\Delta/c)_e$
2.000	.1	31.9	32.0	32.3
2.200	.1	32.0	32.1	32.3
2.400	.1	32.2	32.3	32.3
2.600	.2	32.4	32.6	32.3
2.800	.2	32.9	33.1	32.7
3.000	.4	33.5	33.8	33.6
3.200	.6	34.3	34.9	34.9
3.400	.9	35.6	36.5	36.5
3.600	1.4	37.3	38.6	38.6
3.800	2.1	39.3	41.5	41.9
4.000	3.4	41.5	44.9	45.1
4.200	5.3	43.2	48.5	48.4
4.400	8.1	43.3	51.4	51.6
4.600	12.3	40.4	52.7	52.7
4.800	17.4	34.4	51.7	51.7
5.000	21.9	26.7	48.6	48.5
5.200	23.4	19.3	42.8	41.5
5.400	20.9	13.5	34.3	33.9
5.600	16.3	9.2	25.5	25.9
5.800	11.8	6.3	18.1	18.7
6.000	8.4	4.4	12.8	12.8

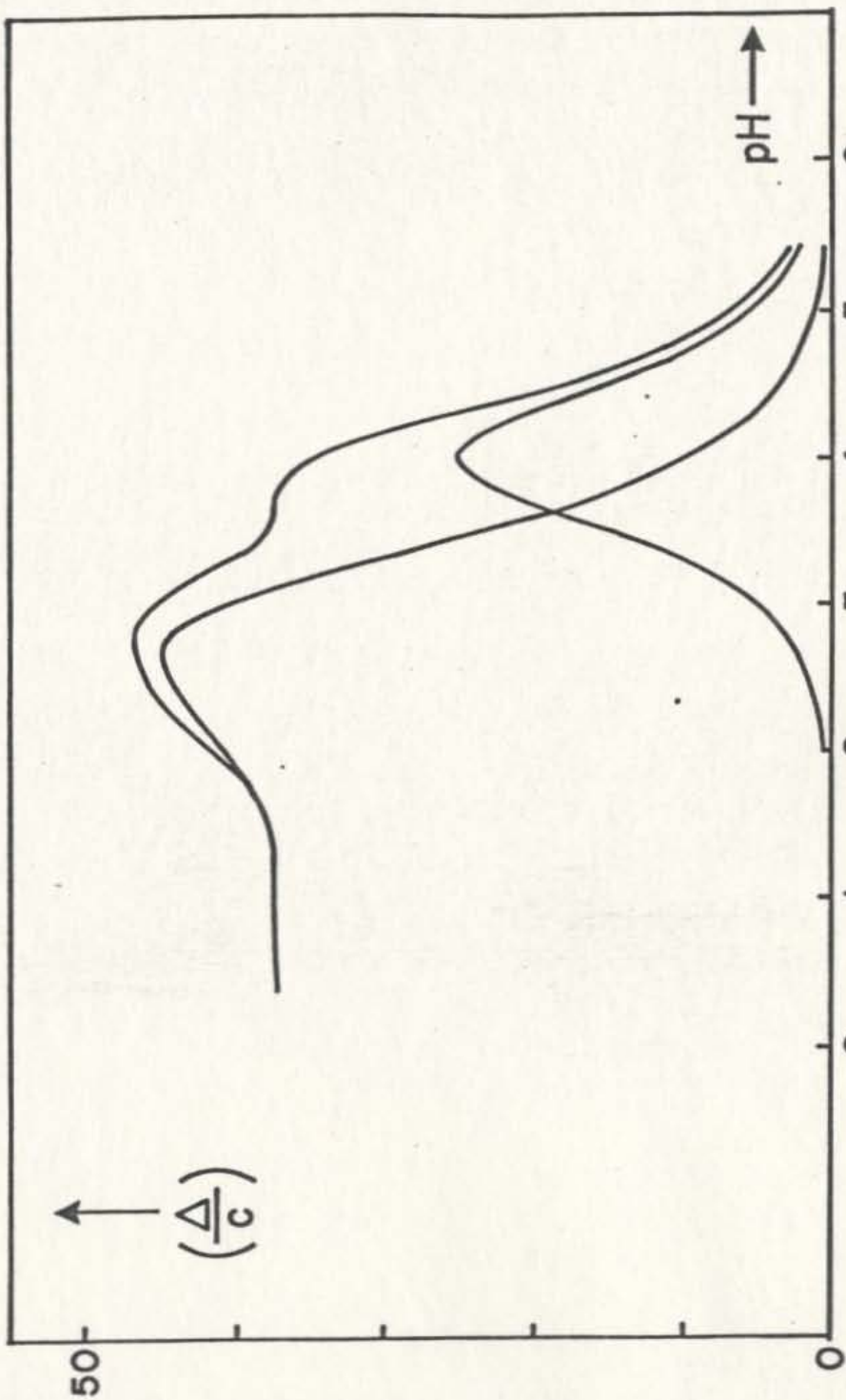

Figure 4.16 Theoretical components of the experimental broadening

The constants derived above were now used to calculate broadenings corresponding to the experiments at high RF. By allowing the RF field and both chemical shifts to move within their estimated error limits where necessary, it was possible to obtain calculated broadenings which were within about 3 (Δ/c) units of the experimental data. Since the experimental uncertainties were estimated to be this high, the agreement was considered to be satisfactory. Better fits could be obtained by adjusting the rate law parameters, but since this data generally extended over small pH ranges and also showed high uncertainty, the modified parameters were of little value. Tables 4.20 to 4.22 show some possible fits.

Dependence of k_2 on Ionic Strength

Inspection of Table 4.14 shows that k_2 increases as the ionic strength increases. Such behaviour is expected from the primary kinetic salt effect for a reaction between two positively charged ions. i.e.

$$\log (k_2) = m_r\sqrt{\mu} + \log (k_2^\circ) \qquad (4.7)$$

where m_r is a constant equal to the gradient of a straight line plot between $\log k_2$ and $\sqrt{\mu}$. The relevant data is listed in Table 4.23 and the plot of $\log k_2$ versus $\sqrt{\mu}$ is shown in Figure (4.17). A linear least squares fit gave

$$m_r = 0.346 \pm 0.037$$

and $$k_2^\circ = (2.80 \pm 0.14) \times 10^7 \text{ l.mole.}^{-1} \text{ sec.}^{-1}.$$

TABLE 4.20[†]

COMPARISON OF THEORETICAL BROADENINGS WITH SMOOTHED EXPERIMENTAL BROADENINGS FOR 2.98×10^{-2} M. HISTAMINE SOLUTIONS WITH RF FIELD AT 2513 RADS. SEC.$^{-1}$

pH	$(\Delta/c)_s$	$(\Delta/c)_r$	$(\Delta/c)_{s+r}$	$(\Delta/c)_e$
3.200	1.4	38.8	40.2	41.6
3.400	2.1	38.9	41.0	41.2
3.600	3.3	37.9	41.3	40.7
3.800	5.2	35.7	40.9	40.1
4.000	7.8	32.0	39.7	39.3
4.200	11.0	26.9	38.0	38.4
4.400	14.0	21.2	35.2	37.3

[†]Values in this Table were calculated using the same rate parameters which were used for the low RF data at this concentration. δ_r was 4860 rads. sec.$^{-1}$, δ_s was 1850 rads. sec.$^{-1}$, and the RF field was set at the measured value of 2513 rads. sec.$^{-1}$.

TABLE 4.21[†]

COMPARISON OF THEORETICAL BROADENINGS WITH SMOOTHED EXPERIMENTAL BROADENINGS FOR 5.95×10^{-2} M. HISTAMINE SOLUTIONS WITH RF FIELD AT 2513 RADS. SEC.$^{-1}$

pH	$(\Delta/c)_s$	$(\Delta/c)_r$	$(\Delta/c)_{s+r}$	$(\Delta/c)_e$
3.200	1.8	39.0	40.8	42.0
3.400	2.8	37.8	40.7	41.8
3.600	4.4	35.1	39.5	40.4
3.800	6.7	30.8	37.5	38.0
4.000	9.7	25.2	35.0	35.1
4.200	13.0	19.4	32.4	31.6
4.400	14.9	14.0	28.9	27.5
4.600	14.1	9.8	23.8	22.5
4.800	11.2	6.6	17.8	17.2
5.000	8.1	4.4	12.5	12.6
5.200	5.6	3.0	8.5	8.9
5.400	3.8	2.0	5.8	6.0
5.600	2.7	1.4	4.1	3.9
5.800	1.9	1.0	3.0	2.6

[†]Values in this Table were calculated using $j_2' = 7.5 \times 10^6$ l.mole. sec.$^{-1}$ and $k_2 = 4.2 \times 10^7$ l.mole.$^{-1}$ sec.$^{-1}$ with all other rate law parameters the same as used for the low RF data at this concentration. δ_r was 4860 rad. sec.$^{-1}$, δ_s was 1850 rads. sec.$^{-1}$ and RF field was set at the measured value of 2513 rads. sec.$^{-1}$.

TABLE 4.22†

COMPARISON OF THEORETICAL BROADENINGS WITH SMOOTHED EXPERIMENTAL BROADENINGS FOR 2.70×10^{-1} M. HISTAMINE SOLUTIONS WITH RF FIELD AT 2819 RADS. $SEC.^{-1}$

pH	$(\Delta/c)_s$	$(\Delta/c)_r$	$(\Delta/c)_{s+r}$	$(\Delta/c)_e$
1.400	.1	28.1	28.2	29.2
1.600	.1	28.6	28.7	29.2
1.800	.1	29.4	29.5	29.2
2.000	.2	30.6	30.7	29.5
2.200	.3	32.1	32.3	31.3
2.400	.4	33.9	34.3	33.3
2.600	.6	36.6	36.2	34.5
2.800	1.0	36.4	37.4	34.7
3.000	1.5	35.4	36.9	33.7
3.200	2.4	32.2	34.6	32.0
3.400	3.7	27.1	30.8	29.8
3.600	5.7	21.2	26.9	27.4
3.800	8.3	15.6	23.9	25.8
4.000	11.2	11.0	22.2	23.6
4.200	13.0	7.4	20.4	20.8
4.400	12.3	4.9	17.2	17.4
4.600	9.7	3.2	13.0	13.0
4.800	6.9	2.1	9.0	8.4
5.000	4.7	1.4	6.0	5.3
5.200	3.1	.9	4.0	3.5
5.400	2.0	.6	2.6	3.0

†Values in this Table were calculated using $j_2' = 4.5 \times 10^6$ 1. $mole.^{-1}$ $sec.^{-1}$, $k_2 = 4.5 \times 10^7$ $1.mole.^{-1}$ $sec.^{-1}$, $k_1' = 7500$ $sec.^{-1}$, $Q = 1500$, and other rate parameters the same as used for the low RF data at this concentration. δ_r was 4700 rads. $sec.^{-1}$, δ_s was 1830 rads. $sec.^{-1}$ and the RF field was set at 3100 rads. sec^{-1}.

TABLE 4.23

THE PRIMARY KINETIC SALT EFFECT ON k_2

Histamine	$\sqrt{\mu}$	$10^{-7} \times k_2$	log (k_2)
6.00×10^{-3}	0.140	3.01	7.48
2.98×10^{-2}	0.311	3.90	7.59
5.96×10^{-2}	0.440	3.90	7.59
2.70×10^{-1}	0.935	5.85	7.77

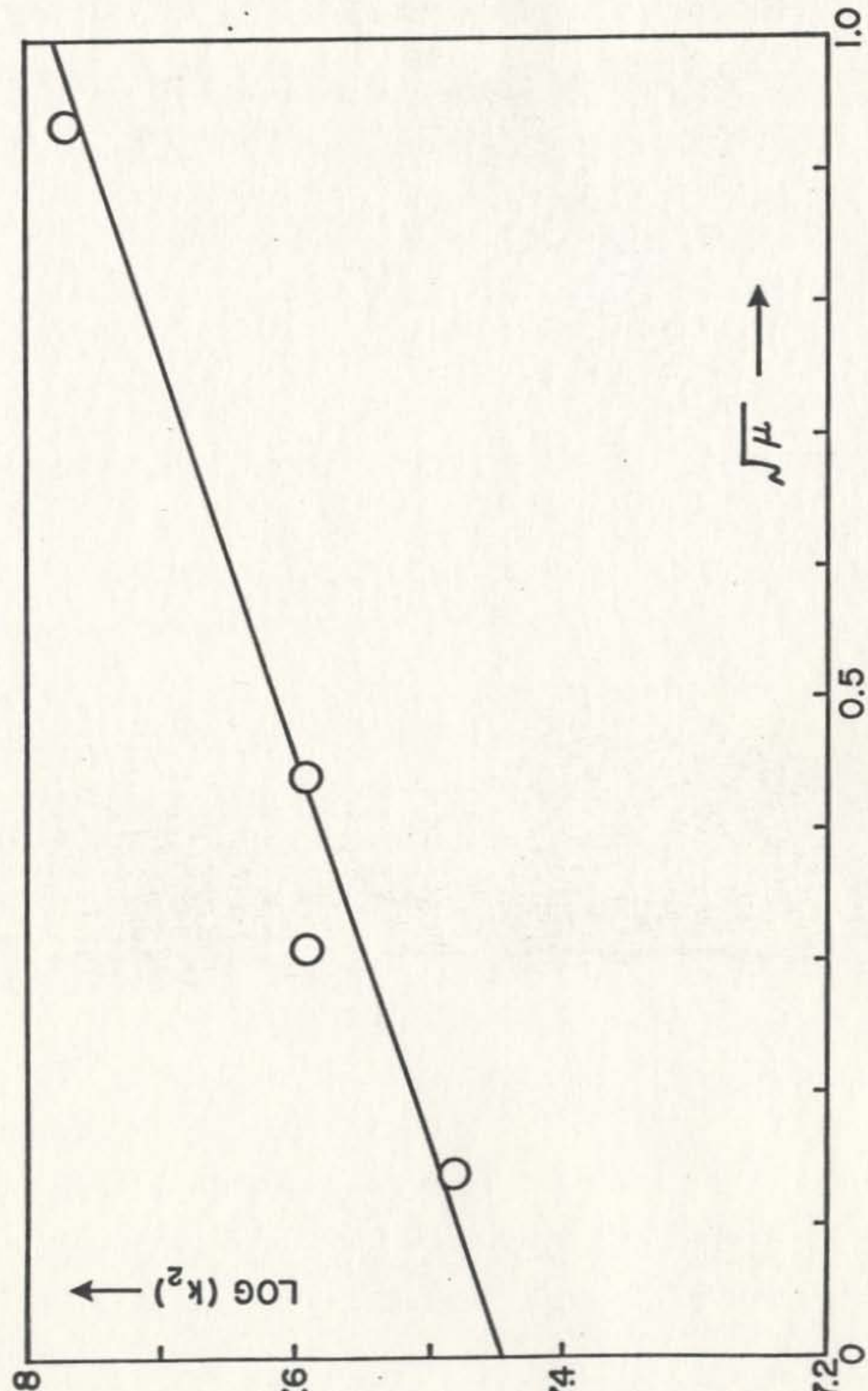

Figure 4.17 The effect of ionic strength on k_2

Consideration of j_2'

Table 4.14 shows the unexpected result that j_2' increases rapidly as the histamine concentration decreases. Since the j_2' values were obtained by linear least squares plots of the ammonium rates versus $[BH^+]$, it follows that all components of j_2' must refer to reactions depending on $[BH^+]$. It was assumed that all reactions depending on $[BH^+]$ would also depend on $[BH_2^{2+}]$. Since each of the kinetic analyses referred to a series of solutions at fixed histamine concentration, it follows that $[BH_2^{2+}]$ was essentially constant in any one analysis. Therefore any fit of the data involving a term $j_x[BH^+]$ $[BH_2^{2+}]$ could have just as well been obtained using a term $j_y[BH^+]$. A reaction following the latter rate law would have been identified in the kinetic analysis with

$$j_y = j_x[BH_2^{2+}]$$

i.e. $$j_x = \frac{j_y}{[BH_2^{2+}]}$$

The rate constants obtained from the different analyses--viz. the apparent second order in histamine j_x values, would therefore be expected to show a larger value from the j_y mechanism when the histamine concentration (and hence the $[BH_2^{2+}]$) was smaller.

We will now attempt to separate the apparent second order term into two components. One component, (j_2), will be due to reactions which are second order with respect to amine, and the other component (j_i), will be due to reactions depending on $[BH^+]$ alone.

Then

$$j_2' [BH^+] [BH_2^{2+}] = j_2 [BH^+] [BH_2^{2+}] + j_i [BH^+]$$

or

$$j_2' [BH_2^{2+}] = j_2 [BH_2^{2+}] + j_i \qquad (4.8)$$

Provided j_2 is constant, Equation (4.8) predicts that a plot of $j_2' [BH_2^{2+}]$ against $[BH_2^{2+}]$ would give a straight line with gradient j_2 and intercept j_i. To allow for variation of j_2 with ionic strength, it was possible to determine a value $m_s = 0.127$ (similar to the value m_r in Equation (4.7)) from a later experiment.

Then

$$\log (j_2) = m_s \sqrt{\mu} + \log (j_2^\circ)$$

or

$$\log \left(\frac{j_2}{j_2^\circ}\right) = m_s \sqrt{\mu} \qquad (4.9)$$

Equation (4.8) could then be rewritten as

$$j_2' [BH_2^{2+}] = \left(\frac{j_2}{j_2^\circ}\right) j_2^\circ [BH_2^{2+}] + j_i \qquad (4.10)$$

Equation (4.9) can be used to evaluate $\left(\frac{j_2}{j_2^\circ}\right)$ for each histamine concentration, and a plot of $j_2' [BH_2^{2+}]$ against $\left(\frac{j_2}{j_2^\circ}\right) [BH_2^{2+}]$ will provide values of j_2° and j_i. Table 4.24 lists the values and Figure (4.18) shows the plot.

A linear least squares fit according to Equation (4.10) gives

$$j_2^\circ = (2.49 \pm 0.07) \times 10^6 \text{ l. mole.}^{-1} \text{ sec.}^{-1}$$

$$j_i = (2.00 \pm 0.12) \times 10^5 \text{ sec.}^{-1}.$$

TABLE 4.24

SEPARATION OF j_2' INTO TWO COMPONENTS

Histamine	$\sqrt{\mu}$	$10^{-6} \times j_2' [BH_2^{2+}]$	$\left(\frac{j_2}{j_2^\circ}\right) [BH_2^{2+}]$
6.00×10^{-3}	0.140	0.195	6.26×10^{-3}
2.98×10^{-2}	0.311	0.289	3.27×10^{-2}
5.96×10^{-2}	0.440	0.385	6.81×10^{-2}
2.70×10^{-1}	0.935	1.085	3.57×10^{-1}

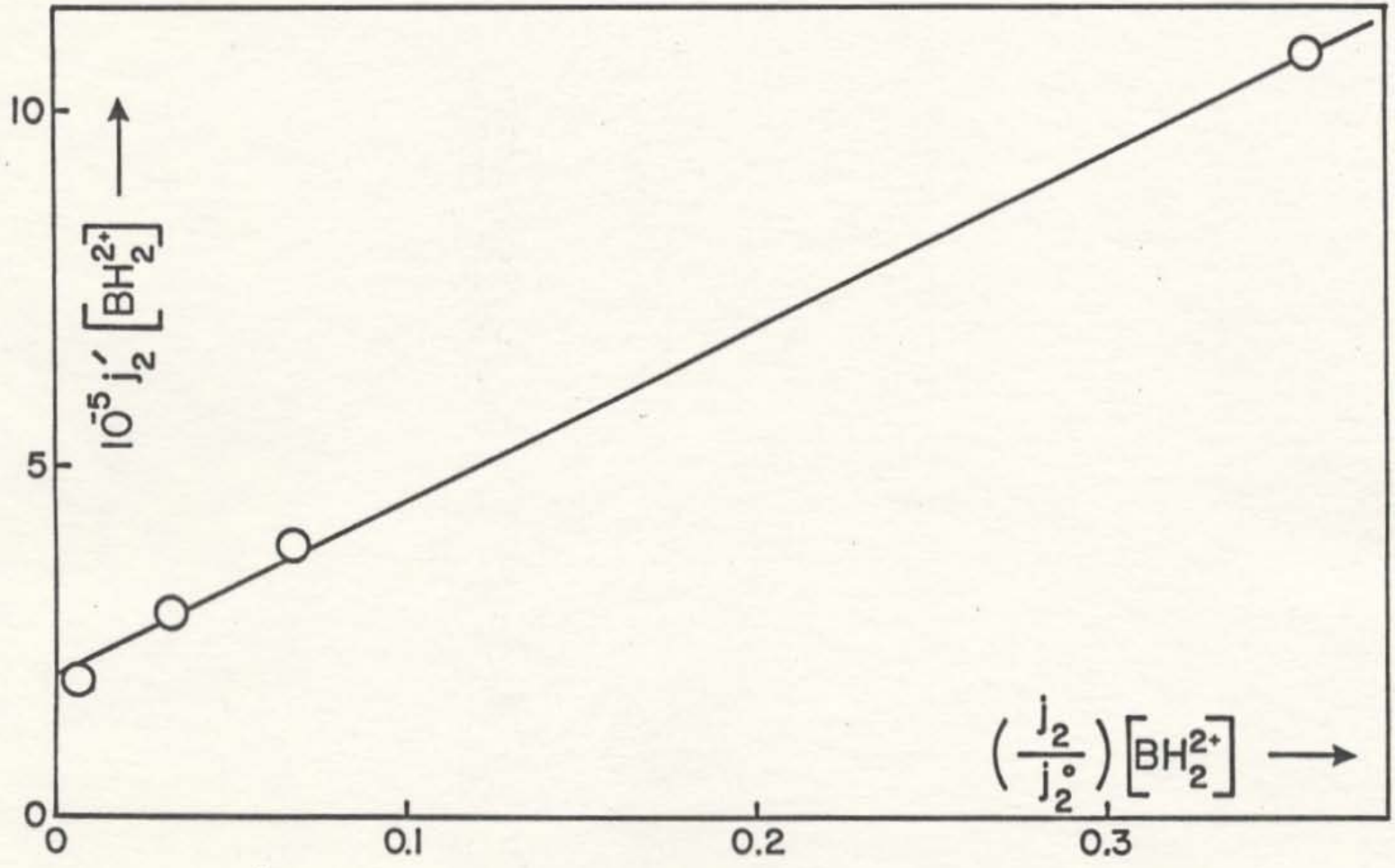

Figure 4.18 Separation of j_2'

If the rapid increase in j_2' is to be explained in this way it is necessary to identify the reaction to which the rate constant j_i applies. An obvious possibility is an intramolecular reaction in which the reactant histamine species is singly protonated at an amino site. The reaction then consists of an intramolecular proton transfer from an amino site to an imidazole site. A second less obvious possibility is a reaction between BH_2^{2+} and OH^-.

$$BH_2^{2+} + OH^- \xrightarrow{k} BH^+ + H_2O$$

The rate constant for this reaction is given by k

where $\text{Rate} = k\,[BH_2^{2+}]\,[OH^-]$

$$\therefore \quad \text{Rate} = \frac{k\,[BH_2^{2+}]\,K_w}{[H^+]}$$

$$\therefore \quad \text{Rate} = \frac{k\,[BH^+]\,K_w}{K_{A1}} \quad .$$

Therefore this reaction can be identified with the rate constant j_i if

$$\frac{k.K_w}{K_{A1}} = j_i$$

so that $k = 2.8 \times 10^{13}$ ℓ.mole.$^{-1}$ sec.$^{-1}$.

Since this is about three orders of magnitude greater than would be expected if the reaction is diffusion controlled, this possibility must be rejected in favour of the intramolecular reaction.

Series Run at Constant Buffer Ratios

Two series of experiments were run in which the ratio $\frac{[BH^+]}{[BH_2^{2+}]}$ was kept constant. One of these was with solutions in 95% D_2O while the other was with natural abundance of the hydrogen isotopes.

Constant Buffer Ratio In Natural Abundance Solutions

The broadenings due to exchange from the imidazolium sites were calculated using the previously determined rate constants. These broadenings (as well as the broadenings due to O^{17}) were then subtracted from the measured broadenings to leave a component which was attributed to ammonium exchange. Ammonium exchange rates ($3/\tau$) were calculated and listed in Table 4.25. The total ammonium exchange rate should be given by

$$(3/\tau) = \frac{\text{Rate}}{[BH_2^{2+}]} = j_2 [BH^+] + j_i \frac{[BH^+]}{[BH_2^{2+}]}$$

or

$$(3/\tau) = j_2 [BH^+] + j_i R \qquad (4.11)$$

where the constant buffer ratio $\frac{[BH^+]}{[BH_2^{2+}]} = R = 0.141$ in this series.

A plot of $(3/\tau)$, as ordinate, against $[BH^+]$ was found to show a slight upward curvature which was interpreted as a primary kinetic salt effect on j_2. As a first approximation the value of m_r obtained previously for the ionic strength dependence of k_2 was used to calculate values of

TABLE 4.25

SERIES RUN AT CONSTANT BUFFER RATIO OF $\frac{[BH^+]}{[BH_2^{2+}]}$ = 0.141

[Histamine]	$(1/T_{1p})$	$(1/T_1)$	Δ_s †	$(3/\tau)$	$\log\left(\frac{3/\tau - {}_1R}{[BH^+]}\right)$	$\sqrt{\mu}$	$\left(\frac{j_2}{j_2^\circ}\right)[BH^+]$
0.0615	0.973	0.344	0.433	39309	6.260	0.411	0.00856
0.1285	1.166	0.346	0.641	55905	6.283	0.594	0.01884
0.1629	1.221	0.349	0.699	65148	6.296	0.669	0.02437
0.2421	1.301	0.353	0.786	86814	6.312	0.815	0.03793
0.2976	1.331	0.358	0.816	102831	6.323	0.903	0.04777
0.3645	1.339	0.363	0.824	124992	6.345	1.001	0.06028
0.4174	1.371	0.368	0.855	136932	6.336	1.071	0.07027
0.4700	1.359	0.373	0.841	157653	6.359	1.136	0.08067
0.5419	1.378	0.380	0.858	178188	6.360	1.220	0.09538

† Broadening due to side chain exchange obtained by subtraction of broadenings due to ring exchange and O^{17} exchange.

$\left(\frac{j_2}{j_2^\circ}\right)$ which were used in a plot of $(3/\tau)$ against $\left(\frac{j_2}{j_2^\circ}\right)[BH^+]$.† This produced curvature in the opposite sense, thus indicating that the ionic strength dependance of j_2 was less than that measured for k_2. Both of these curves were now fitted to quadratic expressions by a least squares technique and, from the intercepts, it was determined that j_i was $(1.80 \pm 0.13) \times 10^5$ sec.$^{-1}$ as a first approximation.

Now from Equation (4.11) we have

$$\left(\frac{3/\tau - j_i R}{[BH^+]}\right) = j_2$$

$$\therefore \log\left(\frac{3/\tau - j_i R}{[BH^+]}\right) = \log (j_2) \qquad (4.12)$$

But the dependance of j_2 on ionic strength is given by

$$\log (j_2) = m_s \sqrt{\mu} + \log (j_2^\circ)$$

so that substitution for $\log (j_2)$ in Equation (4.12) yields

$$\log \left(\frac{3/\tau - j_i R}{[BH^+]}\right) = m_s \sqrt{\mu} + \log (j_2^\circ) \qquad (4.13)$$

Using the above estimate of j_i, a plot of $\log \left(\frac{3/\tau - j_i R}{[BH^+]}\right)$ against $\sqrt{\mu}$ was found to yield a straight line with

---

†The values of this function which are listed in Table 4.25 are not the trial values as calculated from m_r here.

Gradient = m_s = 0.127 ± 0.007

Intercept = 6.209 ± .007

(From the intercept it follows that j_2° = (1.62 ± 0.03) x 10^6 1. mole.$^{-1}$ sec.$^{-1}$ as a first approximation).

Finally, the value m_s = 0.127 was used to calculate values of $\left(\frac{j_2}{j_2^\circ}\right)$, and a plot of $(3/\tau)$ against $\left(\frac{j_2}{j_2^\circ}\right)[BH^+]$ drawn in Figure 4.19. The data for this plot is listed in Table 4.25 and a least squares fit gave

$$j_i = (1.83 \pm 0.07) \times 10^5 \text{ sec.}^{-1}$$
$$j_2^\circ = (1.61 \pm 0.02) \times 10^6 \text{ 1. mole.}^{-1} \text{ sec.}^{-1}.$$

Constant Buffer Ratio in 95% D_2O Solutions

Results for solutions in 95% D_2O at a constant buffer ratio of $\frac{[BH^+]}{[BH_2^{2+}]}$ = 0.146 are listed in Table 4.26. The broadenings due to imidazolium exchange were calculated by assuming that the variation of k_2^* with ionic strength in D_2O was the same as that determined in H_2O (m_r = 0.346). Values of $\left(\frac{j_2^*}{j_2^{\circ *}}\right)^2$ were calculated by making the similar assumption that the value of m_s = 0.127 could be applied to deuterated solutions. A plot of $3/\tau$ against $\left(\frac{j_2^*}{j^{\circ *}_2}\right)[BH^+]$ was found to be linear with

$$j_i^* = (6.23 \pm 0.65) \times 10^4 \text{ sec.}^{-1}$$
$$j_2^{\circ *} = (1.37 \pm 0.03) \times 10^6 \text{ 1.mole.}^{-1} \text{ sec.}^{-1}.$$

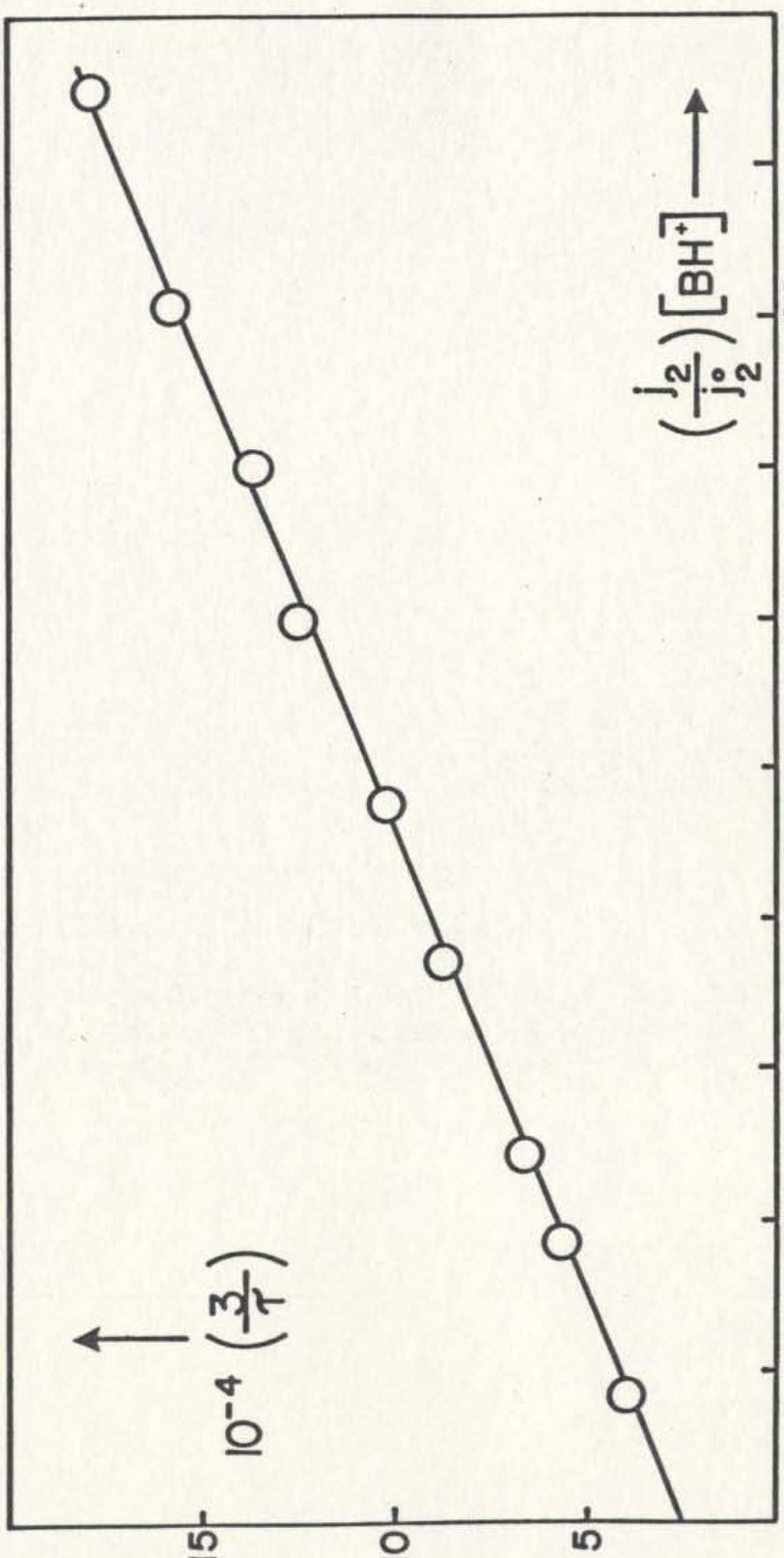

Figure 4.19 Constant buffer ratio plot

TABLE 4.26

SERIES RUN AT CONSTANT BUFFER RATIO OF $\frac{[BH^+]}{[BH_2^{2+}]}$ = 0.146 IN 95% D_2O

[Histamine]	$(1/T_{1p})$	$(1/T_1)$	Δ_s	$(3/\tau)$	$\left(\frac{j_2}{j_2^\circ}\right)$ $[BH^+]$
0.0805	1.496	0.097	0.878	24666	0.01182
0.0972	1.512	0.098	0.903	29547	0.01448
0.1353	1.583	0.100	0.994	38076	0.02074
0.1584	1.654	0.102	1.075	41430	0.02464
0.1809	1.618	0.103	1.049	48846	0.02845
0.2240	1.659	0.106	1.102	57894	0.03614
0.2426	1.686	0.107	1.133	61095	0.0395
0.2622	1.604	0.108	1.056	70908	0.0431
0.2775	1.638	0.109	1.095	72567	0.0460
0.2981	1.654	0.111	1.113	76689	0.0499

Experiments with Solutions Enriched in O^{17}

Three constant buffer ratio series were run with solutions in which the atom fraction of O^{17} was about .01 (Tables 4.27 to 4.29). Values of Δ were obtained by subtracting $(1/T_{1p})_M$ measured in natural abundance from $(1/T_{1p})_e$ in the enriched solutions.

i.e. $\Delta = (1/T_{1p})_e - (1/T_{1p})_n$

The fraction of HOH sites at O^{17}, p, were likewise calculated as the difference between the natural abundance and enriched solutions. (Δ/p) values were then converted to total rates, $(1/\tau)_t$, in the usual way. The rates involving histamine species, $(1/\tau)_h$, were obtained by subtraction of the H^+ and OH^- catalyzed rates from the total rates.

i.e. $(1/\tau)_h = (1/\tau)_t - (1/\tau)_{cat.}$

The rate law for reactions involving histamine species will then be

$$111(1/\tau)_h = n_1\ell_1 [BH^+] + n_2\ell_2 [BH^+][BH_2^{2+}] \qquad (4.14)$$

or

$$\frac{111(1/\tau)_h}{[BH^+]} = n_1\ell_1 + n_2\ell_2 [BH_2^{2+}] \qquad (4.15)$$

In Equation (4.14) the term involving $n_1\ell_1$ will be the total rate for all processes which are first order in histamine concentration and the term involving $n_2\ell_2$ will be the total rate for all processes which are second order in histamine concentration. Since, at this point, it was not possible to predict the ionic strength dependance of the composite rate constant ℓ_2, the initial analysis was performed by plotting

TABLE 4.27

ENRICHED O^{17} SOLUTIONS AT A CONSTANT BUFFER RATIO OF $\frac{[BH^+]}{[BH_2^{2+}]} = 3.88$

[Histamine]	$(1/T_{1p})_e$	$(1/T_{1p})_n$	$(1/\tau)_t$	$\frac{(1/\tau)_h}{[BH^+]}$	$\left(\frac{\ell_2}{\ell_2^\circ}\right)' [BH_2^{2+}]$ †
0.07181	3.460	0.586	1666	16620	0.0198
0.09246	3.305	0.592	2174	19905	0.0265
0.11678	2.903	0.596	3119	25959	0.0349
0.14477	2.415	0.599	4454	32520	0.0453
0.17612	1.985	0.601	6265	39614	0.0575
0.20865	1.771	0.602	7619	41531	0.0710
0.25141	1.477	0.602	10504	48809	0.0899

†Values of $\left(\frac{\ell_2}{\ell_2^\circ}\right)'$ were calculated using $m_a = 0.325$ (see text).

TABLE 4.28

ENRICHED O^{17} SOLUTIONS AT A CONSTANT BUFFER RATIO OF $\frac{[BH^+]}{[BH_2^{2+}]} = 22.9$

[Histamine]	$(1/T_{1p})_e$	$(1/T_{1p})_n$	$(1/\tau)_t$	$\frac{(1/\tau)_h}{[BH^+]}$	$\left(\frac{\ell_2}{\ell_2^\circ}\right)' [BH_2^{2+}]$ †
0.06659	3.422	0.647	1726	8934	0.00320
0.07997	3.336	0.649	2026	10261	0.00389
0.09558	3.252	0.649	2229	9672	0.00472
0.11663	3.018	0.648	2779	11746	0.00585
0.14811	2.700	0.646	3554	13354	0.00761
0.18069	2.331	0.641	4660	16181	0.00948
0.51615	2.069	0.636	5724	17639	0.01158
0.25776	1.816	0.629	7138	19935	0.01412
0.30975	1.540	0.622	9501	23170	0.01743
0.35558	1.373	0.615	11671	25897	0.02043
0.42010	1.213	0.606	14701	28584	0.02481
0.48737	1.048	0.596	19865	34904	0.02957

†Values of $\left(\frac{\ell_2}{\ell_2^\circ}\right)'$ were calculated using $m_a = 0.162$ (see text).

TABLE 4.29

ENRICHED O^{17} SOLUTIONS AT A CONSTANT BUFFER RATIO OF $\frac{[BH^+]}{[BH_2^{2+}]} = 33.7$

[Histamine]	$(1/T_{1p})_e$	$(1/T_{1p})_n$	$(1/\tau)_t$	$\frac{(1/\tau)_h}{[BH^+]}$	$\left(\frac{\ell_2}{\ell_2^\circ}\right)' [BH_2^{2+}]$ †
0.0872	3.199	0.710	2864	12229	0.002770
0.1070	2.984	0.710	3363	13070	0.003434
0.1297	2.787	0.708	3870	13111	0.004209
0.1511	2.569	0.706	4522	14383	0.004950
0.1742	2.408	0.703	5100	14669	0.005763
0.2094	2.097	0.698	6489	17561	0.007019
0.2572	1.792	0.692	8594	21001	0.008761
0.3061	1.553	0.684	11155	24860	0.010594
0.3674	1.361	0.675	14481	28688	0.012939

†Values of $\left(\frac{\ell_2}{\ell_2^\circ}\right)'$ were calculated using $m_a = 0.101$ (see text).

$\frac{111(1/\tau)_h}{[BH^+]}$ against $[BH_2^{2+}]$ for each series of data. As a first approximation, the linear least squares slopes were interpreted as values of $n_2\ell_2$ and these were found to increase quite markedly as the buffer ratio increased. To take the analysis further, it is necessary to consider all the second order processes which may be present.

Possible Reactions Which are Second Order in Histamine

A proton could conceivably be transferred from any BH_2^{2+} or BH^+ species to any BH^+ or B species. In the following second order rate constants, the first suffixed digit indicates the charge of the species losing the proton, and the second suffixed digit indicates the charge of the species gaining the proton. The total second order rate law would then be given by

$$v_2 = n_{21}\ell_{21}[BH_2^{2+}][BH^+] + n_{20}\ell_{20}[BH_2^{2+}][B]$$

$$+ n_{11}\ell_{11}[BH^+][BH^+] + n_{10}\ell_{10}[BH^+][B]$$

$$\therefore v_2 = n_{21}\ell_{21}[BH_2^{2+}][BH^+] + n_{20}\ell_{20}[BH_2^{2+}][BH^+]\left(\frac{[B]}{[BH^+]}\right)$$

$$+ n_{11}\ell_{11}[BH_2^{2+}][BH^+]\left(\frac{[BH^+]}{[BH_2^{2+}]}\right) + n_{10}\ell_{10}[BH_2^{2+}][BH^+]\left(\frac{[BH^+]}{[BH_2^{2+}]}\right)\left(\frac{[B]}{[BH^+]}\right)$$

$$\therefore v_2 = n_{21}\ell_{21}[BH_2^{2+}][BH^+] + n_{20}\ell_{20}[BH_2^{2+}][BH^+]\left[\frac{R.K_{A2}}{K_{A1}}\right]$$

$$+ n_{11}\ell_{11}[BH_2^{2+}][BH^+](R) + n_{10}\ell_{10}[BH_2^{2+}][BH^+]\left[\frac{R.K_{A2}}{K_{A1}}\right]$$

where

$$R = \frac{[BH^+]}{[BH_2^{2+}]} \; ; \; K_{A1} = \frac{[BH^+][H^+]}{[BH_2^{2+}]} \; ; \; K_{A2} = \frac{[B][H^+]}{[BH^+]} \; .$$

$$\therefore \quad \frac{v_2}{[BH_2^{2+}][BH^+]} = n_{21}\ell_{21} + (n_{20}\ell_{20} \cdot K' + n_{11}\ell_{11})\, R + n_{10}\ell_{10}\, K' R^2 \qquad (4.16)$$

where $K' = \frac{K_{A2}}{K_{A1}}$ will be expected to show some concentration dependence.

If the rate constants can be corrected to zero ionic strength, then K' will be equal to the ratio of the ionization constants at zero ionic strength (i.e. the ratio of the thermodynamic values).

The First Approximations for $n_2\ell_2$

In the first analysis according to Equation (4.15), the total second order rate was given by

$$v_2 = n_2\ell_2\, [BH_2^{2+}][BH^+]$$

Substitution for v_2 in Equation (4.16) gives

$$n_2\ell_2 = n_{21}\ell_{21} + (n_{20}\ell_{20}\, K' + n_{11}\ell_{11})R + n_{10}\ell_{10}\, K' R^2 \qquad (4.17)$$

Inspection of the preliminary $n_2\ell_2$ values at the three different buffer ratios showed that $n_2\ell_2$ increased linearly with R to the power 2.2. A plot of $n_2\ell_2$ against R^2 was found to be linear within the limits of experimental error. It was therefore deduced that the coefficient of R was not significant in the present results, and hence the only reactions of importance for the numerical analysis were $n_{21}\ell_{21}$ and $n_{10}\ell_{10}$. The

approximate relative contributions of these two components to each of the three different $n_2\ell_2$ values could now be evaluated.

It was assumed that the contributions of k_2 and j_2 to $n_{21}\ell_{21}$ would be in the same ratio as their previously measured magnitudes (i.e. it was assumed that the number of water molecules involved in k_2 and j_2 would be the same), and a weighted ionic strength correction factor (m_w) was evaluated on this basis.† There is no theoretical primary kinetic salt effect on $n_{10}\ell_{10}$ [75] and previous measurements of second order amine reactions of this charge type have been found to show only a small ionic strength dependence. Therefore for present purposes the ionic strength dependence of $n_{10}\ell_{10}$ was neglected. A total average ionic strength correction factor (m_a) was now calculated for each series and used to determine values of $(\ell_2/\ell_2^\circ)'$ using an equation similar to Equation (4.7). Equation (4.15) can now be rewritten as

$$\frac{111(1/\tau)_h}{[BH^+]} = n_1\ell_1 + n_2\ell_2^\circ\left(\frac{\ell_2}{\ell_2^\circ}\right)'[BH_2^{2+}] \qquad (4.18)$$

Plots of $\frac{(1/\tau)_h}{[BH^+]}$ against $\left(\frac{\ell_2}{\ell_2^\circ}\right)'[BH_2^{2+}]$ were now made for each of the three series of data. The plot of the data from Table 4.28 (which extends over the largest concentration range) is shown in Figure 4.20. Since no curvature can be seen in this plot, it would seem that the various approximations that were made are reasonable.

Linear least squares fits to Equation (4.18) gave the values listed in Table 4.30.

---

†Since k_1 is considerably larger than j_1, any difference in the number of water molecules will only cause very small errors in m_w.

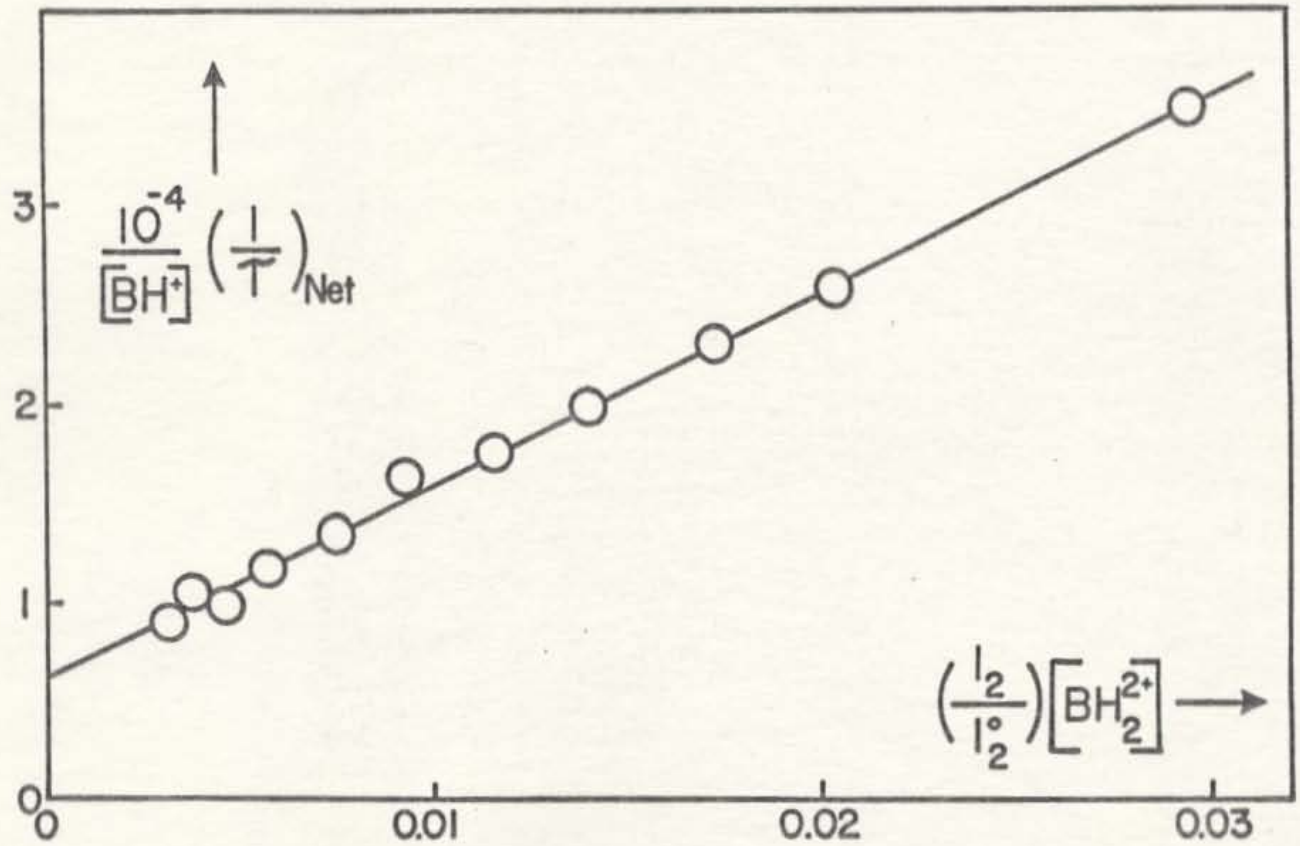

Figure 4.20 Data from second O^{17} experiment

TABLE 4.30

RESULTS FROM O^{17} EXPERIMENTS

Buffer Ratio (R)	$10^{-7} \times n_2 \ell_2^\circ$ (l.mole.$^{-1}$ sec.$^{-1}$)	$10^{-5} \times n_1 \ell_1$ (sec.$^{-1}$)
3.88	5.2 ± 0.4	10.3 ± 2.4
22.9	10.9 ± 0.2	6.67 ± 0.30
33.7	18.7 ± 1.0	7.10 ± 0.76

The values of $n_2\ell_2^\circ$ were plotted against R^2 as shown in Figure 4.21.[†] A least squares fit according to Equation (4.17) (with the coefficient of R set at zero) gave

$$n_{21}\ell_{21}^\circ = (4.85 \pm 0.34) \times 10^7 \text{ l.mole.}^{-1} \text{ sec.}^{-1}$$

and $$n_{10}\ell_{10}^\circ \cdot K' = (1.21 \pm 0.05) \times 10^5 \text{ l.mole.}^{-1} \text{ sec.}^{-1}.$$

Since K′ at zero ionic strength is $(1.25 \pm 0.02) \times 10^{-4}$, it follows that

$$n_{10}\ell_{10}^\circ = (9.7 \pm 0.6) \times 10^8 \text{ ℓ.mole.}^{-1} \text{ sec.}^{-1}.$$

The Data at Low pH

Grunwald and Ralph detected two parallel first order proton exchange mechanisms in their work on acidic solutions of imidazole [44]. To interpret these results, they postulated that the acid dissociation of imidazolium ion occurs in two steps as shown for histamine in Figure 4.22.

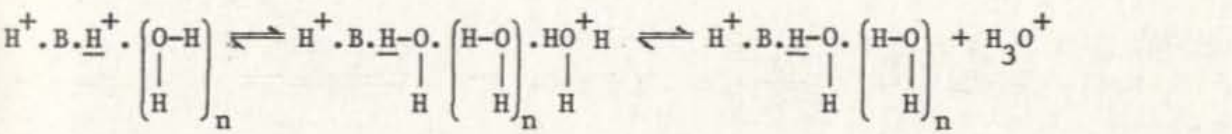

(II) (I)

Figure 4.22

Acid dissociation of histamine

Proton exchange could then arise due to breaking of the B.H bond either

---

[†]The relative proportions of $n\ell_{21}$ and $n\ell_{10}$ in the different $n\ell_2$ values were in good agreement with the original approximations so that a recalculation of the results using a modified ionic strength correction factor (m_a) was considered unnecessary.

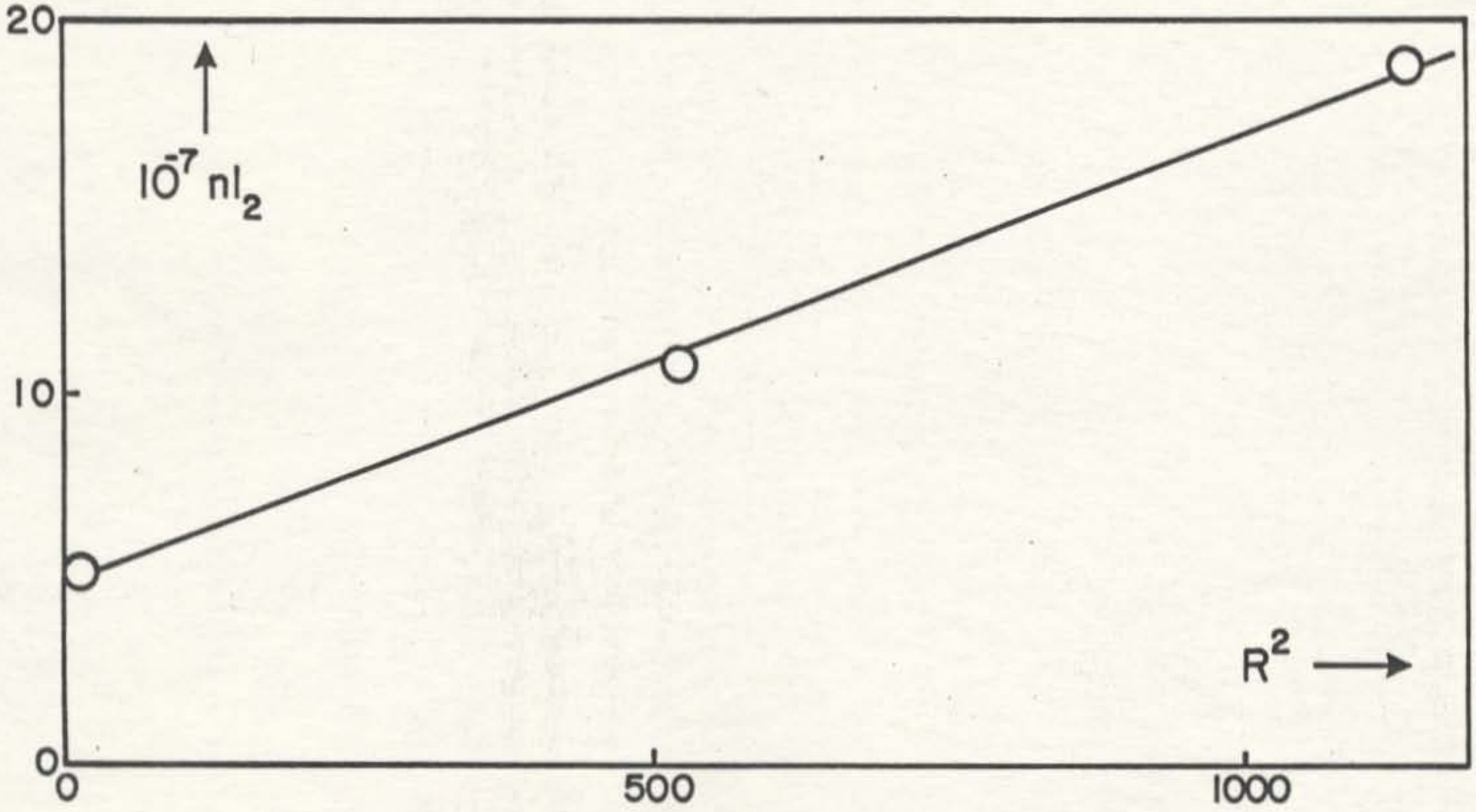

Figure 4.21 Plot to resolve $n\ell_2$ into $n\ell_{21}$ and $n\ell_{10}$

in the dissociated product (I), or in the ionized intermediate (II).

As shown in the introduction to this thesis, the rate of exchange due to dissociated product (I) will be decreased as $[H^+]$ increases according to the expression

$$\text{Rate of proton exchange} = \frac{k_a' [BH_2^{2+}]}{1 + Q [H^+]} \qquad (4.19)$$

For amines with an ionic charge (such as the case here), two separate Q values differing by about two or three orders of magnitude have been observed [35]. These two Q values have been interpreted as corresponding to exchange occurring in the trans and gauche isomers of the amine with the rate of exchange in the gauche isomer being repressed at about two or three pH units higher than the rate of exchange in the trans isomer.

Kinetic analysis predicts that the proton exchange rate in the ionized intermediate (II) is independent of $[H^+]$. In very strong acid, however, a kinetic salt effect would be expected to cause a change in this rate constant [76].

Solutions with Natural Isotopic Abundance

In the case of histamine, a "Q feature" has already been observed to cause a repression of a first order rate component at about pH 3. This could be due to proton exchange in the gauche isomer of the dissociated product (I). The first order rate which is observed in more concentrated acid could possibly contain two further components (i) due to proton exchange in the trans isomer of the dissociated product (I), and (ii) due to proton exchange in the ionized intermediate (II). Accordingly it may be possible to detect up to two further repression

features, (i) a further Q value, and (ii) a kinetic salt effect.

Attempts were made to interpret the repression of rate below pH = 1 in either or both of the above ways. It was not possible to separate two repression features in any of the four series of data which were available for solutions containing natural abundance of isotopes. For reasons which will be discussed later, the preferred single interpretation was of a kinetic salt effect. Tables 4.31 to 4.35 show the treatment of the data for interpretation in this manner.

Using the salt effect interpretation, the listed specific rates will be equal to the k_{cyclic} defined by Ralph and Grunwald [44].† Accordingly plots of $\log\left(\frac{\text{Rate}}{[BH_2^{2+}]}\right)$ against [HCl] were made for each series of data. They were found to be similar to those of imidazole and a least squares fit to a quadratic expression of the form

$$\log\left(\frac{\text{Rate}}{[BH_2^{2+}]}\right) = c_1\,[HCl]^2 + c_2\,[HCl] + c_3 \qquad (4.20)$$

produced the results shown in Table 4.36. Results obtained by Ralph and Grunwald for imidazole [44] are shown for comparison.

Solutions in 95% D_2O

The data listed in Table 4.35 showed some indication of two repression features. Figure 4.23 shows that values of $\log\left(\frac{\text{Rate}}{[BH_2^{2+}]}\right)$ for [HCl] < 0.4 M lie above the extrapolation of the least squares quadratic curve for data above [HCl] = 0.4 M. The appearance of this

†Ralph and Grunwald define k_{cyclic} as shown in the first chapter of this thesis. See Equations (1.40) and (1.41).

TABLE 4.31

ACID REPRESSION DATA FOR 2.98×10^{-2} M. HISTAMINE WITH RF FIELD AT 500 RADS. SEC.$^{-1}$

[HCl]	(Δ/c)	(Δ/p)†	$\frac{\text{Rate}}{[BH_2^{2+}]}$	$\log\left(\frac{\text{Rate}}{[BH_2^{2+}]}\right)$
0.0881	35.9	1997	5080	3.706
0.220	35.5	1978	5030	3.701
0.315	35.5	1980	5052	3.703
0.531	35.4	1978	5078	3.706
0.955	33.9	1902	4802	3.681
2.119	25.8	1458	3358	3.526
2.945	17.1	975	2084	3.319
3.741	9.7	556	1156	3.064
3.976	8.7	501	1018	3.008
4.635	5.6	323	666	2.823
5.580	3.4	199	400	2.601

†For imidazolium exchange assuming broadening due to ammonium exchange is zero.

TABLE 4.32

ACID REPRESSION DATA FOR 5.96×10^{-2} M. HISTAMINE WITH RF FIELD AT 200 RADS. SEC.$^{-1}$

[HCl]	(Δ/c)	(Δ/p)†	$\frac{\text{Rate}}{[BH_2^{2+}]}$	$\log\left(\frac{\text{Rate}}{[BH_2^{2+}]}\right)$
0.041	39.0	2170	5998	3.778
0.083	38.3	2132	5784	3.762
0.180	39.9	2223	6404	3.806
0.318	39.2	2186	6192	3.792
0.501	38.6	2156	6052	3.782
0.846	37.7	2113	5884	3.770
1.360	33.8	1903	4876	3.688
2.038	26.3	1489	3414	3.533
2.968	16.4	936	1974	3.295
3.733	9.6	552	1126	3.052
4.838	4.6	268	538	2.731

†For imidazolium exchange assuming broadening due to ammonium exchange is zero.

TABLE 4.33

ACID REPRESSION DATA FOR 2.70×10^{-1} M. HISTAMINE WITH RF FIELD AT 355 RADS. $SEC.^{-1}$

[HCl]	(Δ/c)	(Δ/p) †	$\frac{\text{Rate}}{[BH_2^{2+}]}$	$\log\left(\frac{\text{Rate}}{[BH_2^{2+}]}\right)$
0.045	36.6	2036	5342	3.728
0.052	38.6	2147	6006	3.779
0.132	37.7	2099	5688	3.755
0.260	36.8	2053	5522	3.742
0.549	36.5	2039	5514	3.741
0.853	36.0	2017	5410	3.733
1.426	32.0	1802	4512	3.654
1.441	30.1	1696	4142	3.617
2.238	23.9	1356	3068	3.487
3.628	11.5	660	1374	3.138
4.789	6.3	365	748	2.874
5.430	4.0	233	476	2.677

†For imidazolium exchange assuming broadening due to ammonium exchange is zero.

TABLE 4.34

ACID REPRESSION DATA FOR 2.70×10^{-1} M. HISTAMINE WITH RF FIELD AT 2819 RADS. $SEC.^{-1}$

[HCl]	(Δ/c)	(Δ/p) †	$\frac{\text{Rate}}{[BH_2^{2+}]}$	$\log\left(\frac{\text{Rate}}{[BH_2^{2+}]}\right)$
0.045	29.3	1630	5376	3.731
0.081	28.6	1591	5189	3.715
0.215	28.9	1612	5284	3.723
0.514	28.0	1564	5093	3.707
0.853	28.2	1580	5146	3.712
1.426	23.2	1306	3929	3.594
2.238	17.8	1010	2893	3.461
3.628	9.8	562	1533	3.185
3.877	8.6	495	1345	3.128
4.789	5.5	319	859	2.934
5.430	2.9	169	453	2.656

†For imidazolium exchange assuming broadening due to ammonium exchange is zero.

TABLE 4.35

ACID REPRESSION DATA FOR 95% DEUTERATED SOLUTIONS WHICH WERE 5.95×10^{-2} M. IN HISTAMINE. RF FIELD 632 RADS. SEC.$^{-1}$

[HCl]	(Δ/c)	(Δ/p) †	$\frac{\text{Rate}}{[BH_2^{2+}]}$	$\log\left(\frac{\text{Rate}}{[BH_2^{2+}]}\right)$
0.003	32.6	1813	4436	3.647
0.006	32.7	1819	4460	3.649
0.015	32.2	1791	4358	3.639
0.016	31.7	1763	4256	3.629
0.049	31.1	1730	4144	3.617
0.079	30.4	1692	4018	3.604
0.145	29.0	1615	3772	3.577
0.252	27.8	1550	3578	3.554
0.427	24.8	1385	3108	3.492
0.747	22.3	1249	2752	3.440
1.160	16.5	927	1970	3.294
1.745	12.2	689	1439	3.158
2.519	7.3	413	850	2.929
3.942	2.2	126	258	2.412

†For imidazolium exchange assuming broadening due to ammonium exchange is zero.

TABLE 4.36

COEFFICIENTS OBTAINED BY FITTING EQUATION 4.20 TO DATA AT LOW pH

Data from Tables	-10^2c_1	-10^2c_2	c_3
4.31	2.43	7.76	3.740
4.32	3.42	6.35	3.807
4.33	2.45	7.17	3.773
4.34	2.51	5.81	3.737
4.35 when [HCl] > 0.4 M	2.32	20.6	3.588
4.35 all points	1.59	24.2	3.621
Imidazole †	2.58	16.6	3.54

†Data listed for imidazole by Ralph and Grunwald [44].

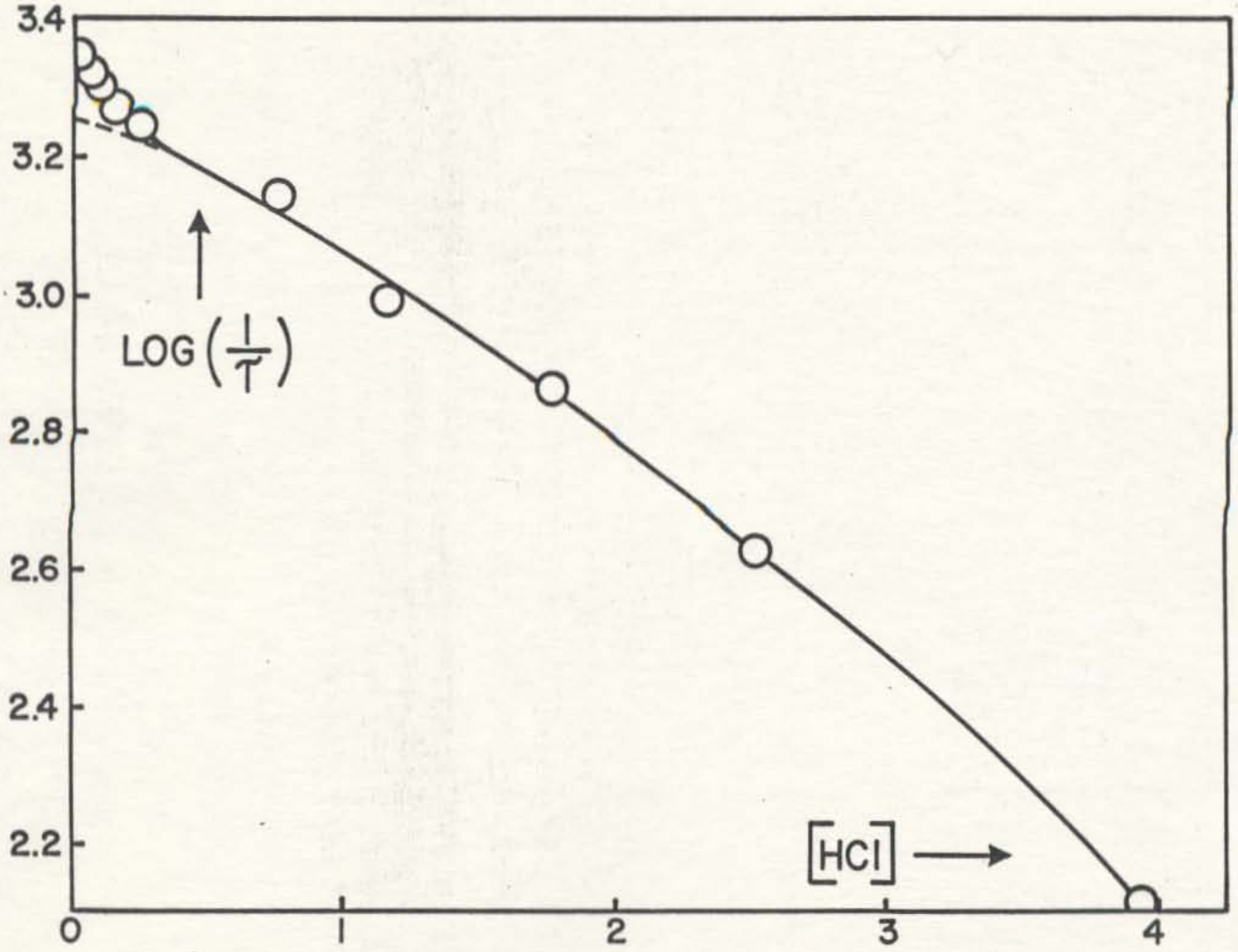

Figure 4.23 Acid repression in deuterated histamine solutions

plot is very similar to that shown by Ralph and Grunwald for imidazole [44], but the upward step when [HCl] < 0.4 M is somewhat smaller in the present case. In view of this similarity, an attempt was made to calculate a Q value (Q_2) for the apparent step in the rate when [HCl] < 0.4 M. To perform these calculations, estimates of k_{cyclic} were made by extrapolation of the least squares fit of the data for [HCl] > 0.4 M. These estimates were subtracted from the measured values of $\left(\frac{\text{Rate}}{[BH_2^{2+}]}\right)$ and the residual rates used in Equation (4.19) to calculate Q_2. The k_a' value in this equation was determined as 488 l.mole.$^{-1}$ sec.$^{-1}$ by extrapolating the log $\left(\frac{\text{Rate}}{[BH_2^{2+}]}\right)$ curve to [HCl] = 0 and subtracting the resulting value of k°_{cyclic} from the measured specific rate on the plateau. The results of these calculations are shown in Table 4.37, and the mean value for Q_2 = 10.0 ± 2.4. This corresponds to a k_H of 2 x 10^8 sec.$^{-1}$.

Since the above attempt to determine a Q_2 step involved only small changes in rates, and since no Q_2 step could be determined in the natural abundance solutions, it must follow that the very existance of "Q_2" is suspect. Accordingly an attempt was made to fit all the data shown in Figures 4.23 to a single least squares quadratic curve. The coefficients defined by Equation (4.20) are listed in Table 4.36, and they are used to calculate the theoretical (Δ/c) values (without Q_2) which are shown in Table 4.38. Comparison of these calculated (Δ/c) values with the experimental (Δ/c) values in Table 4.38 shows that the maximum discrepancy without including a Q_2 feature is about 1.5 (Δ/c) units. This is possibly outside the limits of experimental uncertainty, but not conclusively so. The (Δ/c) values calculated with the Q_2 term

TABLE 4.37

ATTEMPTS TO CALCULATE A SECOND Q FOR
DATA IN 95% DEUTERATED SOLUTIONS

[HCl]	Residual Rate	Q_2
0.0156	416	11.1
0.0493	366	6.8
0.0792	292	8.5
0.1447	164	13.7
0.2519	142	9.7

TABLE 4.38

COMPARISON OF THEORETICAL AND EXPERIMENTAL (Δ/c) VALUES FOR SOLUTIONS IN 95% D_2O AT LOW pH

[HCl]	(Δ/c) Calculated with Q_2	(Δ/c) Calculated without Q_2	(Δ/c) Experimental
0.003	32.1	31.3	32.6
0.006	32.0	31.2	32.7
0.015	31.8	31.1	32.2
0.016	31.8	31.1	31.7
0.049	30.9	30.6	31.1
0.079	30.3	30.4	30.4
0.145	29.3	29.5	29.0
0.252	27.7	28.0	27.8
0.427	25.7	25.9	24.8
0.747	21.8	21.9	22.3
1.160	17.6	17.4	16.5
1.745	12.4	11.9	12.2
2.519	7.3	7.0	7.3
3.942	2.3	2.2	2.2

can be seen to give a better fit with the experimental data.

Further Consideration of the Double Irradiation Experiments

In the initial treatment of the data obtained from these experiments, it was assumed that j_1 remained constant, and on this basis j_2' was determined to be $(7.6 \pm 2.6) \times 10^6$ 1.mole.$^{-1}$ sec.$^{-1}$ in 0.326 M histamine solutions at pH 0.3 to 1.0. Results from the series of experiments at constant histamine concentration can now be used to predict that $j_2' = (4.0 \pm 0.2) \times 10^6$ 1.mole.$^{-1}$ sec.$^{-1}$ under the same conditions. It can be seen that these two values for j_2' do not agree within the limits of their standard errors. Extra systematic errors may make the discrepancy less pronounced, but the agreement is poor.

Since the double irradiation measurements were made with [HCl] as high as 0.5 M., the possibility of acid repression of j_1 should be considered. If acid repression of j_1 is present, then the initial analysis (in which j_1 was kept constant) would lead to an artificially high value for j_2' and an artificially low value for j_1. The data in Table 4.11 was therefore treated in an alternative fashion with j_2' fixed at 4.0×10^6 1.mole.$^{-1}$ sec.$^{-1}$ and the j_1 of Equation (4.3) changed to $\left(\frac{j_1}{1 + Q_s[H^+]}\right)$. Values obtained were

$$j_1 = (21.2 \pm 4.0) \text{ sec.}^{-1}$$

$$Q_s = 0.8 \pm 0.6.$$

If this be so, then the value of j_1 used in the main analysis should have been 21.2 sec.$^{-1}$ rather than 14.2 sec.$^{-1}$. Inspection of the analysis showed that the difference between these two values always

led to differences of less than one tenth of a (Δ/c) unit. Since this amount is insignificant, the main analysis was not modified.

CHAPTER 5

DISCUSSION OF HISTAMINE RESULTS

Steps in the Pseudo First Order Rate Laws

The step detected at pH 3 to 4

In the results the fit for the 0.03M and 0.06M data was improved by including a Q factor in the rate expression for imidazolium proton exchange. The data at 0.006M and 0.27M could be fitted to the rate expressions within the limits of experimental error without invoking such a step. In the case of the data at 0.006M, the errors in the measurements were very high and also the overlap of the two broadening components was most severe. There is, therefore, little surprise that the goodness of fit of the data at this concentration was insensitive to the introduction of the step. An important consequence is that k_1' may, for example, be fixed at much lower values with k_2 (and possibly also j_2) having correspondingly higher values. While such a set of constants will not produce as good a fit of the experimental data as was shown for the set of constants given in the results, nevertheless the fit will still be within the limits of experimental error. Accordingly the error limits on k_1', k_2 and j_2 at this concentration must be very large. For the data at 0.27M., the second order rate of exchange (i.e. the k_2 process) was large in the pH region 3 to 4. Accordingly, the percentage of the (Δ/c) measurements which were affected by the step had become small and the error limits on k_1' at this concentration will be large.

The possibility that the step should have been included in the rate expression for ammonium exchange

The step in the pH 3 to 4 region of the .03M and .06M data was considered to be present in the rate law for imidazolium proton exchange. The possibility that this step could be present in the ammonium proton exchange law will now be considered. A step in the pH 3 to 4 region of the ammonium rate expression could conceivably arise in two ways.

(i) The first order rate in the region of pH 0 may be due to a cyclic process as proposed by Ralph and Grunwald for imidazolium [44] and the k_H process would cause the step in the region of pH 3 to 4.

(ii) The trans and gauche isomers of the histamine may give rise to two different k_H values in the two different pH regions [35].

In either case the total first order ammonium exchange rate would have to have a minimum value of about 3000 $sec.^{-1}$ at pH 4 in order to account for the magnitude of the Δ/c step which is observed. However the ammonium group is primarily associated with a pK_A of about 10 and therefore has a very weak acidic character. Such a group is unlikely to have a large rate of proton exchange due to acid disassociation. In fact the ammonium rate of proton exchange is known to be very low at pH 1 since the slow sweep spectrum showed no significant exchange broadening of the ammonium resonance at this pH. It should also be noted that if the step is to be accounted for by the first explanation, then the only k_H process would be exceptionally slow for an alkylamine. In addition the cyclic process postulated in the first explanation has not previously been observed for an alkylamine.

Acid Repression of j_1

In the double irradiation experiments, the acid repression of j_1 was possibly present with a Q value of about 0.8. If this is so then we can evaluate a k_H for the process:

$$j_H = \frac{j_{-1}}{Q} = \frac{j_1}{QK_{A1}'} \tag{5.1}$$

where K_{A1}' is the acid dissociation constant for the reaction

$$^+HIm.NH_3^+ + H_2O \rightleftharpoons {}^+HIm.NH_2 + H_3O^+ \tag{5.2}$$

$$K_{A1}' = \frac{[^+HImNH_2][H_3O^+]}{[^+HImNH_3^+]} \tag{5.3}$$

Consideration of the microscopic acid dissociation constants will provide a relationship between K_{A1}' and the experimental acid dissociation constants K_{A1} and K_{A2}. The full ionization scheme for histamine can be represented by

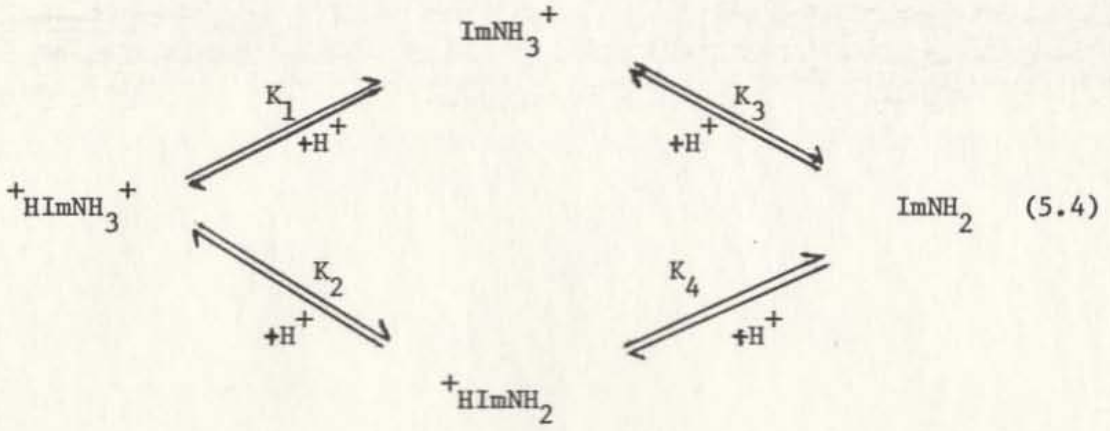

(5.4)

where the microscopic acid dissociation constants are

$$K_1 = \frac{[ImNH_3^+][H_3O^+]}{[^+HImNH_3^+]} \tag{5.5}$$

$$K_2 = \frac{[^+HImNH_2][H_3O^+]}{[^+HImNH_3^+]} \tag{5.6}$$

$$K_3 = \frac{[ImNH_2][H_3O^+]}{[ImNH_3^+]} \tag{5.7}$$

$$K_4 = \frac{[ImNH_2][H_3O^+]}{[^+HImNH_2]} \tag{5.8}$$

The experimental acid dissociation constants are

$$K_{A1} = \frac{([ImNH_3^+] + [^+HImNH_2])[H_3O^+]}{[^+HImNH_3^+]} = K_1 + K_2 \tag{5.9}$$

$$K_{A2} = \frac{[ImNH_2][H_3O^+]}{([ImNH_3^+] + [^+HImNH_2])} = \frac{1}{(1/K_3 + 1/K_4)} \tag{5.10}$$

Since the imidazolium ion is much more acidic than the ammonium ion, we expect that $K_1 >> K_2$ so that $K_{A1} \simeq K_1$. Similarly we expect $K_4 >> K_3$ so that $K_{A2} \simeq K_3$. K_{A1}' is identical to K_2 and it refers to the same process as K_3 (which can be measured by K_{A2}) but with the presence of an extra proton at the imidazole end of the molecule. In the same way the microscopic constant K_1 (which can be measured by K_{A1}) refers to the same process as the K_A of imidazolium ion but with an extra proton at the ammino end of the molecule. If we assume that the effect of the extra

proton on the acid dissociation constant is confined to coulombic repulsion, then the electrostatic field will be the same in both cases. Therefore the ΔG° electrostatic which δpK_A measures will be the same in both cases so that

$$pK_A - pK_1 = pK_3 - pK_2$$

or $$pK_A - pK_{A1} = pK_{A2} - pK_{A1}' \qquad (5.11)$$

where pK_A is the acid dissociation constant of imidazole which was reported to be 6.98 ± 0.01 by Ralph and Grunwald [44]. Paiva et al. [68] report pK_{A2} for histamine as 9.75 while Randolf v. Schalien [67] reports a value of 9.756. Assuming a mean value of 9.75 for pK_{A2} and recalling that pK_{A1} was determined as 5.85 ± 0.01 in the present work, Equation (5.11) can be used to determine an estimate for pK_{A1}' of 8.62. Hence $K_{A1}' = 2.4 \times 10^{-9}$ and Equation (5.1) provides

$$j_H = \frac{j_1}{Q.K_{A1}'} = \frac{21.2}{0.8 \times 2.4 \times 10^{-9}} = 1.1 \times 10^{10} \text{ sec.}^{-1}$$

While recognizing that the assumptions made, as well as the uncertainties of measurements, will cause large uncertainties in the foregoing, it is nevertheless interesting to note that the magnitude of j_H is as expected for a primary alkylamine in water [35]. It is, therefore, quite reasonable to suppose that acid repression of j_1 was detected in the double irradiation experiments.

Acid Repression of k_1

The step in the region of pH 3 to 4 has been interpreted as a k_H process with $k_H = 4 \times 10^6$ sec.$^{-1}$. Such a value might be quite reasonable

for the gauche rotamers of histamine [35]. The trans isomer might show a k_H value at about pH = 0. This was the case for imidazole where k_H was found to be 1.8×10^9 [44]. Accordingly an attempt was made to interpret the acid repression data as a k_H process rather than as a salt effect. When this procedure was applied to the different data series, k_H was evaluated as $(6 \pm 1) \times 10^{10}$ sec.$^{-1}$. Such a value is unacceptably high for a k_H process at the imidazole ring so that the interpretation of the acid repression as a salt effect is preferred. However, a k_H value comparable to that found in imidazole may well be superimposed on the salt effect and be inseparable from the salt effect.

Rate Constants from the 0^{17} Experiments

(a) $n_1 l_1$

This rate constant is a composite rate constant for all reactions involving one molecule of histamine. Three types of reaction may be present:

(i) The usual pseudo first order reactions of the j_1 and k_1 type.

(ii) The intramolecular proton transfer between amino and imidazole sites. This process was detected in the NH data and it was designated by the rate constant j_i.

(iii) At high pH, Chang and Grunwald [77] have detected an intramolecular process in imidazole. In this process, a proton is transferred from one imidazole nitrogen to the other imidazole nitrogen in the same ring with one or more water molecules participating.

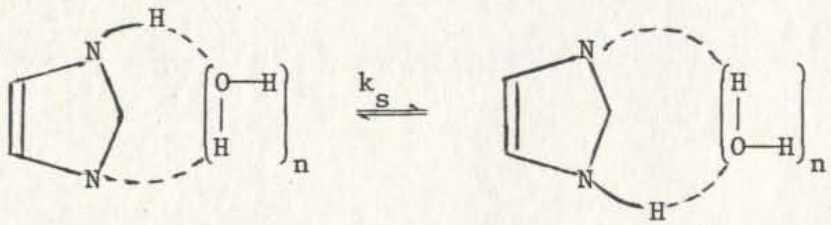

(5.12)

This reaction might be detected in the O^{17} rate data for histamine.

Inspection of the values for n_1l_1 (which are listed in Table 4.30) shows that the contribution from j_1 and k_1 will be insignificant provided that the number of water molecules is "normal" (i.e. between one and two). The value of n_1l_1 must therefore arise from one or both of the intramolecular processes. While it is not possible to clearly distinguish between these two processes, upper and lower limits can be placed on their relative contributions as follows.

It is first noted that the j_i process must take place with the participation of at least one water molecule since otherwise it would not have been detected in the NH data. In the n_1l_1 measurement the minimum contribution from this process must therefore be 3.74×10^5 sec.$^{-1}$.† If this minimum contribution due to j_i is subtracted from the n_1l_1 values listed in Table 4.30 we obtain the weighted mean for the maximum value of n_sk_s to be $(3.4 \pm 0.8) \times 10^5$. This compares with the value of n_sk_s in imidazole of $(1.5 \pm 0.5) \times 10^6$. Therefore if this k_s process is present at all in histamine, it must be appreciably slower than in imidazole

---

†Using $j_i = 1.87 \times 10^5$ sec.$^{-1}$ (this is the weighted mean of the two values determined in the results). In the n_1l_1 data the j_i contribution will be doubled due to the measurement of both the forward and reverse proton transfers.

itself. Since the rate determining step is not known it is difficult to specify the reason for this difference. The difference in the acidity of the imidazolium ion in the two cases is one factor which may cause the k_s mechanism and rate to change.

The second limiting case would arise if $n_s k_s$ had become so small as to be negligible. In this case $n_1 l_1$ will become $2n_i j_i$ and the weighted mean for the number of water molecules in the intramolecular j_i process will be 1.9 ± 0.2. The weighted means given here are weighted as the reciprocal of the square of the standard deviation.

(b) $n_2 \ell_2^\circ$

This rate constant refers to all reactions which involve two histamine species and it has already been deduced that reactions involving different charge types are included. Thus reactions involving a +2 ion and a +1 ion have been designated by the component

$$n_{21}\ell_{21}^\circ = (4.85 \pm 0.34) \times 10^7 \text{ ℓ.mole.}^{-1} \text{ sec.}^{-1}.$$

Reactions involving a +1 ion and an unchanged histamine molecule were also detected with

$$n_{10}\ell_{10}^\circ = (9.7 \pm 0.6) \times 10^8 \text{ ℓ.mole.}^{-1} \text{ sec.}^{-1}.$$

Reactions in which the two histamine species have a total charge of +2 might also be expected. The rate constants $n_{20}\ell_{20}^\circ$ and $n_{11}\ell_{11}^\circ$ (which were included in Equation (4.17) refer to such reactions. Analysis of the experimental data, however, showed no evidence for these reactions since the value of $n_2\ell_2$ increased slightly more rapidly than the square

of the buffer ratio. Reactions in which the total reactant charge is +2 will cause $n_2\ell_2^\circ$ to increase as the first power of the buffer ratio, while reactions in which the total reactant charge is +1 (i.e. $n_{10}\ell_{10}^\circ$) will cause $n_2\ell_2^\circ$ to increase as the square of the buffer ratio. If reactions of both charge type are present, $n_2\ell_2^\circ$ should increase as the buffer ratio raised to some power between one and two. In order to understand why $n_{20}\ell_{20}^\circ$ and $n_{11}\ell_{11}^\circ$ were not detected, we must examine the uncertainties in the values of $n_2\ell_2^\circ$ which are listed in Table (4.30). For the maximum possible contribution from these two reactions, we must find the maximum portions of $n_2\ell_2^\circ$ (i.e. portions proportional to the first power of the buffer ratio) which can be subtracted while leaving residual parts which will still give a linear plot (within the limits of the experimental uncertainties) versus the square of the buffer ratio. By this procedure the limit

$$(n_{20}\ell_{20}^\circ K^- + n_{11}\ell_{11}^\circ) \leq 1.1 \times 10^6 \text{ ℓ.mole.}^{-1} \text{ sec.}^{-1}$$

was determined. Hence the experimental results require that

$$n_{11}\ell_{11}^\circ \leq 1.1 \times 10^6 \text{ ℓ.mole.}^{-1} \text{ sec.}^{-1}$$

and $$n_{20}\ell_{20}^\circ \leq 9 \times 10^9 \text{ ℓ.mole.}^{-1} \text{ sec.}^{-1}$$

The main component of $n_{20}\ell_{20}^\circ$ will be a "downhill" reaction in which a proton is transferred from an imidazolium site to an amino site. Such a reaction might be expected to be diffusion controlled but even so the rate constant would not be expected to exceed 9×10^9 ℓ.mole.$^{-1}$ sec.$^{-1}$ where this size of ion is involved. Hence the limits imposed by the

failure to detect this reaction are not anomalous.

When the least squares fit to Equation (4.17) is repeated after the above component has been subtracted, it is found that

$$n_{10}\ell_{10}^{\circ} = (7.3 \pm 0.8) \times 10^{8}\ \ell.\text{mole.}^{-1}\ \text{sec.}^{-1}$$

Hence very little change in this rate constant will result if $n_{20}\ell_{20}^{\circ}$ and/or $n_{11}\ell_{11}^{\circ}$ are in fact present.

Components of the Second Order Rate Constants

The rate constants j_2 and k_2 were both derived from a rate law dependence on $[BH_2^{2+}][BH^{+}]$. The reactions which would have this dependence are listed below but without including the water participation which will be at least one water molecule in each case.

For j_2:

$$^{+}\text{HIm.NH}_3^{+} + \text{Im.NH}_3^{+} \overset{q_1}{\rightarrow} {}^{+}\text{HIm.NH}_2 + {}^{+}\text{HIm.NH}_3^{+} \qquad (5.13)$$

and

$$^{+}\text{HIm.NH}_3^{+} + {}^{+}\text{HIm.NH}_2 \overset{q_2}{\rightarrow} {}^{+}\text{HIm.NH}_2 + {}^{+}\text{HIm.NH}_3^{+} \qquad (5.14)$$

For k_2:

$$^{+}\text{HIm.NH}_3^{+} + \text{Im.NH}_3^{+} \overset{q_3}{\rightarrow} \text{Im.NH}_3^{+} + {}^{+}\text{HIm.NH}_3^{+} \qquad (5.15)$$

and

$$^{+}\text{HIm.NH}_3^{+} + {}^{+}\text{HIm.NH}_2 \overset{q_4}{\rightarrow} \text{Im.NH}_3^{+} + {}^{+}\text{HIm.NH}_3^{+} \qquad (5.16)$$

If we designate the rate constants for reactions (5.13) to (5.16) by q_1 to q_4 respectively while remembering that

$$\frac{[\ Im.NH_3^+]}{[^+HIm.NH_2]} = \frac{K_{A1}}{K'_{A1}} = 5.9 \times 10^2$$

we have for j_2

$$j_2\ [BH_2^{2+}][BH^+] = q_1\ [BH_2^{2+}][BH^+] + q_2\ \frac{[BH_2^{2+}][BH^+]}{5.9 \times 10^2}$$

where $[BH^+] = [Im.NH_3^+] + [^+HIm.NH_2] \simeq [Im.NH_3^+]$

$$\therefore\ j_2 = q_1 + \frac{q_2}{5.9 \times 10^2}$$

and a mean value of $j_2 = 1.9 \times 10^6$ $\ell.mole.^{-1}$ $sec.^{-1}$ gives

$$1.9 \times 10^6 = q_1 + \frac{q_2}{5.9 \times 10^2} \qquad (5.17)$$

and similarly for k_2

$$k_2\ [BH_2^{2+}][BH^+] = q_3\ [BH_2^{2+}][BH^+] + q_4\ \frac{[BH_2^{2+}][BH^+]}{5.9 \times 10^2}$$

The value of $k_2^\circ = 2.4 \times 10^7$ $\ell.mole.^{-1}$ $sec.^{-1}$ determined later gives

$$2.4 \times 10^7 = q_3 + \frac{q_4}{5.9 \times 10^2} \qquad (5.18)$$

We can obtain a third relationship by recognising that reactions (5.13) and (5.16) are the reverse of each other. Accordingly the principle of microscopic reversibility will apply

$$q_1\ [BH_2^{2+}][BH^+] = q_4\ \frac{[BH_2^{2+}][BH^+]}{5.9 \times 10^2}$$

$$q_1 = \frac{q_4}{5.9 \times 10^2} \qquad (5.19)$$

We therefore have three equations with four unknown rate constants and a solution will not be possible. However some limiting values for these rate constants may be estimated. From Equation (5.17) we have

$$q_2 \leq 1.1 \times 10^9 \text{ ℓ.mole.}^{-1} \text{ sec.}^{-1}$$

and also

$$q_1 \leq 1.9 \times 10^6 \text{ ℓ. mole.}^{-1} \text{ sec.}^{-1}$$

From Equation (5.19) it follows that

$$q_4 \leq 1.1 \times 10^9 \text{ ℓ. mole.}^{-1} \text{ sec.}^{-1}$$

and from Equation (5.18)

$$2.2 \times 10^7 \leq q_3 \leq 2.4 \times 10^7 \text{ ℓ. mole.}^{-1} \text{ sec.}^{-1}$$

If q_4 (for a "downhill" reaction) is larger than q_2 (for a "symmetrical" reaction) then both q_1 and q_4 will be near their upper limits. However, the steric features of hydrogen bonding have a marked effect on the rates of reactions with solvent participation so that free energy considerations alone do not provide conclusive evidence that q_4 will be greater than q_2. There are further indications from the present work which lead to the same conclusion. The main component in the reaction referred to by the ℓ_{10} rate constant concerns the same proton transfer as reaction (5.14). Due to electrostatic repulsion between the

reactant ions, q_2 will be expected to be smaller than k_{10} [18]. A similar electrostatic repulsion is expected to result in q_3 having a smaller value than the rate constant for the parallel reaction in imidazole itself (k_{Im}). If we assume that the ratio of q_2 to k_{10} is the same as the ratio of q_3 to k_{Im}, we can estimate q_2 from the values of $4.8 \times 10^8 \leq k_{10} \leq 9.7 \times 10^8$ l. mole.$^{-1}$ sec.$^{-1}$ (see later), $2.2 \times 10^7 \leq q_3 \leq 2.4 \times 10^7$ l. mole.$^{-1}$ sec.$^{-1}$, and $k_{Im} = 1 \times 10^8$ l. mole.$^{-1}$ sec.$^{-1}$ [44]:

$$1.1 \times 10^8 \leq q_2 \leq 2.3 \times 10^8 \text{ l. mole.}^{-1} \text{ sec.}^{-1}$$

Equations (5.17) and (5.19) then lead to the estimates

$$1.5 \times 10^6 \leq q_1' \leq 1.7 \times 10^6 \text{ l. mole.}^{-1} \text{ sec.}^{-1}$$

and $0.9 \times 10^9 \leq q_4 \leq 1.0 \times 10^9$ l. mole.$^{-1}$ sec.$^{-1}$

Equation (5.18) then gives

$$q_3 = 2.2 \times 10^7 \text{ l. mole.}^{-1} \text{ sec.}^{-1}$$

A reaction such as (5.16) for which $\Delta G° < 0$ would be expected to be diffusion controlled providing intramolecular hydrogen bonding does not make the hydrogen bond alignment unfavourable for the q_4 proton transfer. Calculation of the diffusion controlled rate will show whether the presence of such unfavourable hydrogen bonding has led to the upper experimental limit being significantly less than the diffusion controlled rate. A method of calculating the diffusion controlled rate of reaction between two ions has been given by Alberty and Hammes [20]. The theory is consistent with a Brönsted limiting law as used in the

present work for the effect of ionic strength on the rate of reaction (Equation 4.7). The rate constant for a diffusion controlled reaction between two ions at zero ionic strength is given by

$$q_4 = \frac{4\pi N}{1000} D_{12} R_{12} f \qquad (5.20)$$

where N is Avagadro's number,

$D_{12} = D_1 + D_2$ where D_1 and D_2 are the diffusion coefficients of the two reacting ions

and R_{12} is the reaction radius.

Repulsion of the ionic charges is allowed for by the factor f which can be calculated from

$$f = \frac{L/R_{12}}{\exp.(L/R_{12})-1} \qquad (5.21)$$

with $$L = \frac{Z_1 Z_2 e^2}{\epsilon k T} \qquad (5.22)$$

where Z_1 and Z_2 are the number of charges on the reacting ions (with signs) and e, ϵ, k and T have their usual significance. Thus q_4 may be calculated if estimates can be made for the reaction radius and for the diffusion coefficients of the reacting ions. Eigen [78] used Equation (5.20) to calculate the rate constants of several reactions between two ions where one of the ions was a hydrogen or hydroxyl ion. He found that a reaction radius of 5×10^{-8} cm. (about two hydrogen bond lengths) accounted for the rate constants. Alberty and Hammes [20] estimated the same value for R_{12} when using Equation (5.20) to calculate the rate constant for the reaction of fumarase with fumarate ions. The indications of water participation in the present case make the estimation of the

same value for R_{12} seem reasonable. It was assumed that the diffusion coefficients of the two reacting ions, would be about the same and an estimate of this value was made from conductivity data available for tetramethylammonium ion and tetraethylammonium ion [79]. By assuming that the diffusion coefficient is proportional to the reciprocal of the cube root of the molar mass it was determined that $D_1 = D_2 = 0.79 \times 10^{-5}$ cm.^{2} sec.$^{-1}$. Equation (5.20) then provides the estimate

$$q_4 = 1.0 \times 10^9 \text{ ℓ. mole.}^{-1} \text{ sec.}^{-1}$$

Since this value is in good agreement with the experimental value, the possibility that the reaction is diffusion controlled is consistent with this calculation.

Number of Water Molecules in the Second Order Reactions

The experiments using solutions which were enriched in O^{17} showed that

$$n\ell_{21}^{\circ} = (4.85 \pm 0.34) \times 10^7 \text{ ℓ. mole.}^{-1} \text{ sec.}^{-1}$$

The value of ℓ_{21}° can be obtained from

$$\ell_{21}^{\circ} = j_2^{\circ} + k_2^{\circ} = (2.63 \pm 0.11) \times 10^7 \text{ ℓ. mole.}^{-1} \text{ sec.}^{-1}$$

so that the average number of water molecules

$$n = 1.8 \pm 0.2$$

This result applies to the composite second order rate constant. Since the previous analysis showed that reaction (5.15) makes the

dominant contribution to this composite constant, it follows that this result must be true for that component, but with a slightly larger uncertainty.

Consideration of j_i

It was deduced that this rate constant refers to an intramolecular process in the BH^+ species involving an average of one to two water molecules. The initial arrangement may be written as follows using two water molecules for the example.

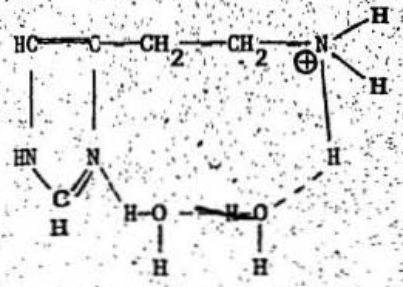

and for present purposes we can abbreviate this to

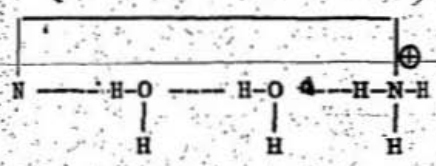

The reaction scheme for the j_i process will then be

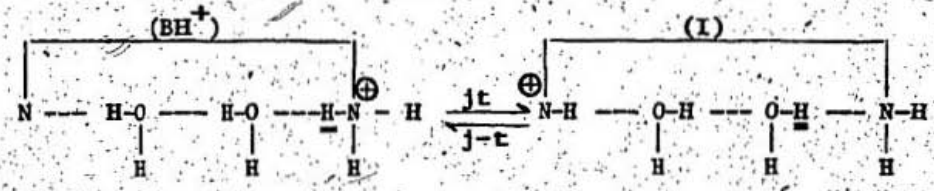

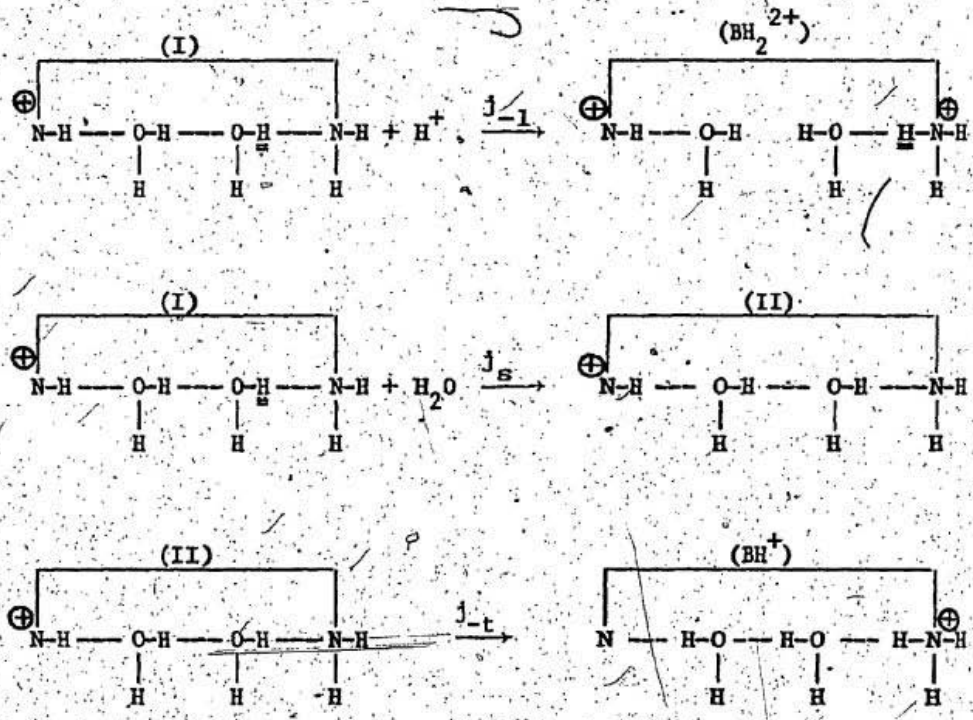

The formation of I from BH_2^{2+} is neglected since the rate constant for such a process has been shown to be very small ($j_1 \simeq 20$ sec.$^{-1}$). The j_s step may occur by rotation of the marked water molecule rather than by its substitution. The n.m.r. experiment measures the rate of breaking of the N-H bond, so that the rate equation is

$$\text{Rate} = j_i[BH^+] = j_s[I] \qquad (5.23)$$

By application of steady state theory to the intermediate designated as I.

$$\frac{d[I]}{dt} = 0 = j_t[BH^+] - I\,(j_{-t} + j_s + j_{-1}[H^+])$$

$$\therefore [I] = \frac{j_t [BH^+]}{j_{-t} + j_s + j_{-1} [H^+]}$$

Substituting for [I] in Equation (5.23)

$$j_i = \frac{j_s j_t}{j_{-t} + j_s + j_{-1} [H^+]} \qquad (5.24)$$

There are now three simplified cases.

Case 1

$$j_{-1} [H^+] >> j_{-t}, j_s.$$

then $$j_i = \frac{j_s j_t}{j_{-1} [H^+]}$$

In this case, acid repression of j_i would occur. This was not observed and would in fact only be expected at low pH values.

Case 2

$$j_s >> j_{-t}, j_{-1}[H^+]$$

then $$j_i = j_t$$

$$\therefore j_t = 1.9 \times 10^5 \text{ sec.}^{-1}.$$

Also by the principle of microscopic reversibility,

$$j_t [BH^+] = j_{-t} [I]$$

$$\therefore \quad j_{-t} = \left(\frac{[BH^+]}{[I]}\right) j_t$$

but $$\frac{[BH^+]}{[I]} = \frac{K_{Al}}{K_{Al}} = \frac{1.41 \times 10^{-6}}{2.4 \times 10^{-9}} = 5.9 \times 10^2$$

$$\therefore \quad j_{-t} = 5.9 \times 10^2 \times 1.9 \times 10^5$$

$$\therefore \quad j_{-t} = 1.1 \times 10^8 \text{ sec.}^{-1}.$$

By our initial assumption therefore

$$j_s \gg 1.1 \times 10^8 \text{ sec.}^{-1}.$$

In this case the rate determining step is a proton transfer and the high measured isotope effect of 3.1 ± 0.5 on j_i is consistent with such a case (see Chapter 1 and Reference 19).

Case 3

$$j_{-t} \gg j_s, \; j_{-1}[H^+]$$

then $$j_i = \frac{j_t \cdot j_s}{j_{-t}} = \frac{j_s}{5.9 \times 10^2}$$

so $$j_s = 1.1 \times 10^8 \text{ sec.}^{-1}.$$

In this case the rate determining step is the rotation or exchange of a water molecule. For such cases a normal isotope effect of about 1.4 (or in the case of a co-operative process about 1.4 squared) is expected. The present higher isotope effect therefore favours Case 2.

A Consequence of the Principle of Microscopic Reversibility

The intramolecular process must occur at the same total rate in both directions and this rate has been determined to be $j_t[BH^+]$ where $j_t = 1.9 \times 10^5$. The intramolecular process will make a contribution to the apparent second order law for imidazole exchange such that

$$j_t [BH^+] = k_x [BH_2^{2+}] [BH^+]$$

$$\text{i.e.} \quad k_x = \frac{j_t}{[BH_2^{2+}]}$$

where k_x is the contribution to k_2 from the intramolecular process. Table 5.1 shows the residual k_2 for the different data series after subtracting the expected intramolecular contributions. As explained previously, the value of k_2 in 0.006M solutions has large error limits† so that the anomalous result for this concentration is not surprising.

A plot of log $(k_2 - k_x)$ against $\sqrt{\mu}$ for the three points available provides a straight plot with a new value for the second order rate constant extrapolated to zero ionic strength.

$$k_2^\circ = (2.43 \pm .06) \times 10^7 \text{ ℓ. mole.}^{-1} \text{ sec.}^{-1}$$

This is slightly lower than the value of $(2.80 \pm 0.14) \times 10^7$ ℓ. mole.$^{-1}$ sec.$^{-1}$ which had been obtained without allowing for the intramolecular reaction.

---

†For example one possible fit of this data had k_2' set at zero. In this case all discrepancies were less than 2 (Δ/c) units and the value of k_2 was 6.7×10^7 ℓ. mole.$^{-1}$ sec.$^{-1}$

TABLE 5.1

ALLOWANCE FOR THE INTRAMOLECULAR REACTION

IN THE k_2 VALUES

$[BH_2^{2+}]$	$\sqrt{\mu}$	$10^{-7} \times k_2$	$10^{-7} \times k_x$	$10^{-7} \times (k_2 - k_x)$	$\log(k_2 - k_x)$
2.70×10^{-1}	0.935	5.85	.06	5.8	7.76
5.96×10^{-2}	0.440	3.9	0.3	3.6	7.56
2.98×10^{-2}	0.311	3.9	0.6	3.3	7.52
6.00×10^{-3}	0.140	3.0	3.1		

Summary of Constants Determined in This Work

Table 5.2 lists the main constants which have been deduced from this study of histamine. k_2°, j_2°, pI_{10}°, and K_{A1}° are values obtained by extrapolating to zero ionic strength. Any salt effects on k_1, k_1', k_H and j_1 are neglected. Since no consistent trend with ionic strength could be determined, k_1 is taken as the mean of the values obtained at the four different concentrations. As indicated previously, k_1' and k_H both had large uncertainties in the 0.006M. data and their values at this concentration were much different from their values at the other three concentrations. Accordingly the 0.006M results were omitted when calculating the means for k_1' and k_H. The uncertainty listed for k_2° is a least squares error only and errors due to corrections for salt effects and allowance for an intramolecular process will cause larger total uncertainty in the value. Values for j_2° and j_1 were obtained from the constant buffer experiments and also from separation of j_2'. The mean of the two values is reported in each case. The large uncertainty for j_2° arises from a large discrepancy between the two values. This discrepancy is not very surprising when the possible sources of error are considered. For both determinations of j_2° it was necessary to separate j_1 and also to make an allowance for salt effects on j_2°. The possibility of a salt effect on j_1 had to be ignored in each case. Furthermore in the constant buffer experiment, allowance had to be made for broadening due to imidazolium exchange and, in view of the complicated rate laws, this correction may introduce considerable error.

Values of j_1 obtained from the two procedures showed good agreement and the weighted mean is listed in the Table.

TABLE 5.2

SUMMARY OF THE MAIN CONSTANTS

Constant	Value	Isotope effect	Activation energies (E_a), and average number of water molecules (n).
k_1	$(5.54\pm0.45)\times10^{3}$	1.3±0.2	$E_a = 9.2\pm0.6$ k.cals. mole^{-1}
k_{-1}	$(5.67\pm0.21)\times10^{3}$	67	
k_H	$(4.6\pm0.4)\times10^{6}$	97	
k_2°	$(2.43\pm0.06)\times10^{7}$	2.7±0.2	n=1.8±0.2
j_2°	$(2.05\pm0.45)\times10^{6}$	1.5±0.4	
j_1	21.2±4.0		
j_H	$(1.1\pm1.0)\times10^{10}$		
j_i	$(1.87\pm0.09)\times10^{5}$	3.1±0.5	1≤n≤1.9
$n1_{10}^\circ$	$(9.7\pm0.6)\times10^{8}$		
K_{Al}°	$(1.41\pm0.03)\times10^{-6}$	2.9±0.1	

Consideration of the Isotope Effects

Isotope effects listed in Table 5.2 for k_1, k_1', k_H, k_2° and K_{A1}° were obtained by dividing natural abundance rates by rates in 95% D_2O for the solutions which were approximately 0.06M. Although it was possible to obtain natural abundance values of j_2° and j_1 as the mean of two different values, the available data for deuterated solutions only permitted one determination of these constants i.e. the determination from the constant buffer ratio experiments. The isotope effects listed for j_2° and j_1 in Table 5.2 were obtained by dividing the mean natural abundance values by the constant buffer ratio deuterated values.

The isotope effect listed for k_1 will be reasonable provided that k_1 refers essentially to proton exchange in an ionized intermediate as found by Ralph and Grunwald for imidazole [44]. If k_1 were concerned with proton transfer via acid dissociation, however, then k_1 would be identified with k_a as shown by the two possible mechanisms in Equations 1.30 to 1.39. If this were true, then the isotope effects on k_1 and K_{A1}° would lead to the prediction of an inverse isotope effect on k_{-a}. Since there appears to be no reason to anticipate such an inverse effect, the interpretation of k_1 as proton exchange in an ionized intermediate again appears to be favored.

Due to the small value of k_1' in 95% D_2O, the values of k_1' and k_H were very uncertain in these solutions and hence the isotope effects on these constants are very uncertain. They are entered in Table 5.2 for completeness but their usefulness is dubious.

The isotope effect on j_2° was determined as 1.5 ± 0.4 as explained previously. If this isotope effect is determined by consideration of

the constant buffer experiments alone (and such a procedure may lead to some cancellation of errors) then its value would be listed as 1.2 ± 0.1. Rosenthal and Grunwald [42] reconsidered work by Day and Reilley [56] and deduced that reactions of this type involving two molecules of amine and one molecule of water would be expected to show an isotope effect of 1.2. Reactions involving two molecules of amine and more than one water molecule usually show a higher isotope effect as found for k_2° in the present work.

The isotope effect of 3.1 ± 0.5 which was determined for j_1 is indicative of a mechanism in which the proton transfer is the rate determining step (see Chapter 1 and Reference 19). The earlier analysis of the j_1 process used this fact to deduce that the value of j_1 refers to the rate constant for the proton transfer step (j_t).

The Number of Water Molecules taking Part in the Reactions

In the last section it was indicated that the isotope effect on j_2° may well indicate that one water molecule takes part in this reaction. The value of n = 1.8 ± 0.2 was determined for the composite rate constant (l_{21}) which involves the species BH_2^{2+} and BH^+. This number of water molecules will therefore be a weighted average of the number of water molecules taking part in the j_2° and the k_2° processes. If we make the assumption that one water molecule is involved in the j_2° process, then we can use the weighted average of 1.8 ± 0.2 water molecules to determine the number of water molecules in the k_2° process. Such a procedure provides the value of 1.9 ± 0.2 water molecules for the k_2° reaction which could be exactly two within the limits of experimental error. This result is consistent with the isotope effect of 2.7 which was found for k_2°.

Another case in which the number of water molecules is of interest in the present work is in the determination of nl_{10}°. In the pH region at which the NH broadenings were measured, this reaction was too slow to be measured and hence a value for l_{10}° could not be obtained. As was pointed out in Chapter one, however, in all cases where the number of water molecules has been measured for such a process involving two amine molecules, the result has been between one and two water molecules. Such a range of values in the present case would place l_{10}° between 4.8×10^{8} and 9.7×10^{8} ℓ. mole.$^{-1}$ sec.$^{-1}$. This range seems reasonable when one considers that the equivalent reaction of methylamine has a rate constant of 6.1×10^{8} [30].

Comparison with Other Known Rate Constants

Many of the rate constants determined here for histamine have no parallel in previously determined rate constants. Nevertheless it is possible to make some tests of the presently measured values.

(a) The value of $k_2^{\circ} = 2.4 \times 10^{7}$ ℓ. mole.$^{-1}$ sec.$^{-1}$ refers primarily to a reaction in which a proton is transferred from the imidazolium site of a doubly protonated histamine molecule to the imidazole site of a previously singly protonated histamine molecule. This is specifically the reaction for which 2.2×10^{7} ℓ. mole.$^{-1}$ sec.$^{-1}$ $\leq q_3 \leq 2.4 \times 10^{7}$ ℓ. mole.$^{-1}$ sec.$^{-1}$. Such a symmetrical transfer shows close similarity to the process for which k_2° was determined to be 3.0×10^{7} ℓ. mole.$^{-1}$ sec.$^{-1}$ for piperazine in Chapter three of this thesis. These two values are probably not distinguishable within the limits of the total errors in both measurements. Such a similarity of values seems reasonable for such similar processes. A further test of

the main component of the histamine k_2° value can be made from the measurements which Ralph and Grunwald made on imidazole [44]. These workers determined a rate constant $k_{Im} = 1 \times 10^8$ ℓ. mole.$^{-1}$ sec.$^{-1}$ for a process in which a proton was transferred from a singly charged imidazolium ion to a previously uncharged imidazole molecule. The presently measured q_3 for histamine refers to the same proton transfer but it will be expected to be slower due to electrostatic repulsion caused by the positively charged ammonium side chains. Reductions by factors of four to nine have been found due to the presence of similar electrostatic repulsions in recombination reactions with protons [18]. In the imidazole comparison a reduction by a factor of slightly more than four is measured. Different hydrogen bonding in the cases of imidazole and histamine may also contribute to the difference in rate.

(b) In the analysis of the histamine results, the rate constant j_1 was interpreted as the rate of acid dissociation of the doubly protonated histamine molecule at the amino site. We can therefore calculate a rate constant j_{-1} for the recombination reaction using the previous estimate for K_{A1}'.

$$^+HIm.NH_3^+ + H_2O \underset{j_{-1}}{\overset{j_1}{\rightleftharpoons}} {}^+HIm.NH_2 + H_3O^+ \qquad (5.2)$$

$$K_{A1}' = \frac{j_1}{j_{-1}}$$

$$\therefore \quad j_{-1} = \frac{j_1}{K_{A1}'} = \frac{21.2}{2.4 \times 10^9} = 8.8 \times 10^9 \text{ ℓ. mole.}^{-1} \text{ sec.}^{-1}$$

Although the recombination rate for methylamine or ethylamine

(which may be the best models for recombination at the amino site of an unchanged histamine molecule) are not available, it is noted that this recombination rate varies only from 4.3×10^{10} sec.$^{-1}$ to 1.3×10^{10} sec.$^{-1}$ for such varied amines as ammonia itself and dibenzylmethylamine [18, 35, 39]. Allowing for a reduction of the recombination rate by a factor of one-half to one-third due to electrostatic repulsion [18], the present estimate of j_{-1} leads to a prediction of the recombination rate at the amino site of an unchanged histamine molecule of between 1.6×10^{10} sec.$^{-1}$ and 2.6×10^{10} sec.$^{-1}$. The estimate for j_{-1} is therefore quite reasonable.

(c) A comparison involving the rate constant 1_{10} has been made previously.

Some Conclusions Arising from This Work

It has been shown that by varying the radio frequency field in the adiabatic half passage experiment it is possible to separate two broadening components arising from exchange at two different types of reactive site. This method has been applied to study aqueous solutions of histamine. Although there is insufficient data in the literature to provide a thorough check of the accuracy of the results obtained from this approach, it has been possible to show that the method can provide rate constants which are certainly not in conflict with previous measurements. It is estimated that uncertainties arising from all errors in the method are generally within about ± 20%.

The experiments on histamine have shown that, given the proper structure of hydrogen bonding, water participation allows facile intramolecular proton transfer over fairly large distances. Since the distances between active centers in enzymes is sometimes comparable to that

in histamine, it follows that intramolecular proton transfer in enzymes is possible and perhaps even probable. If intramolecular proton transfer similar to the histamine reaction does occur in enzymes, there are two important consequences.

(i) The intramolecular reaction can compete favourably with bimolecular reactions at physiological pH as shown by the following. For an enzyme the bimolecular reaction

$$E + H^+ \rightarrow EH^+$$

typically has a rate constant of about 10^9 to 10^{10} $\ell.\ mole.^{-1}\ sec.^{-1}$. Therefore at a pH of 7.4 the mean lifetime of the enzyme will be $\tau_E \approx 10^{-2}$ sec. For an intramolecular proton transfer from an ammonium to an imidazole site, however, if the rate is the same as found in histamine, $\tau_E = \frac{1}{j_i} = 5 \times 10^{-6}$ sec.

(ii) The ability of the hydrogen bonded water molecules to fit the contours of the enzyme means that the intramolecular process can result in proton transfer between centers which are severely sterically crowded.

REFERENCES

1. T. C. Bruice and S. J. Benkovic, Bio-organic Mechanisms, Vol. 1. pp. 119 ff., Benjamin, New York, 1966.

2. W. P. Jencks, Catalysis in Chemistry and Enzymology, McGraw-Hill New York, (1969).

3. W. P. Jencks, Advan. Enzymol., 43, 219 (1975).

4. D. E. Koshland Jr., Proc. Natl. Acad. Sci (U.S.) 44, 98 (1958). For a review and further references see Citri, N., Advan. Enzymol., 37, 397 (1973).

5. B. L. Vallee and J. F. Riordan, Ann. Rev. Biochem. 38, 745 (1969).

6. W. P. Jencks in 'Chemical Reactivity and Biological Role of Functional Groups in Enzymes', Biochemical Society Symposium No. 31, 59 (1970) Academic Press Inc., London.

7(a). D. M. Blow, J. J. Birktoft and B. S. Hartley, Nature, 221, 337 (1969).

7(b). D. M. Blow, Accounts of Chemical Research, 9, 145 (1976).

8. J. H. Wang, Science 161, 328 (1968).

9. G. G. Hammes, Accounts of chemical research, 1, 321 (1968).

10. S. A. Bernhard, The Structure and Function of Enzymes., Benjamin, New York, (1968).

11. M. Eigen and G. G. Hammes, Advan. Enzymol., 25, 1 (1963).

12. A. Williams and W. P. Jencks, J. Chem. Soc., Perkin II, 1760 (1974).

13. E. H. Cordes and M. Childers, J. Org. Chem., 29, 968, (1964).

14. C. G. Overberger and H. Maki., Macromolecules, 3, 220 (1970) and references cited therein.

15(a). D. Findlay, D. G. Herries, A. P. Mathias, B. R. Rabin and C. A. Ross, Biochem. J. 85, 152 (1962).

15(b). G. G. Hammes, Adv. Prot., Chem., 23, 1, (1968).

15(c). G. G. K. Roberts, D. H. Meadows and O. Jardetzky, Biochemistry, 8, 2053 (1969).

15(d). D. A. Usher, Proc. natl. Acad. Sci., U.S. 62, 661 (1969).

16. F. Covitz and F. J. Westheimer, J. Am. Chem. Soc., 85, 1773 (1963).

17. M. Eigen, Disc. Far. Soc. 39, 7 (1965).

18. M. Eigen, W. Kruse, G. Maass and L. De Maeyer, Progress in Reaction Kinetics, 2, 285 (1964).

19. M. Eigen, Angew Chem. Internat. Edit., 3, 1 (1964).

20. R. A. Alberty and G. G. Hammes, J. Phys. Chem., 62, 154 (1958).

21. J. N. Bronsted, Z. physik. Chem. 102, 169 (1922).

22. S. L. Friess, E. S. Lewis, and A. Weissberger, editors, Technique of Organic Chemistry, Vol. VIII, chapters XV to XVIII, Interscience, New York, (1963).

23. Z. Luz and S. Meiboom, J. Am. Chem. Soc., 85, 3923 (1963).

24(a). E. Grunwald, C. F. Jumper and S. Meiboom, J. Am. Chem. Soc., 85, 522 (1963).

24(b). E. Grunwald and S. Meiboom, J. Am. Chem. Soc., 85, 2047 (1963).

25. M. Sheinblatt and H. S. Gutowsky, J. Am. Chem. Soc., 86, 4814 (1964).

26. E. Grunwald and E. K. Ralph, Dynamic Nuclear Magnetic Resonance Spectroscopy. page 621. F. A. Cotton and L. Jackman editors. Academic Press, New York (1975).

27. J. A. Pople, W. G. Schneider and H. J. Bernstein, High Resolution Nuclear Magnetic Resonance, McGraw-Hill, Toronto (1959).

28. R. A. Ogg and J. D. Ray, J. Chem. Phys., 26, 1515 (1957).

29. E. Grunwald, A. Loewenstein and S. Meiboom, J. Chem. Phys., 27, 630 (1957).

30. E. Grunwald and M. Cocivera, Dis., Far. Soc., 39, 105 (1965).

31. T. C. Farrar and E. D. Becker, Pulse and Fourier Transform N.M.R. Academic Press, New York (1971).

32. S. Meiboom, J. Chem. Phys, 34, 375 (1961).

33. E. Grunwald and E. Price, J. Am. Chem. Soc., 86, 2970 (1964).

34. Z. Luz and S. Meiboom. J. Chem. Phys., 39, 366 (1963).

35. E. Grunwald and E. K. Ralph, Accounts of Chemical Research, 4, 107 (1971).

36. M. Sheinblatt, J. Chem. Phys., 36, 3103 (1962).

37. C. G. Swain, J. T. McKnight and V. T. Kreiter, J. Am. Chem. Soc., 79, 1088 (1957).

38. E. Grunwald, J. Phys. Chem. 67, 2211 (1963).

39. E. Grunwald and E. K. Ralph, J. Am. Chem. Soc., 89, 4405 (1967).

40. M. T. Emerson, E. Grunwald, M. L. Kaplan and R. A. Kromhout. J. Am. Chem. Soc., 82, 6307 (1960).

41. E. Grunwald, R. L. Lipnick and E. K. Ralph, J. Am. Chem. Soc., 91, 4333 (1969).

42. D. Rosenthal and E. Grunwald, J. Am. Chem. Soc., 94, 5956 (1972).

43. M. Cocivera, J. Phys. Chem., 72, 2520 (1968).

44. E. K. Ralph and E. Grunwald, J. Am. Chem. Soc., 91, 2422, (1969).

45. M. T. Emerson, E. Grunwald and R. A. Kromhout, J. Chem. Phys., 33, 547 (1960).

46. E. Grunwald, P. J. Karabatsos, R. A. Kromhout and E. L. Purlee. J. Chem. Phys., 33, 556 (1960).

47. A. Loewenstein and S. Meiboom, J. Chem. Phys., 27, 1067 (1957).

48. A. Loewenstein, J. Phys. Chem., 67, 1728 (1963).

49. E. Grunwald, J. Phys. Chem., 67, 2208 (1963).

50. E. Grunwald and A. Y. Ku, J. Am. Chem. Soc., 90, 29 (1969).

51. T. H. Marshall and E. Grunwald, J. Am. Chem. Soc., 91, 4541 (1969).

52. E. K. Ralph and E. Grunwald, J. Am. Chem. Soc., 89, 2963 (1967).

53. E. Grunwald and M. S. Puar, J. Phys. Chem., 71, 1842 (1967).

54. M. Sheinblatt, J. Chem. Phys. 39, 2005 (1963).

55. E. K. Ralph and E. Grunwald, J. Am. Chem. Soc., 90, 517 (1968).

56. R. J. Day and C. N. Reilly, J. Phys. Chem., 71, 1588 (1967).

57. H. C. Torrey, Phys. Rev., 76, 1059 (1949).

58. I. Solomon, Compt. Rend., 248, 92 (1959) and 249, 1631 (1959).

59. B. D. Sykes, J. Am. Chem. Soc., 91, 949 (1969).

60. F. Bloch, Phys. Rev., 70, 460 (1946).

61. B. D. Sykes and J. M. Wright, Rev. Sci. Instr., 41, 876 (1970).

62. A. L. Bacarella, E. Grunwald, H. P. Marshall and E. L. Purlee, J. Org, Chem., 20, 747 (1955).

63. H. S. Gutowsky and A. Saika, J. Chem. Phys., 21, 1688 (1953).

64. G. C. Hood, O. Redlich and C. A. Reilly, J. Chem. Phys., 22, 2067 (1954).

65. M. A. Paul and F. A. Long, Chem. Revs., 57, 1 (1957).

66. J. L. Sudmeier and G. Occupati, J.A.C.S. 90, 154 (1968).

67. S. N. R. v.Schatien, Suomen Kemistalehli, 31B, 372 (1958).

68. T. B. Paiva, M. Tominga and A. C. M. Paiva, J. Med. Chem. 13, 689 (1970).

69. I. D. Chawla and A. C. Andrews, J. Inorg. and Nuclear chem. 31, 3809 (1969).

70. W. Channing Nicholas and W. Conard Femelius, J. Phys. Chem., 65, 1047 (1961).

71. E. Grunwald and E. Price, J.A.C.S. 86, 2965 (1964).

72. L. H. Meyer, A. Saika and H. S. Gutowski, J.A.C.S. 75, 4567 (1953).

73. Dr. E. K. Ralph, unpublished results.

74. S. Forsen and R. A. Hoffman, J. Chem. Phys. 39, 2892 (1963).

75. W. J. Moore, Physical Chemistry, Prentice-Hall, Englewood Cliffs, N.J. (1972).

76. F. A. Long and W. F. McDevit, Chem. Rev., 51, 119 (1952).

77. K. C. Chang and E. Grunwald, J. Am. Chem. Soc., 98, 3737 (1976).

78(a). M. Eigen, Z. Physik. Chem., 1, 3/4, 176 (1954).

78(b). M. Eigen and L. De Maeyer, Z. Electrpchem., 59, 986 (1955).

79(a). R. L. Kay and D. F. Evans, J. Phys. Chem., 69, 4216 (1965).

79(b). H. G. Herz, B. Lindman and V. Siepe. Berichte, 73, 542 (1969).